Institute of Thermoelectricity, Academy of Sciences and Ministry of Education and Science of Ukraine

Journal of THERMOELECTRICITY

International Research

Founded in December, 1993

published 6 times a year

No. 4 *2018*

Editorial Board

International Editorial Board

Founders – National Academy of Sciences, Ukraine
Institute of Thermoelectricity of National Academy of Sciences and Ministry of Education and Science of Ukraine

Certificate of state registration № КВ 15496-4068 ПР

Address of editorial office:
Ukraine, 58002, Chernivtsi, General Post Office, P.O. Box 86.
Phone: +(380-372) 90 31 65.
Fax: +(380-3722) 4 19 17.
E-mail: jt@inst.cv.ua
http://www.jt.inst.cv.ua

Signed for publication 25.09.18. Format 70×108/16. Offset paper №1. Offset printing.
Printer's sheet 11.5. Publisher's signature 9.2. Circulation 400 copies. Order 5.

Printed from the layout original made by "Journal of Thermoelectricity" editorial board in the printing house of "Bukrek" publishers,
10, Radischev Str., Chernivtsi, 58000, Ukraine

CONTENTS

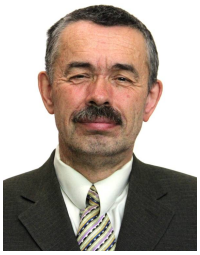

P.V. Gorskiy

P.V. Gorskiy, *doctor Phys.-math. science*

Institute of Thermoelectricity of the NAS and MES of Ukraine,
1, Nauky str, Chernivtsi, 58029, Ukraine;
[2]Yu.Fedkovych Chernivtsi National University, 2, Kotsiubynskyi str.,
Chernivtsi, 58000, Ukraine, *e-mail: anatych@gmail.com*

IMATION OF THE ELECTRICAL AND THERMAL CONTACT RSISTANCES AND THERMOEMF OF "THERMOELECTRIC MATERIAL-METAL" TRANSIENT CONTACT LAYER DUE TO SEMICONDUCTOR SURFACE ROUGHNESS

The impact of semiconductor surface roughness on the electrical and thermal contact resistances and thermoEMF of "thermoelectric material (TEM)-metal" transient contact layer is studied theoretically. The distribution of "hollows" and "humps" on the rough surface is simulated by the "truncated Gaussian distribution". The impact of distribution parameters on the electrical contact resistance and thermoEMF of "thermoelectric material-metal" contact is studied. Specific numerical calculations and plotting is made for the case of bismuth telluride-nickel contact. It turned out that the electrical and thermal contact resistances and thermoEMF at low root-mean-square deviations of profile height nonmonotonically depend on the average profile height, however, as the distribution of "hollows" and "humps" approaches the uniform, they tend to certain asymptotic values. In so doing, both the thermal and electrical contact resistances and thermoEMF increase at high relative values of the average profile height and decrease and its low values. Bibl. 10, Fig. 5.
Key words: electrical contact resistance, thermoEMF, surface roughness, transient layer, elementary bars, average value, root-mean-square deviation.

Introduction

The previous authors published a number of theoretical works dedicated to calculations of "TEM-metal" electrical and thermal contact resistances [1 – 4]. These works dealt with the barrier and emission mechanisms of formation of "TEM-metal" electrical contact resistance, diffusion phonon scattering on surface irregularities as a mechanism of formation of "TEM-metal" thermal contact resistance, as well as the influence of metal diffusion into semiconductor and coefficient of charge collection by metal electrode on "TEM-metal" electrical contact resistance. On the other hand, from the experimental data [5 – 8] it is known that the quality of semiconductor surface treatment has a considerable impact on "TEM-metal" contact resistance, and, hence, on the quality of thermoelectric energy conversion. However, the author of this article is not familiar with the works which would logically, with regard to specific numerical characteristics of TEM surface roughness, consider its impact on the electrical resistance and thermoEMF of "TEM-metal" contact. Exactly this consideration is the purpose of the present study.

It should also be noted that in [9] the limits of the depth of the disturbed layer, which arises when cutting the ingot of thermoelectric material into legs, are given. It is believed that this depth can vary from 20 to 150 μm.

Calculation of the electrical contact resistance and thermoEMF of "TEM-metal" transient contact layer due to TEM surface roughness and discussion of the results obtained

We will first describe the physical model that was used in the calculation process. Let us have a TEM with a non-flat surface. Since such a surface can be imagined as a set of random "hollows" and "humps"

with random depths and heights, we will draw imaginary horizontal planes through the "top" of the highest "hump" and through the "bottom" of the deepest "hollow". The distance between these parallel planes will be considered to be the known thickness d_0 of the transient layer. To "construct" the transient layer, we will fill with metal all the spaces between the horizontal planes free of TEM. To the author of this article, such a statistical approach seems to be more correct than modeling irregularities with objects of a particular geometric shape, for example, hemispheres [10].

We now describe the methods of calculation of the electrical contact resistance and thermoEMF of "TEM-metal" transient contact layer in the framework of this physical model.

Let us start with the calculation of the contact resistance. Breaking contact area into elementary pads of size *ds,* we thereby break our transient contact layer into elementary bars of length d_0, interconnected in parallel. Each of them consists of a "metal" part of length d_0x and a "semiconductor" part of length $d_0(1–x)$, where x is a random number from the range [0;1]. Therefore, the total conductivity of the contact is equal to:

$$\Sigma = \int_S \frac{ds}{d_0\left[\rho_m x + \rho_s(1-x)\right]}, \tag{1}$$

where ρ_m and ρ_s are resistivities of metal and TEM, respectively, S is contact area. Applying mean value theorem to (1), we find the following resultant expression for the electrical contact resistance:

$$r_c = d_0\left\langle \frac{1}{\rho_m x + \rho_s(1-x)} \right\rangle^{-1}, \tag{2}$$

where angular brackets mean averaging over rather large sequence of random (pseudorandom) numbers from the range [0;1]. Another model assumption we will make is that our pseudorandom numbers will be assumed to be distributed in the specified interval in accordance with the so-called "truncated Gaussian distribution", which we will present in the form:

$$f(x) = \frac{\exp\left[-(x-a)^2/2s^2\right]}{\int_0^1 \exp\left[-(x-a)^2/2s^2\right]dx}, \tag{3}$$

where a and s are certain parameters, and $0 \le a \le 1$. The boundary $\sigma \to \infty$ corresponds to uniform distribution for which $f(x) \equiv 1$. Then the contact resistance is decidedly equal to:

$$R_c = d_0\left[\int_0^1 \frac{f(x)dx}{\rho_m x + \rho_s(1-x)}\right]^{-1}. \tag{4}$$

Using formulae (3) and (4), we consider the impact of distribution parameters which characterize the quality of semiconductor surface treatment on the value of contact resistance. The result of calculations of contact resistance for bismuth telluride-nickel couple are given in Fig.1 for the thickness $d_0 = 20\,\mu$m and the values of a equal to 0.928, 0.5 and 0.072, respectively. In so doing, we assumed that $\rho_m = 8.7\cdot10^{-6}\,\Omega\cdot$cm, and $\rho_s = 1.25\cdot10^{-3}\,\Omega\cdot$cm.

From the figure it is seen that with increasing s, the electrical contact resistance rather quickly

(already at $s = 20$) reaches the asymptotic value which corresponds to $s = \infty$, i.e. the uniform distribution of "hollows" and "hills" along the rough surface. This value is equal to:

$$R_c = \frac{d_0(\rho_s - \rho_m)}{\ln(\rho_s/\rho_m)}, \quad (5)$$

i.e. about $5 \cdot 10^{-7}\ \Omega \cdot cm^2$.

Moreover, from the figure it is seen that at low values of s the electrical contact resistance is the lower, the closer to unity is the value of a. The value of $s = 0$ at $a = 1$ corresponds to absolutely smooth surface, so it is clear that in this case $R_c = 0$ (in the figure this case is not shown).

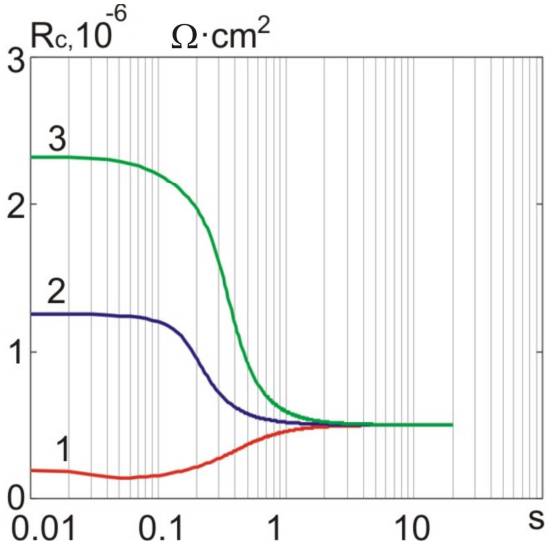

Fig. 1. Dependence of the electrical contact resistance of bismuth telluride-nickel at d_0 =20μm on the value of s at a equal to: 1) 0.928; 2)0.5; 3)0.072

The figure also shows that, with decreasing *a*, the contact resistance increases, since a decrease in *a* corresponds to an increase in the length of the "semiconductor" and to a decrease in the length of the "metal" part of each elementary bar that forms the transient layer. Thus, according to curve 1, the lowest value of the contact resistance under the investigated conditions is about $2 \cdot 10^{-7}\ \Omega \cdot cm^2$.

The results of similar calculations for $d_0 = 150\ \mu m$ are given in Fig. 2.

Under these conditions the lowest value of the contact resistance is $10^{-6}\ \Omega \cdot cm^2$, and its asymptotic value is $3.75 \cdot 10^{-6}\ \Omega \cdot cm^2$.

Thus, from the calculations it is seen that the character of surface treatment which is assigned by the distribution parameters (4) has a significant impact on the value of the contact resistance. The best situation is realized when the difference in heights is significantly larger than surface roughness. Under these conditions, the "metal" part of the elementary bars is substantially larger than the "semiconductor", which explains the relatively low value of the contact resistance in this case.

Quite similarly, one can determine the thermal contact resistance due to surface roughness. It is given below:

$$R_t = d_0\left[\int_0^1 \frac{f(x)dx}{\kappa_m^{-1}x + \kappa_s^{-1}(1-x)}\right]^{-1}, \qquad (6)$$

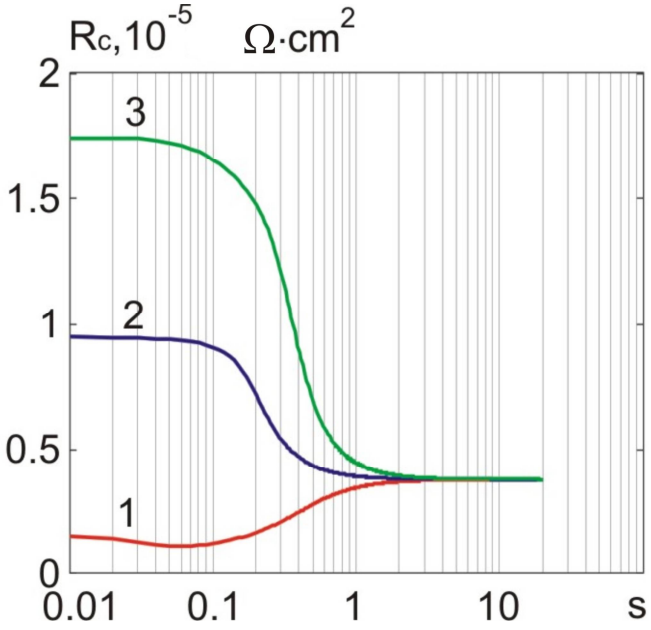

Fig. 2. Dependence of the electrical contact resistance of bismuth telluride-nickel couple at d_0 =150μm on the value of s at a equal to: 1) 0.928; 2)0.5; 3)0.072

The results of calculations of the thermal contact resistance by formula (6) are given in Figs. 3, 4.

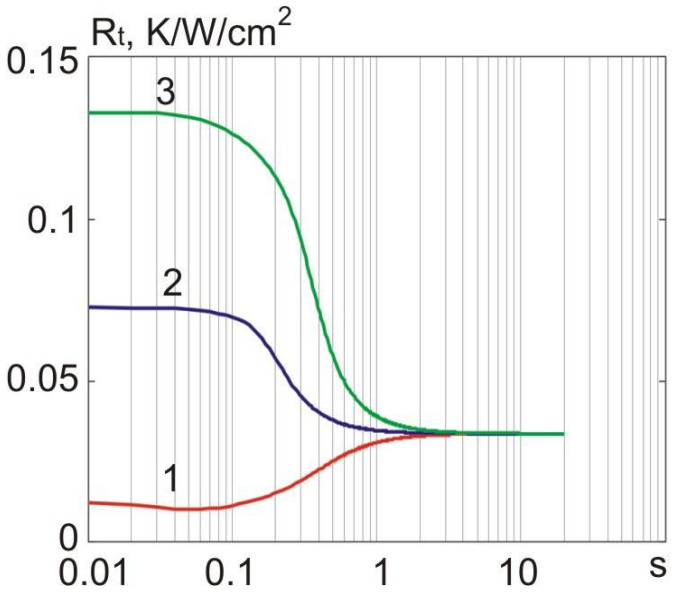

Fig. 3. Dependence of the thermal contact resistance of bismuth telluride-nickel couple at d_0 =20μm on the value of s at a equal to: 1) 0.928; 2)0.5; 3)0.072

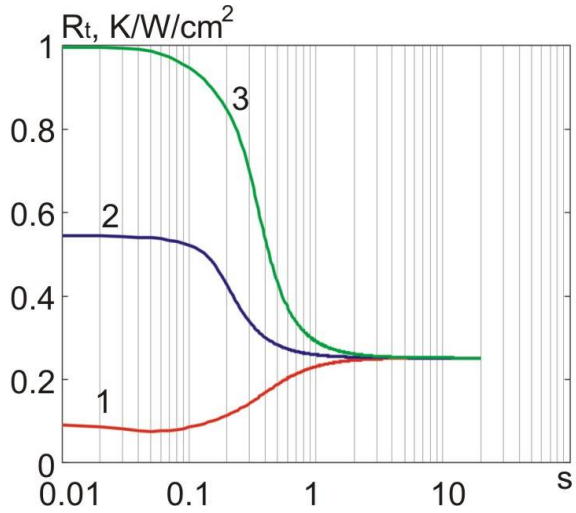

Fig. 4. Dependence of the thermal contact resistance of bismuth telluride-nickel couple at d_0 =150μm on the value of s at a equal to: 1) 0.928; 2)0.5; 3)0.072

From the figures it is seen that the behavior of the thermal contact resistance as a function of *s* is quite similar to the behavior of the electrical contact resistance due to analogy between heat and charge transfer. The lowest value of the thermal contact resistance under conditions in question is equal to 0.01 K·cm^2/W, and the asymptotic values at transient layer thicknesses 20 and 150 μm are equal to 0.033 and 0.251 K·cm^2/W, respectively.

The thermoEMF of the contact layer is found as the EMF of the parallel connected elementary bars, each of which has its own EMF and internal resistance, due to the ratio of lengths of the "metal" and "semiconductor" parts of each of them. Taking this into account, we first find the thermoEMF of an elementary bar. By definition, this thermoEMF is equal to the ratio of the difference of thermoelectric voltage on the bar to the temperature difference on it. So, first one must find the temperature distribution in the elementary bar. To this end, we write down the stationary equation of heat conductivity in the absence of external heat sources for the one-dimensional case. It will look like:

$$\frac{d}{dy}\left(\kappa\frac{dT}{dy}\right)=0\,, \tag{7}$$

where κ – coordinate-dependent thermal conductivity of the bar material. The general solution of this equation is as follows:

$$T=C_1\int\frac{dy}{\kappa}+C_2\,, \tag{8}$$

where C_1, C_2 – arbitrary constants that can be found from the initial conditions. Therefore, the thermoEMF of the elementary bar is:

$$\alpha_b=\frac{\int_0^{d_0}\alpha dT}{\int_0^{d_0}dT}=\frac{\int_0^{d_0}(\alpha/\kappa)dy}{\int_0^{d_0}(1/\kappa)dy}=\frac{(\alpha_m/\kappa_m)x+(\alpha_s/\kappa_s)(1-x)}{(1/\kappa_m)x+(1/\kappa_s)(1-x)}\,, \tag{9}$$

where $\alpha_m, \alpha_s, \kappa_m, \kappa_s$ – the thermoEMF and thermal conductivities of metal and TEM, respectively.

Thus, the general thermoEMF of transient layer due to surface roughness is equal to:

$$\alpha_c = \frac{\int_0^1 [\rho_m x + \rho_s(1-x)]^{-1}[(\alpha_m/\kappa_m)x + (\alpha_s/\kappa_s)(1-x)][(1/\kappa_m)x + (1/\kappa_s)(1-x)]^{-1} f(x)dx}{\int_0^1 [\rho_m x + \rho_s(1-x)]^{-1} f(x)dx}. \quad (10)$$

The results of calculation of the thermoEMF of bismuth telluride-nickel couple are given in Fig. 5.

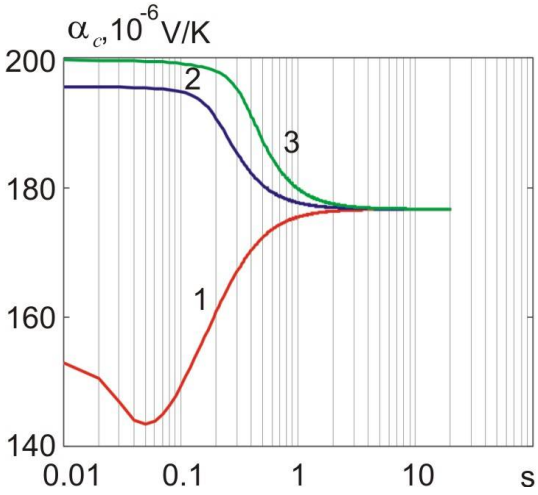

Fig. 5. Dependence of the thermoEMF of bismuth telluride-nickel couple at d_0 =150μm on the value of s at a equal to: 1) 0.928; 2)0.5; 3)0.072

From the figure it is seen that the thermoEMF of bismuth telluride-nickel couple qualitatively depends on the value of *s* at different *a,* just as the electrical and thermal contact resistances. This similarity is due to the fact that as a result of the low thermal conductivity of TEM in comparison with the metal, other things being equal, the bulk of the temperature drop on the elementary bar falls on its semiconductor part. The lowest value of the thermoEMF in this case is about 145 μV / K, and its asymptotic value, which corresponds to the uniform distribution of "hollows" and "humps", is 176 μV/K. The case of "short circuit", when the transient layer is completely composed of metal, is not considered in this article.

Conclusions

1. It was established that the electrical contact resistance of "TEM-metal" transient layer due to deviation of semiconductor surface from the ideal plane, for the "nickel-bismuth telluride" couple at transient layer thickness 20 μm is $5 \cdot 10^{-7}$, and at the thickness of 150 μm – $3.8 \cdot 10^{-6}$ Ohm·cm^2 under the condition of uniform distribution of "hollows" and "humps" within the layer.
2. It was established that the thermal contact resistance of "TEM-metal" transient layer due to deviation of semiconductor surface from the ideal plane, for the "nickel-bismuth telluride" couple at transient layer thickness 20 μm is 0.033 and at the thickness of 150 μm – 0.251 K·cm^2/W under the condition of uniform distribution of "hollows" and "humps" within the layer.
3. It was established that the thermoEMF of "nickel-*p*-type bismuth telluride" transient contact layer due to semiconductor surface roughness, does not depend on contact layer thickness and is 176 μV/K.
4. Since the value of the contact resistance that has to be "assigned" in order to match the real and estimated values of thermoelectric module parameters is an order of magnitude higher than that given in

this article, this indicates, firstly, that the main part of the contact resistance is not due to semiconductor surface roughness, and secondly, that there are reserves for the contact resistance reduction. However, for their detection and use, further in-depth, including experimental, studies of the mechanisms of contact resistance formation are needed.

References

1. Anatychuk L.I., Dugaev V.K., Litvinov V.I., Volkov V.L. (1994). Contact resistance between metal and thermoelectric material. *J. Thermoelectricity*, 1, 70-77.
2. Da Silva L.W., Kaviany M. (2004). Micro-thermoelectric cooler: interfacial effects on thermal and electrical transport. *Int. Journ of Heat and Mass Transfer*, 478, 2417-2435.
3. Vikhor L.M., Gorskiy P.V. (2015). Electrical resistance of "thermoelectric material-metal" contact. *J.Thermoelectricity*, 2, 16-24.
4. *Vikhor L.M., Gorskiy P.V. (2015). Heat and charge transport at "thermoelectric material-metal" boundary.* J.Thermoelectricity*, 6, 5-15.*
5. Alieva T.D., Abdinov D.Sh., Salaev E.Yu. (1981). Vlianiie obrabotki poverkhnoctei termoelektricheskikh materialov na svoistva termoelemntov izgotovlennykh iz tverdykh rastvorov $Bi_2Te_3 – Sb_2Te_3$ i $Bi_2Te_3 – Bi_2Se_3$ [The influence of processing of thermoelectric material surfaces on the properties of thermoelements made of $Bi_2Te_3 – Sb_2Te_3$ and $Bi_2Te_3 – Bi_2Se_3$ solid solutions]. *Izvestiia Akademii nauk SSSR. Neorganicheskiie materialy – Bulletin of the USSR Academy of Sciences. Inorganic Materials,* 17(10), 1773-1776 [in Russian].
6. Gupta R.P., McCarty R., Sharp J. (2013). Practical contact resistance measurement method for bulk Bi_2Te_3-based thermoelectric devices. *J. of Electron. Mat*., 1-5 (doi: 10.10007/s11664-013-2806-6).
7. *Ilzycer D., Sher A., Shilon M. (1980). Electrical contacts to thermoelectric bismuth telluride based alloys.* Proc of Third International Conf. on Thermoelectric Energy Conversion *(March 12-14, 1980), 200-202.*
8. *Belonogov E.K., Dybov V.A., Kostiuchenko A.V. et al. (2017). Modification of surface of thermoelectric legs based on Bi_2Te_3 –Bi_2Se_3 solid solution by pulse phonon treatment method.* Condensed Matter and Interphases*, 19(4), 479-488.*
9. Sabo E.P. (2011). Technology of chalkogen thermoelements. Physical foundations. Section 3. Technology of connection of thermoelement legs. Continuation. 3.5. Electrochemical metallization. *J.Thermoelectricity*, 1, 26-35.
10. Holm R. (1981). Elektricheskiie kontakty [Electrical contacts]. Moscow: Inostrannaia literatura [Russian transl].

Submitted 24.08.2018.

Горський П.В. *докт. фіз.-мат. наук*

Інститут термоелектрики НАН і МОН України,
вул. Науки, 1,Чернівці, 58029, Україна,
[2]Чернівецький національний університет
ім. Юрія Федьковича, вул. Коцюбинського 2,
Чернівці, 58000, Україна
e-mail: anatych@gmail.com

ОЦІНКА ЕЛЕКТРИЧНОГО ТА ТЕПЛОВОГО КОНТАКТНИХ ОПОРІВ ТА ТЕРМОЕРС ПЕРЕХІДНОГО КОНТАКТНОГО ШАРУ ТЕРМОЕЛЕКТРИЧНИЙ МАТЕРІАЛ-МЕТАЛ, ЗУМОВЛЕНИХ НЕПЛОЩИННІСТЮ ПОВЕРХНІ НАПІВПРОВІДНИКА

Теоретично досліджено вплив шорсткості поверхні напівпровідника на електричний та тепловий контактні опори та термоЕРС перехідного контактного шару «термоелектричний матеріал-метал». Розподіл «западин» і «горбів» на шорсткій поверхні модельовано «усіченим розподілом Гауса». Досліджено вплив параметрів розподілу на електричний контактний опір та термоЕРС контакту «термоелектричний матеріал-метал». Конкретні числові розрахунки та побудову графіків виконано для випадку контакту телуриду вісмуту з нікелем. Виявилось, що електричний та тепловий контактні опори та термоЕРС за малих середньоквадратичних відхилень висоти профілю немонотонно залежить від середньої висоти профілю,але з наближенням розподілу «западин» та «горбів» до рівномірного прямують до певних асимптотичних значень. При цьому як тепловий та електричний контактні опори, так і термоЕРС у міру наближення розподілу западин та горбів до рівномірного зростають за великих відносних значень середньої висоти профілю і зменшуються за малих його значень Бібл. 10, рис. 5.

Ключові слова: електричний контактний опір, термоЕРС, шорсткість поверхні, перехідний шар, елементарні бруски, середнє значення, середньоквадратичне відхилення.

Горский П.В., *докт. физ.-мат. наук*

Институт термоэлектричества, ул. Науки, 1,
Черновцы, 58029, Украина
[2]Черновицкий национальный университет
им. Юрия Федьковича, ул. Коцюбинского 2
Черновцы, 58000, Украина
e-mail: anatych@gmail.com

ОЦЕНКА ЭЛЕКТРИЧЕСКОГО И ТЕПЛОВОГО КОНТАКТНЫХ СОПРОТИВЛЕНИЙ И ТЕРМОЭДС ПЕРЕХОДНОГО КОНТАКТНОГО СЛОЯ ТЕРМОЭЛЕКТРИЧЕСКИЙ МАТЕРИАЛ-МЕТАЛЛ,ОБУСЛОВЛЕННЫХ НЕПЛОСКОСТНОСТЬЮ ПОВЕРХНОСТИ ПОЛУПРОВОДНИКА

Теоретически исследовано влияние шероховатости поверхности полупроводника на электрическое и тепловое контактные сопротивления и термоЭДС переходного контактного слоя «термоэлектрический материал-металл». Распределение «впадин» и «горбов» на шероховатой поверхности моделируется «усеченным распределением Гаусса». Исследовано влияние параметров распределения на электрическое и тепловое контактное сопротивление и термоЭДС контакта «термоэлектрический материал-металл». Конкретные численные расчеты и построение графиков выполнены для случая контакта теллурида висмута с никелем. Оказалось, что электрическое и тепловое контактные сопротивления и термоЭДС при малых среднеквадратичных отклонениях высоты профиля немонотонно зависят от средней высоты профиля, но с приближением распределения «впадин» и «горбов» к равномерному стремятся к определенным асимптотическим значениям. При этом как тепловое и электрическое контактные сопротивления, так и термоЭДС по мере приближения распределения впадин и

горбов к равномерному возрастают при больших относительных значениях средней высоты профиля и уменьшаются при малых ее значениях. Библ. 10, рис. 5.
Ключевые слова: электрическое контактное сопротивление, термоЭДС, шероховатость поверхности, переходной слой, элементарные бруски, среднее значение, среднеквадратичное отклонение

References

1. Alieva T.D., Barkhalov B.Sh., Abdinov D.Sh. (1995). Struktura i elektricheskie svoistva granits razdela kristallov $Bi_{0.5}Sb_{1.5}Te_3$ i $Bi_2Te_{2.7}Se_3$ s nekotorymi splavami [Structure and electrical properties of interfaces of $Bi_{0.5}Sb_{1.5}Te_3$ and $Bi_2Te_{2.7}Se_3$ crystals with some alloys]. *Neorganicheskie materialy – Inorganic Materials*, 31(2), 194-198 [in Russian].
2. Chuang C.-H., Lin Y.-C., Lin C.-W. (2016). Intermetallic reactions during the solid-liquid interdiffusion bonding of $Bi_2Te_{2.55}Se_{0.45}$ thermoelectric materials with Cu electrodes using a Sn interlayer. *Metals*, 6(92), 1-10. (doi: 103390/met.6040092).
3. Sabo E.P. (2011). Technology of chalkogen thermoelements. Physical foundations. Section 3. Technology of connection of thermoelement legs. Continuation. 3.5. Electrochemical metallization. *J.Thermoelectricity*, 1, 26-35.
4. Kuznetsov G.D., Polystanskiy Y.G., Evseev V.A. (1995). The metallization of the thermoelement branches by ionic sputtering of the nickel and cobalt. *Proc. of XIV International Conference on Thermoelectrics* (Russia, St.Petersburg, June 27-30, 1995) (pp.166-167).
5. Bublik V.T., Voronin A.I., Ponomarev V.F., Tabachkova N.Yu. (2012). Izmeneniie struktury prikontaktnoi oblasti termoelektricheskikh materialov na osnove telluride vismuta pri povyshennykh temperaturakh [Change in the structure of near-contact area of thermoelectric materials based on bismuth telluride at elevated temperatures] *Izvestiia vysshykh uchebnykh zavedenii*. Materialy elektronnoi tekhniki - *News of Higher Educational Institutions. Electronic Technique Materials,* 2, 17-20 [in Russian].
6. Snarskiy A.O., Zhenirovskiy M.I., Bezsudnov I.V. (2006). On the law of Wiedemann-Franz in thermoelectric composites. *J.Thermoelectricity*, 3, 59-65.
7. Tikhonov A.N., Samarskii A.A. (1972). *Uravneniia matematicheskoi fiziki [Equations of Mathematical Physics].* Moscow: Nauka [in Russian].
8. Kittel Charles. *Vvedeniie v fiziku tverdogo tela [Introduction to Solid State Physics].* Moscow: Nauka, 1978 [Russian transl].
9. Gupta R.P., McCarty R., Sharp J. (2013). Practical contact resistance measurement method for bulk Bi_2Te_3-based thermoelectric devices. *J. of Electron. Mat*., 1-5 (doi: 10.10007/s11664-013-2806-6).
10. Drabkin I.A., Osvenskiy V.B., Sorokin A.I. et al. (2017). Kontaktnyie soprotivleniia v sostavnykh termoelektricheskikh vetviakh [Contact resistances in composite thermoelectric legs]. *Fizika i Tekhnika Poluprovodnikov – Semiconductors,* 51 (8), 1038-1040.

Submitted 24.08.2018.

Manyk O.M., *Cand. of Phys. and Math. Sciences*[1.2]
Manyk T.O., *Cand. of Phys. and Math. Sciences* [1.2]
Bilynskyi-Slotylo V.R., *Cand. of Phys. and Math. Sciences*[1.2]

[1]Institute of Thermoelectricity of the NAS and MES of Ukraine,
1, Nauky str., Chernivtsi, 58029, Ukraine,
[2]Yuriy Fedkovych Chernivtsi National University,
2, Kotsiubynskyi str., Chernivtsi, 58012, Ukraine
e-mail: anatych@gmail.com

THEORETICAL MODELS OF CADMIUM ANTIMONIDE ORDERING ALLOYS

An integrated approach has been developed for calculating the configurational energy of cadmium antimonide ordering alloys. On the basis of the thermodynamic and statistic approaches, dependences of the free energy on the degree of long-range order are calculated from the standpoint of chemical bond, taking into account the molecular structures of cadmium antimonide melts. The obtained results can be used in the development of technological modes of obtaining new materials based on cadmium antimonides, which have high sensitivity, stability and identity of characteristics, especially necessary for thermal converters of metrological purpose. Bibl. 16, Fig. 3.

Key words: theory of ordering alloys, chemical bond, molecular models, phase transitions, polymorphous transformations, configurational energy of ordering alloys, state diagrams.

Introduction

Cadmium antimonide is one of the promising thermoelectric materials [1]. Depending on the heat treatment mode and cooling method, cadmium alloys with antimony can crystallize in accordance with stable and metastable state diagrams [2].

A stable compound of cadmium with antimony is *CdSb* which congruently melts at 456 °C and forms two eutectics: *CdSb* + *Cd* (at 290 °C, composition 7 at.% of antimony) and *CdSb* + *Sb* (T_{melt} 445 °C, composition 57 at.%) of antimony.

Metastable crystallization of alloys, depending on the cooling rate and the temperature of the melt, can take place in different ways. Thus, it was possible to observe the crystallization of the compound Cd_4Sb_3 (T_{melt} 430 ° C) in the range of compositions of 8-70 wt.% of antimony, if the melts were quenched from the temperature of 500 ° C. Cd_3Sb_2 is formed during quenching from 390 ° C of alloys containing 35–41.9 at.% of antimony, and melts at 410 ° C according to the peritectic reaction of $Cd_3Sb_2 = Cd_4Sb_3$ + melt.

Thermal effects at 325-375 ° C in the alloys containing 20-47 at.% of antimony are explained by the reaction $3Cd_3Sb_2 \rightarrow 2Cd_4Sb_3 + Cd$. Effects at 200-290 ° C on thermograms of alloys from the region of 20-70 at.% of antimony correspond to the reaction $Cd_4Sb_3 \rightarrow 3CdSb + Cd$.

A detailed review of state diagrams, phase transitions, thermodynamic properties of cadmium antimonides is given in [2]. It should be noted that these are mainly the results of experimental studies. As for the theoretical studies of ordering *CdSb* alloys, they are not yet available due to the fact that in the framework of simplified models used at present, it is not possible to reflect the specific features of cadmium antimonides, and consistent statistical and thermodynamic theory describing the effect of structure on the physicochemical properties of the resulting materials does not exist yet.

In this connection, in the present work the task was set to develop theoretical models of ordering alloys, which make it possible to generalize the possibilities of the already existing ones by combining statistical and thermodynamic approaches with regard to chemical bond.

To solve this problem, it was necessary to generalize methods for calculating the thermodynamic and static theory of the ordering of atoms in alloys [3], the quasi-chemical approach [4] using molecular structures of short-range order [5] and solving the inverse problem of the statistical theory of almost completely ordered alloys and to test the developed thermodynamic description of melts of low-symmetry crystals by the example of cadmium antimonides.

Theoretical models of ordering atoms in alloys

As numerous experimental studies have shown, the results of which are given in [6], the order of the arrangement of atoms in alloys has a great influence on their various properties. Not only alloys with metallic properties, but also alloys or compounds that are semiconductors can be in the ordered state. In a number of stoichiometric alloys, at sufficiently low temperatures, there is a distribution of atoms when atoms of each kind occupy only certain type of sites in the crystal lattice. Such an alloy is called well ordered. With a rise in temperature, there is a transition of atoms from "own" to "foreign" sites: such an alloy is called partially ordered. With increasing temperature, the concentration of atoms of this kind at the "foreign" sites increases, and at the "own" sites decreases, and the concentrations of atoms at the sites of various types become identical: such an alloy is called disordered. The temperature at which such a transition takes place is called the phase transition temperature.

Order-disorder phase transitions take place not only in the alloys of stoichiometric composition, but also in the alloys of other compositions. In this case, the temperature of ordering depends on the composition of the alloy.

Unlike the case of pure metal with an ideal crystal lattice, the alloy does not have translational symmetry. However, this symmetry is possessed by the probabilities of substitution of sites of different types with different atoms. The indicated symmetry changes upon order-disorder transition. In so doing, two cases are possible. In the first case, the probabilities of substitution of sites at transition point change abruptly, and the first-order phase transition takes place. In the second case, these probabilities change as the continuous second-order phase transition.

The ordering of atoms at the crystal lattice of an alloy can be characterized by how fully the sites of various types (forming the sublattices) are occupied by atoms of different kinds. In this case, the ordering is considered with respect to the lattice sites. The degree of ordering in this case is determined by the distribution of atoms in the whole crystal and is called the degree of long-range order. Quantitatively, it can be introduced as follows [3]: consider a binary alloy consisting of N_A atoms A and N_B atoms B, in which a crystal lattice contains $N^{(1)}$first-type sites, legal for A atoms, and $N^{(2)}$ second-type sites legal for atoms B. We denote by $v = N^{(1)}/N$ the relative concentration of first-type sites, and by $C_A = N_A/N$ the relative concentration of first-kind atoms (which may not be equal to v). Further, by $N_A^{(1)}$, $N_A^{(2)}$, $N_B^{(1)}$, $N_B^{(2)}$ we denote the numbers of A and B atoms at the sites of the first and second types, and by

$$P_A^{(1)} = \frac{N_A^{(1)}}{N}, \quad P_A^{(2)} = \frac{N_A^{(2)}}{N^{(2)}}, \quad P_B^{(1)} = \frac{N_B^{(1)}}{N^{(1)}}, \quad P_B^{(2)} = \frac{N_B^{(2)}}{N^{(2)}} \tag{1}$$

the probabilities of substitution of first and second-type sites by A and B atoms. In so doing

$$\left.\begin{aligned} &N_A^{(1)} + N_A^{(2)} = N_A, \quad N_B^{(1)} + N_B^{(1)} = N_B \\ &N_A + N_B = N^{(1)} + N^{(2)} = N, \\ &N_A^{(1)} + N_B^{(1)} = N^{(1)}, \quad N_A^{(2)} + N_B^{(2)} = N^{(2)} \end{aligned}\right\}. \tag{2}$$

hence,

$$\left.\begin{array}{c} P_A^{(1)} + P_B^{(1)} = 1, \quad P_A^{(2)} + P_B^{(2)} = 1, \\ vP_A^{(1)} + (1-v)P_A^{(2)} = C_A \end{array}\right\}. \tag{3}$$

The degree of long-range order η is determined by the formula

$$\eta = \frac{P_A^{(1)} - C_A}{1-v}. \tag{4}$$

The assignment of η and C_A determines all the probabilities (1). From (3) and (4) it follows:

$$\left.\begin{array}{ll} P_A^{(1)} = C_A + (1-v)\eta, & P_B^{(1)} = 1 - C_A - (1-v)\eta, \\ P_A^{(2)} = C_A - v\eta, & P_B^{(2)} = 1 - C_A + v\eta, \end{array}\right\} \tag{5}$$

where v is determined by the structure of crystalline lattice.

The degree of long-range order η, introduced by formula (4), is proportional to the deviation of the probability $P_A^{(1)}$ from its value C_A in a disordered alloy. Therefore, in a disordered alloy (of any composition), η = 0, and in the ordered alloys, this value will take on the larger values, the more “ideal" the crystal is and η = 1 for a well-ordered alloy (stoichiometric composition).

The state of ordering can also be characterized by how many atoms of different kinds surround (on the average, in a crystal) an atom of given kind. In this case, one speaks of the degree of short-range order, which can be defined in various ways. For example, for alloys in which first-type sites are always surrounded with second-type sites and vice versa, the degree of short-range order σ can be determined as follows:

$$\sigma = \frac{2N_{AB} - N^*}{N^*}, \tag{6}$$

where N_{AB} is the number of pairs of neighbouring atoms A and B, and N^* is the total number of pairs of neighbouring atoms. In this case, the degree of the short-range order varies from a unity (with complete ordering, when $N_{AB} = N^*$) to zero (with a completely random distribution, when $N_{AB} = N^*/2$.

In the general case, the short-range order can be characterized by other parameters (for instance, correlation parameters for different coordination spheres). As such parameters, for a binary *A*-*B* alloy one can choose the values $\varepsilon_{AB}^{LL'}(S_e)$, determined by the formula

$$\varepsilon_{AB}^{LL'}(S_e) = P_{AB}^{LL'}(S_e) - P_A^L P_A^{L'}. \tag{7}$$

here $P_{AB}^{LL'}(S_e)$ is the probability that the site of L type is occupied by atom A, and located at a distance S_e from it (in the 1-st coordination sphere), the site of L' type is occupied by atom B, and P_A^L, $P_B^{L'}$ – the above introduced probabilities of the substitution of sites of L and L' types, by atoms A and B,respectively.

In the case when the probabilities of substitution by atoms A and B of the given type of sites do not depend on the arrangement of atoms at other sites, $P_{AB}^{LL'}(S_e)$ is equal to the product of P_A^L, $P_B^{L'}$ and $\varepsilon_{AB}^{LL'}$ is equal to zero. In this case there is no correlation between filling of various types of sites with atoms A and B.

In the case of an alloy of stoichiometric composition AB in which the sites of the first type are surrounded only with sites of the second type and vice versa, there is a simple relation between parameter $\varepsilon_{AB}^{12}(\rho_1)$ for the first coordination sphere and the degrees of short-range and long-range order σ and η [3],

$$\sigma = \eta^2 + 4\varepsilon_{AB}^{12}(\rho_1). \tag{8}$$

From formula (8) it follows that correlation parameter $\varepsilon_{AB}^{12}(\rho_1)$ tends to zero both with a rise in temperature, when $\eta = 0$, $\sigma \to 0$, and with a decrease in temperature, when almost fully ordered state is realized, i.e. when η and σ tend to unity.

The physical reason leading to ordering is the fact that in the alloys capable of being ordered for atoms of any kind it is energetically more beneficial to be surrounded with atoms of a different kind. At sufficiently high temperatures (whereby long-range order is still absent) this brings about the appearance of short-range order. (In this case $\sigma > 0$ and $\varepsilon_{AB}(\rho_1) > 0$).

In the case when for atoms of given kind it is more beneficial to be surrounded with atoms of the same kind, we will have $\sigma < 0$ and $\varepsilon_{AB}^{(\rho 1)} < 0$. Accordingly, alloys in which long-range order can exist are referred to as ordering, and alloys that can disintegrate into disordered solutions – disintegrating.

In the construction of ordering theory, two ways of consideration of the problem are possible. One can perform calculation within a specific model of alloy, calculate the energies corresponding to various arrangements of atoms at crystal lattice sites and then determine a partition function and free energy of the alloy. From the condition of free energy minimum to find the equilibrium properties of alloys, the values of the degree of long-range order and correlation parameters corresponding to given temperature. This type of consideration of ordering problem is given in statistical theory.

Another approach is based on the use of general thermodynamic relations, on the account of crystal symmetry properties and on the proposal of the possibility of certain type of series expansions of thermodynamic quantities. Such thermodynamic theory allows describing two types of phase transitions. First-order phase transitions whereby there is an abrupt change in the first derivatives of thermodynamic potential $\Phi(P,T)$ with respect to temperature T and pressure P, i.e. entropy $S = -d\Phi/dt$ and volume $v = -d\Phi/dP$, and, hence, the energy E of alloy (thermodynamic potential $\Phi = E-TS+PV$ remains continuous with such a transition). With the first-order phase transitions the heat of transformation is released or absorbed.

In the case of second-order phase transitions, the thermodynamic potential Φ and its first derivatives (i.e. entropy and volume) remain continuous, and the second derivatives of Φ with respect to T and P change abruptly – heat capacity

$$C_p = T\frac{\partial S}{\partial T} = -T\frac{\partial^2 \Phi}{\partial T^2}. \tag{9}$$

compressibility

$$æ = -\frac{1}{V}\frac{\partial V}{\partial p} = -\frac{1}{V}\frac{\partial^2 \Phi}{\partial p^2}, \tag{10}$$

coefficient of thermal expansion

$$\alpha = \frac{1}{V}\frac{\partial V}{\partial T} = \frac{1}{V}\frac{\partial^2 \Phi}{\partial T \partial V} \tag{11}$$

Note that these values can also change abruptly during first-order transitions, however, due to continuity of entropy there is no absorption or release of heat.

Hence, during ordering which is first-order phase transition, the composition of ordered and disordered phases must be different, i.e. on the state diagram there must exist a two-phase area. For second-order phase transitions the transition is possible without the appearance of a two-phase area.

Two approaches are possible in the construction of second-order phase transitions. The first approach postulates the possibility of such phase transition, and the symmetry of ordered and disordered

phases is considered to be specified. The temperature and concentration dependences of the degree of long-range order close to phase transition point is studied, and a change in various thermodynamic quantities during transition is considered.

The second possible approach does not suppose beforehand the existence of second-order phase transition. Using common symmetry properties of probability density function it becomes possible to clear out whether second-order phase transitions can occur in the alloy of this structure. The results of studying the possibilities of realization of such approach for alloys of different structures given in [3] have shown that second-order phase transitions are possible in the alloys with bulk-centered and face-centered cubic lattices, as well as closely packed hexagonal lattice.

This approach yielded a dependence of the degree of long-range order on temperature, pressure and alloy composition for the temperatures close to ordering temperature (with a second-order phase transition), as well as in the case of almost fully ordered alloy. Owing to the fact that in thermodynamic theory calculations are carried without the use of a specific alloy model, the results given in [3] possess rather high generality.

However, the results obtained in the thermodynamic theory are valid not in the entire area of parameter change, to the degrees of which the thermodynamic potential was expanded, but only in that range of their values, where only the first terms of these expansions can be used. This method does not allow investigating order-disorder transition which is the first-order phase transition, since at transition into ordered state η immediately takes on high values.

Analysis of the possibilities of models currently used in ordering theory (both thermodynamic and statistical taken separately) does not yield reliable results. Therefore, it is expedient to combine the possibilities of these approaches in a single statistically-thermodynamic approach with the use of molecular models of initial components and chemical bond models of the melts of their compounds.

Statistically-thermodynamic approaches and chemical bond models of ordering melts

Unlike the thermodynamic theory, the statistical theory evidently employs a specific atomic alloy model. On the basis of this model, free energy is determined and the equilibrium properties of the system are found. In so doing, it is not supposed that the degree of long-range order is low or close to unity, and one can obtain the results that are valid in the entire area of change in the degree of long-range order and composition.

Parameters forming part of statistical theory may be related to atomic interaction energies, the values characterizing alloy structure. In principle, it is also possible in the framework of the accepted model to clear out the issue of the peculiarity of thermodynamic potential of alloy at a point of phase transition.

In statistical theory, the atomic structure of alloy is taken explicitly, various arrangements of atoms at the sites are considered and the energies of such arrangements are calculated.

The interaction energies of individual pairs are supposed to be independent on alloy composition, the degree of long-range order, the temperature and the atoms with which this pair is surrounded. In such assumptions, to determine the equilibrium properties of alloy at given temperatures T, volumes V and component concentrations, it is necessary to calculate the partition function

$$Z = \sum_n e^{-E_n/kT}. \tag{12}$$

here, n is the number of system state which is determined by configuration of atoms at the sites and quantum numbers characterizing thermal oscillations of atoms, the state of electrons, etc. All this allows representing alloy energy E_n as a sum:

$$E_n = E_m + E_i, \tag{13}$$

where E_i is configuration energy of crystal (the energy of basic state at given i-th configuration), and E_m independent of configuration number i part of energy determined by quantum number m.

The partition function Z can be written as a product

where
$$\left.\begin{array}{c} Z = Z_0 Z_K, \\ Z_0 = \sum_m e^{-E_m/kT}, \quad Z_K = \sum_i e^{-E_i/kT}, \end{array}\right\} \tag{14}$$

and free energy of alloy $F = kT\ln Z$ takes on the form

$$\left.\begin{array}{c} F = F_0 + F_K, \\ F_0 = -kT\ln Z_0, \quad F_K = -kT\ln Z_K, \end{array}\right\} \tag{15}$$

F_K is the configuration part of free energy.

Configuration energy E_i in traditional approach [3] is expressed through interaction energies of pairs of different atoms located at different distances. In the case of binary alloy A-B this energy is equal to

$$E_i = -\sum_{e=1}^{\infty}\left[N_{AA}^{(e)}\upsilon_{AA}(\rho_e) + N_{BB}^{(e)}\upsilon_{BB}(\rho_e) + N_{AB}^{(e)}\upsilon_{AB}(\rho_e)\right], \tag{16}$$

where $\upsilon_{AA}(\rho_e)$, $\upsilon_{BB}(\rho_e)$, $\upsilon_{AB}(\rho_e)$ are taken with the opposite sign interaction energies of pairs of atoms A-A, B-B and A-B in the crystal at the distances ρ_e, equal to radius of the i-th coordination sphere, and $N^{(e)}_{AA}$, $N^{(e)}_{BB}$, $N^{(e)}_{AB}$ are the numbers pairs of atoms A-A, B-B and A-B, spaced at a distance ρ_e.

In the approximation that takes into account the interaction of only nearest neighbours E_i takes on the form

$$E_i = -\left(N_{AA}\upsilon_{AA} + N_{BB}\upsilon_{BB} + N_{AB}\upsilon_{AB}\right), \tag{17}$$

Here, the numbers of pairs N_{AA}, N_{BB}, N_{AB} and interaction energies $-\upsilon_{AA}$, $-\upsilon_{BB}$, $-\upsilon_{AB}$ must be taken for the nearest atoms.

The number of pairs N_{AA} can be expressed through the number N_A of atoms A in the alloy and the number of pairs N_{AB}. The total number of atoms adjacent to atoms A, is equal to ZN_A (Z – coordination number for the first coordination sphere). Subtracting from this number the number of pairs of different atoms N_{AB}, we obtain a double number of pairs N_{AA}:

$$N_{AA} = \frac{1}{2}\left(ZN_A - N_{AB}\right) \tag{18}$$

Similarly,

$$N_{BB} = \frac{1}{2}\left(ZN_B - N_{AB}\right) \tag{19}$$

Substituting (18), (19) into (17), we obtain another expression for configurational energy

$$E_i = -\frac{1}{2}\left[\omega N_{AB} + Z\left(N_A\upsilon_{AA} + N_B\upsilon_{BB}\right)\right] \tag{20}$$

where

$$\omega = 2\upsilon_{AB} - \upsilon_{AA} - \upsilon_{BB} \tag{21}$$

The value ω is called ordering energy. The second term in (20) traditionally [3] is referred to configuration-independent part of energies E_m. The first term in (20) depends on configurations.

To determine the equilibrium properties of alloy related to arrangement of atoms at the lattice sites, it is necessary to use the condition of minimum configuration part of free energy $F_к$. However, despite the

simplifications made, calculation of partition function is a complicated mathematical problem, which was precisely solved only in the one-dimensional case and in the case of flat lattices. In the tree-dimensional case for its solution one has to resort to approximate calculation methods. The simplest is ordering theory which disregards correlation in alloy (Gorsky, Bragg and Williams [7], [8]).

Solution of ordering problem is reduced to calculation of configuration multiplier of partition function by formulae (14) and (20) for an alloy with given numbers N_A and N_B of atoms A and B.

The approximation lies in the fact that energies E_i of different configurations corresponding to this value of the degree of long-range order are assumed to be identical and calculated on the assumption of random distribution of atoms at the sites of each type. This means that the total number N_{AB} of pairs AB, which according to (20) determines E_i, is found assuming that the probabilities of substitution of given site with atoms A and B do not depend on the configuration of atoms at the surrounding sites and are equal to probabilities (1) – (5), i.e. identical for all sites of given type. Thus, in this approximation the correlation in the alloy is disregarded. At the same time, this approach allows calculating the degree of long-range order of different composition as a function of temperature, ordering temperature as a function of alloy composition, makes it possible to explain a number of phenomena occurring in the ordering alloys.

On order to illustrate the solution of ordering problem for binary alloys A-B, considered are structures having the same number (N/2) of the first and second type of sites, and the site of given type is surrounded with sites of different kind. Such structures are inherent in alloys of the type β-brass (coordination number Z=8), crystals of NaCl type (Z=6), flat square mesh (Z=4). The value N_{AB} is equal to sum of pairs of atoms in which atom A is at the site of the first type, and atom B-at the site of the second type, and vice versa. For such alloys

$$N_{AB} = \frac{ZN}{2}(P_A^{(1)}P_B^{(2)} + P_A^{(2)}P_B^{(1)}) \tag{22}$$

Substituting this expression into (20) and using (1)-(5) (where it is necessary to assume $\upsilon = \frac{1}{2}$), we find that in the nearest-neighbour approximation energy E_i is equal to

$$E_i = -\frac{ZN}{2}\left[C_A\upsilon_{AA} + C_B\upsilon_{BB} + \omega\left(C_AC_B + \frac{\eta^2}{4}\right)\right], \tag{23}$$

where $C_B = 1\text{-}C_A$. In formula (14) in the accepted approximation all terms $e^{-Ei/kT}$, corresponding to different configurations of atoms at the solution sites are identical. The total number of terms is equal to the number of various permutations W of atoms A and B at the sites of the first and second type with a given value of the degree of long-range order in the alloy of given composition. In order to determine W, one must obtain the numbers of such permutations at the sites of each type at given values of numbers of atoms $N^{(1)}{}_A$, $N^{(1)}{}_B$, $N^{(2)}{}_A$ and $N^{(2)}{}_B$ (that are determined by assignment of the composition and degree of long-range order) and multiply the results:

$$W = \frac{(N/2)!}{N_A^{(1)}!N_B^{(1)}!}\frac{(N/2)!}{N_A^{(2)}!N_B^{(2)}!}. \tag{24}$$

Thus, free energy in this case is equal to

$$F = -kT\ln Z_k = E_i - kT\ln W. \tag{25}$$

Substituting into (25) the expressions (23) and (24), using Stirling formula $\ln x! = x(\ln x - 1)$ (valid for large values of x) and considering (1) – (5) we obtain the expression for free energy.

Differentiating this expression with respect to η, from condition $\frac{\partial F}{\partial \eta} = 0$ we find the equation for the equilibrium value of the degree of long-range order, the temperature of order-disorder transition. Differentiating with respect to temperature, we find the configuration part of alloy entropy

$$S = \frac{\partial F}{\partial T}.$$

Thus, in the considered approximation of ordering theory for the above mentioned structures at point of transition entropy changes continuously, i.e. there is no transition heat, and heat capacity undergoes finite jump.

We have the second-order phase transition.

The considered approximation also leads to zero configuration part of heat capacity above ordering temperature, i.e. does not allow taking into account heat capacity related to change in the short-range order in the alloy.

More precise results that are in quantitative agreement with experiment can be obtained in the theories taking into account correlation in the alloy.

One of the methods to determine free energy F which make it possible to take into account correlation in the alloy is calculation of F in the form of a series according to degrees of ordering energy ω relation to kT. This method was proposed by Kirkwood, and its detailed description is given in [3]. This method allows calculating only several first expansion terms. So, the resulting expression for F is rather precise at high temperatures and worse approximates the accurate expression for free energy at low temperatures. Moreover, this method is rather cumbersome and not always convenient for practical calculations. Therefore, in practice, use is more often made of another method of considering the process of ordering in the alloys – quasi-chemical [4], the simplest variant of which is based on considering individual pairs of neighbouring atoms. Free energy of this alloy is found as the function of temperature, the degree of long-range order and the number N_{AB} of pairs of neighbouring atoms AB, which characterize correlation in the alloy. In more controversial variants of this method, as independent "molecules" considered are atoms composing tetrahedron, etc. [9]. With increasing the number of atoms entering one "molecule", the accuracy of the method is increased, and in such a theory we already obtain the first-order phase transition, but in a more complicated way.

Molecular structures of ordering melts of cadmium antimonides

With a view to simplify the statistical and thermodynamic calculations on the one hand and take into account correlation in the melt on the other hand, this paper proposes a comprehensive approach to calculation of thermodynamic functions of ordering melts of low-symmetry crystals by the example of cadmium antimonides. To solve the formulated problem, it was necessary to generalize methods of ordering theory for the case of low-symmetry crystals; develop the method of calculation of the reciprocal problems of statistical theory of almost fully ordered alloys allowing drastic simplification of the number of permutations W of atoms of different kinds with a given value of the degree of long-range order in the alloy of given composition and calculate ordering energy ω by microscopic theory methods depending on the interatomic distances. This will enable calculations of the configuration part of thermodynamic functions, conditions for implementation of phase transitions, polymorphous transformations, stable and metastable phases.

Generalization of ordering theory methods was made from the standpoint of multifactor approach [10]. The essence of such generalization is that in the construction of ordering theory there are two ways to consider the problem. It is possible to perform calculation within a specific model of alloy, calculate the

energies corresponding to different locations of atoms at the lattice sites, and then determine the partition function and free energy of the alloy. Such type of consideration of ordering problem is used in statistical physics, but due to serious mathematical difficulties for a number of alloys such theories do not yield reliable results.

Another approach to the construction of an ordering theory is based on the application of general thermodynamic relationships, on taking into account the properties of crystal symmetry and on the assumption of certain type of series expansion of thermodynamic quantities. Such a theory does not contain the disadvantages associated with the choice of a simplified model of the alloy. However, the results obtained will not apply to the entire range of values of the order parameters.

In fact, these two approaches reflect separately the long-range and short-range order.

Therefore, when generalizing these approaches, it is necessary to take into account factors of both thermodynamic and statistical theory. In this connection, in the present work, the unit cell of cadmium antimonide was considered as consisting of two sublattices: the cadmium sublattice and the antimony sublattice. In addition, each cadmium atom has three nearest neighbors in the antimony sublattice and one neighbor in the cadmium sublattice. Similarly, an antimony atom - has three nearest neighbors in the cadmium sublattice and one in the antimony sublattice. Further, according to [11], CdSb has a rhombic structure, the space group is D152h, and the unit cell contains 16 atoms (Fig. 1).

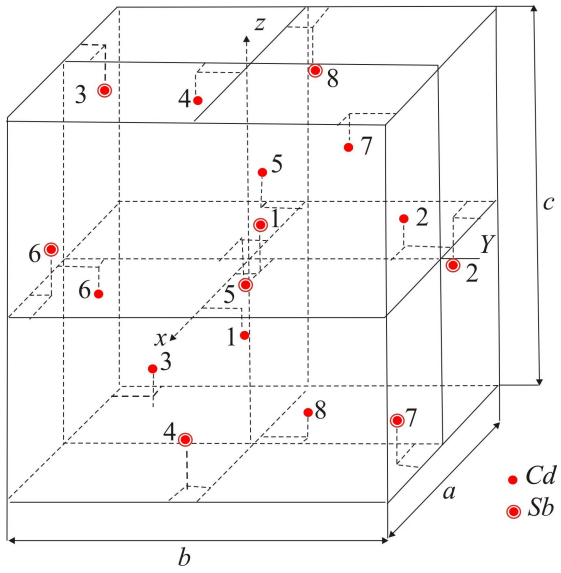

Fig 1. Unit cell of CdSb

Lattice parameters and interatomic distances given in [11] are as follows:

$$\left.\begin{aligned} &a = 6.471\text{Å}; b = 8.253\text{Å}; c = 8.526\text{Å}, \\ &R_{Sb-Sb} = 2.81\text{Å}; R_{Cd-Cd} = 2.99\text{Å}, \\ &R_{Cd-Sb} = 2.81\text{Å};\ 2.91\text{Å};\ 2.84\text{Å} \end{aligned}\right\} \qquad (26)$$

These data were repeatedly checked and refined by various authors. A detailed review of these papers is given in [10].

It follows from the above results that CdSb should have anisotropic properties, as indicated by the various values of the lattice parameters (26). Therefore, these issues (related to the crystal structure of a substance) should be considered together with chemical bond.

As follows from the reviews cited in [2], [10], the issues of chemical bond in CdSb crystals were considered in a number of papers, both experimental and theoretical. Their common shortcoming was that these issues were considered extremely simplified, taking into account only one factor and the comparison of chemical bond and physical properties was based only on probable considerations and allowed to make only rough conclusions that were not always true.

Strict consideration of the nature of the CdSb chemical bond is possible only with comprehensive consideration of various factors, including the coordination structure, the electron configuration of atoms, the interatomic distances, and the angles between the directions of bonds in the crystal. In [10], the results of the study of chemical bond in CdSb with regard to the factors listed above are given. Analysis of factors characterizing various aspects of chemical bond in CdSb crystals made it possible to draw the following conclusions:

1) In the *CdSb* compound, bonds between *Sb-Sb* atoms (as in the layers of pure antimony) and between *Cd-Cd* atoms (as in cadmium crystals), have been preserved, and new *Cd-Sb* bonds of different length have appeared.

2) The *CdSb* lattice can be considered as a strongly deformed diamond lattice, each atom of which is surrounded with one similar atom and three atoms of another kind that are located at the vertices of a deformed tetrahedron.

3) Different distances between atoms in *CdSb*, the presence of different angles between bonds indicate the existence of different types of bonds, but the interactions that determine the bonds almost always come down to a quantitative redistribution of the electron charge on the bonds.

Multifactor analysis allowed us to propose a molecular model of *CdSb*, shown in Fig. 2

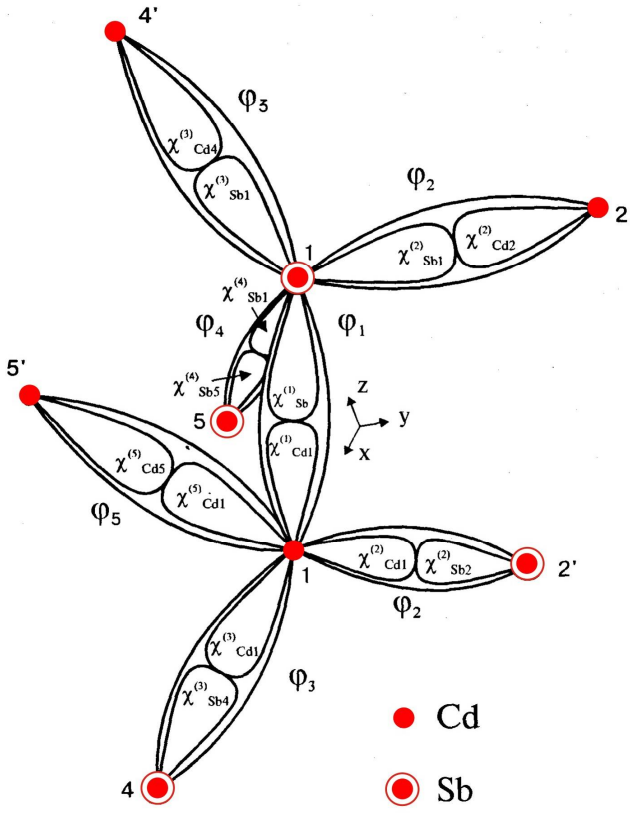

Fig. 2. Molecular model of CdSb.

The molecular model gives an idea of the spatial arrangements of bonds described using nonequivalent hybrid orbitals (NHOs) (all bonds in *CdSb* φi crystals can be distributed over 5 families, according to five different interatomic distances, namely: φ1, φ2, φ3 correspond to three different *Cd -Sb*

distances; φ4 *Sb-Sb* and φ5 *Cd-Cd*. The type of hybrid orbitals is determined by the angles between bond directions, which are experimental criteria for the type of hybrid atomic orbitals that form a bond.

The fact that the rhombic *CdSb* structure can be viewed as a strongly deformed diamond lattice on one side and the presence of cadmium and antimony sublattices in *CdSb*, in which each atom of one sublattice has three neighbors in another sublattice and one in its own, suggests the following theoretical model of ordering for *CdSb* alloy.

It was proposed to consider ordering for a binary alloy of *A-B* type rhombic structure having equal number of sites of the first and second type as ordering of two independent alloys with a deformed face-centered cubic lattice of AB_3 and A_3B type, where the number of sites of one type is three times less than the number of sites of another type (ν = 1/4). The number of AB pairs for each sublattice with such an approach, unlike (22), is equal to:

$$N_{AB} = \frac{3N}{4}(P_A^{(1)}P_A^{(2)} + P_B^{(2)}P_B^{(1)}) + \frac{N}{4}(P_A^{(1)}P_B^{(1)} + P_A^{(2)}P_B^{(2)}), \tag{27}$$

where the designations are the same as in (1)-(5). Thus, in the nearest-neighbour approximation for the total energy E_i of both sublattices we get the expression:

$$E_i = -4N[C_A\upsilon_{AA} + C_B\upsilon_{BB} + \omega(C_AC_B + \frac{\eta^2}{16})], \tag{28}$$

where the designations are the same as in (23).
The number of different permutations of atoms at the sites of each of the sublattices is equal to:

$$W = \frac{(N/4)!}{N_A^{(1)}!N_B^{(1)}!}\cdot\frac{(3N/4)!}{N_A^{(2)}!N_B^{(2)}!} \tag{29}$$

Therefore, free energy according to (15) for both sublattices takes on the form:

$$\begin{aligned} F = &-4N[C_A\upsilon_{AA} + C_B\upsilon_{BB} + \omega(C_AC_B + \frac{\eta^2}{16})] + \\ &+\frac{N\kappa T}{4}[(C_A + \frac{3}{4}\eta)\ln(C_A + \frac{3}{4}\eta) + (C_A - \frac{3}{4}\eta)\ln(C_A - \frac{3}{4}\eta) + \\ &+(C_B - \frac{3}{4}\eta)\ln(C_B - \frac{3}{4}\eta) + (C_B + \frac{3}{4}\eta)\ln(C_B + \frac{3}{4}\eta) + 3(C_A - \frac{1}{4}\eta)\ln(C_A - \frac{1}{4}\eta) + \\ &+3(C_A + \frac{1}{4}\eta)\ln(C_A + \frac{1}{4}\eta) + 3(C_B + \frac{1}{4}\eta)\ln(C_B + \frac{1}{4}\eta) + 3(C_B - \frac{1}{4}\eta)\ln(C_B - \frac{1}{4}\eta)] \end{aligned} \tag{30}$$

Using (29), a study was made of the dependence of the configurational combined energy of *CdSb* alloy on η. The correlation was taken into account by using the digital values of the dissociation energy on nonequivalent hybrid orbitals in *CdSb* crystals given in our published paper [12]. As follows from Fig. 3, when ordering melts, 3 individual NHOs behave differently and make it possible to analyze the dynamics of the formation of a chemical bond in *CdSb* crystals.

Designations given in Fig.3 are as follows: 1, 2, 3 – correspond to chemical bonds of *Cd-Sb* with interatomic distances $R_{Cb-Sb} = 2.81\text{Å}; 2.91\text{Å}; 2.84\text{Å}$ 4 – corresponds to chemical bonds of *Sd-Sb*, 5 – corresponds to chemical bonds of *Cd- Cd*.

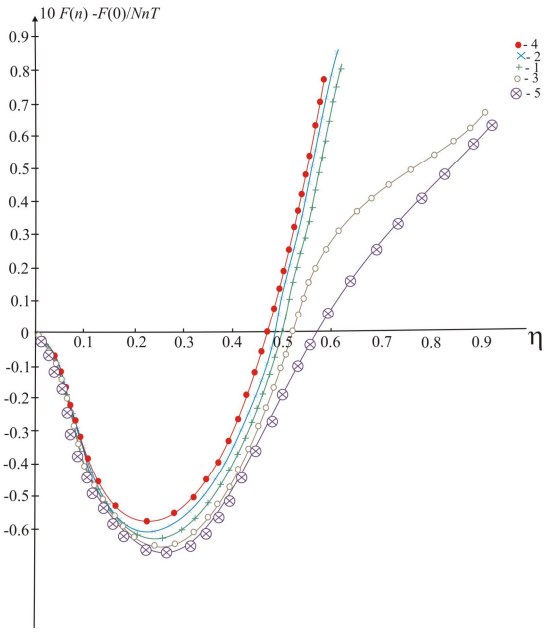

Fig. 3. Curves of dependence of configuration free energy of nonequivalent hybrid orbitals of CdSb (The numbers at the curves mean NHOs).

The results given in Fig.3 are consistent with:

- studies of the interaction of electronic properties and structure of melts with the state diagrams [13], [14];

- the results of studies on the peculiarities of crystallization of melts in the area of existence of a metastable compound Cd_4Sb_3 [15];

- thermal rearrangement of atoms in *Cd-Sb* melts and structurally-functional change in the structure of atoms in the substance [16].

Thus, the obtained results provide an opportunity not only to explain the "fine structure" of the processes of melting and crystallization of cadmium antimonides, but also to refine the technological regimes of the synthesis of new materials with predicted properties by calculating the temperature ranges of superheating and supercooling of chemical bonds responsible for the appearance of the necessary properties.

Discussion of the results

Analysis of the results obtained in this work has shown that the generalization of the methods of thermodynamic and statistical ordering theory from the standpoint of chemical bond and solving inverse problems of the theory of almost completely ordered alloys allows not only to simplify the calculation of the partition function and to obtain analytical expressions for the cumulative energy, which will enable further studies of various thermodynamic functions, phase transitions, polymorphic transformations, when the degree of long-range order in the ordered alloy is determined by the degree of short-range order and correlation using multifactor molecular models.

Such an approach made it possible to consider the configuration component of energy at the molecular level, which in turn makes it possible to use further information about the initial components (dependences of thermodynamic functions on temperature and pressure) in developing technology for producing new materials based on superlattices (sphalerites, skutterudites, cluster formations, stable and metastable phases).

Conclusions

1. Based on the thermodynamic and statistical theory of the ordering of alloys, an integrated approach has been developed for calculating the configurational energy of ordering cadmium antimonide alloys from the standpoint of chemical bond.

2. A method was developed for taking correlation into account by using the dissociation energy of nonequivalent hybrid orbitals as a function of interatomic distances.

3. Calculations of the dependence of the configurational free energy on the degree of the long-range order were carried out taking into account the molecular structures of *CdSb* melts.

References

1. Anatychuk L.I. (1979). *Termoelementy i termoelektricheskiie ustroistva [Thermoelements and thermoelectric devices]*. Kyiv: Naukova dumka [in Russian].
2. Lazarev V.B., Shevchenko V.Ya., Grinberg Ya.Kh., Sobolev V.V. (1978). *Poluprovodnikovyie soiedineniia gruppy $A^{II}B^{V}$ [Semiconductor compounds of $A^{II}B^{V}$ group]*. Moscow: Nauka [in Russian].
3. Krivoglaz M.A., Smirnov A.A. (1958). *Teoriia uporiadochivaiushchikhsia splavov [Theory of ordering alloys]*. Moscow: Fizmatlit Publishers [in Russian].
4. Smirnov A.A. (1966). *Molekuliarno-kineticheskaia teoriia metallov [Molecular-kinetic theory of metals]*. Moscow: Nauka [in Russian].
5. Anatychuk L.I., Manik O.N. (1994). A combined approach for thermoelectric material parameters calculation. 1 Methods of simulation in physics-chemical systems. *J. Thermoelectricity*, 1, 56-62.
6. Bugaiev V.A., Tatarenko V.A. (1989). *Vzaimodeistviie i raspredeleniie atomov v splavakh vnedreniia na osvove plotnoupakovannykh metallov [Interaction and distribution of atoms in the interstitial alloys based on closely packed metals]*. Kyiv: Naukova dumka [in Russian].
7. Gorsky V.S. (1928). *Zs. Phys*., 50, 64.
8. Bragg W.L., Williams E.S. (1935). *Proc. Roy. Soc. A*., 151, 540.
9. Golosov I.S., Pudan L.Ya., Golosova G.S., Popov L.E. (1972). Vlianiie sootnosheniia energii vzaimodeistviia v granetsentrirovannykh kubicheskikh nverdykh rastvorakh [The effect of the ratio of the interaction ratio in FCC solid solutions]. *Physics of the Solid State*, 14(5), 1494 - 1502.
10. Manik O.M. (1999). *Bahatofaktornyi pidhid v teoretychnomu materialoznavstvi [Multi-factor approach in theoretical materials research]*. Chernivtsi: Prut [in Ukrainian].
11. Almin K. E. The crystal structure of *CdSb* and *ZnSb* (1948). *Acta Chem. Scand*., 2, 400-407.
12. Manik O.N., Manik T.O., Bilinsky-Slotylo V.R. (2016). Peculiarities of electronic structure of hybrid orbitals and interatomic interaction in cadmium antimonide crystals. *J. Thermoelectricity*, 5, 57-64.
13. Belotskii D.P., Manik O.N. (1996). On the relationship between thermoelectric materials melts properties and structures and the state diagrams. 1. Regularities of cleavage manifestation in the state diagrams. *J. Thermoelectricity*, 1, 21-47.
14. Belotskii D.P., Manik O.N. (1996). On the relation of electronic properties and structure of melts to the diagrams of state in thermoelectric materials. 2. Phase changes and electronic properties of melts. *J.Thermoelectricity*, 2, 23-57.
15. Kirii V.G., Kirii A.V., Nikishchina I.V., Marenkin S.F. (1997). Sintez metastabilnogo soiedineniia Cd_4Sb_3 [Synthesis of metastable compound Cd_4Sb_3] *Neorganicheskiie materialy – Inorganic Materials*, 33(7), 781-783 [in Russian].
16. Psarev V.I. (1997). Termicheskaia peregruppirovka atomov v rasplavakh *Cd-Sb* [Technical rearrangement of atoms in *Cd-Sb* melts]. *Zhurnal fizicheskoi khimii- Journal of Physical Chemistry*, 21(6), 1022-1059 [in Russian].

Submitted 17.08.2018

Маник О.М., *канд. фіз.-мат. наук*[1,2]
Маник Т.О., *канд. фіз.-мат. наук*[1,2]
Білинський-Слотило В.Р., *канд. фіз.-мат. наук*[1,2]

[1]Інститут термоелектрики НАН і МОН України,
вул. Науки, 1, Чернівці, 58029, Україна,
e-mail: anatych@gmail.com;
[2]Чернівецький національний університет
імені Юрія Федьковича, вул. Коцюбинського 2,
Чернівці, 58012, Україна

ТЕОРЕТИЧНІ МОДЕЛІ УПОРЯДКОВУВАНИХ СПЛАВОВ АНТИМОНІДІВ КАДМІЮ

Розроблено комплексний підхід для розрахунків конфігураційної енергії упорядковуваних сплавів антимонідів кадмію. На основі термодинамічного та статистичного підходів з позицій хімічного зв'язку проведено розрахунки залежності вільної енергії від ступеня далекого порядку з урахуванням молекулярних структур розплавів антимонидів кадмію. Отримані результати можуть бути використані при розробці технологічних режимів отримання нових матеріалів на основі антимоніді кадмію, що володіють високою чутливістю, стабільністю і ідентичністю характеристик, особливо необхідних для термоперетворювачів метрологічного призначення. Бібл. 16, рис. 3.

Ключові слова: теорія упорядковуваних сплавів, хімічний зв'язок, молекулярні моделі, фазові переходи, поліморфні перетворення, конфігураційна енергія упорядковуваних сплавів, діаграми станів.

Маник О. Н., *канд. физ.-мат. наук,* [1,2]
Маник Т. О., *канд. физ.-мат. наук,* [1,2]
Билинский-Слотыло В. Р., *канд. физ.-мат. наук*[1,2]

[1]Институт термоэлектричества НАН и МОН Украины, ул. Науки, 1,
Черновцы, 58029, Украина; *e-mail: anatych@gmail.com*
[2]Черновицкий национальный университет имени Юрия Федьковича,
ул. Коцюбинского, 2, Черновцы, 58012, Украина

ТЕОРЕТИЧЕСКИЕ МОДЕЛИ УПОРЯДОЧИВАЮЩИХСЯ СПЛАВОВ АНТИМОНИДОВ КАДМИЯ

Разработан комплексный подход для расчетов конфигурационной энергии упорядочивающихся сплавов антимонидов кадмия. На основе термодинамического и сиатистического подходов с позиций химической связи проведены расчеты зависимости свободной энергии от степени дального порядка с учетом молекулярных структур расплавов антимонидов кадмия. Полученные результаты могут быть использованы при разработке технологических режимов получения новых материалов на основе антимонидив кадмия, обладающих высокой чуствительностью, стабильностью и

идентичностью характеристик, особенно необходимых для термопреобразователей метрологического назначения. Библ. 16, рис. 3.

Ключевые слова: теория упорядочивающихся сплавов, химическая связь, молекулярные модели, фазовые переходи, полиморфные превращения, конфигурационная энергия упорядочивающихся сплавов, диаграммы состояний.

References

1. Anatychuk L.I. (1979). *Termoelementy i termoelektricheskiie ustroistva [Thermoelements and thermoelectric devices]*. Kyiv: Naukova dumka [in Russian].
2. Lazarev V.B., Shevchenko V.Ya., Grinberg Ya.Kh., Sobolev V.V. (1978). *Poluprovodnikovyie soiedineniia gruppy $A^{II}B^{V}$ [Semiconductor compounds of $A^{II}B^{V}$ group]*. Moscow: Nauka [in Russian].
3. Krivoglaz M.A., Smirnov A.A. (1958). *Teoriia uporiadochivaiushchikhsia splavov [Theory of ordering alloys]*. Moscow: Fizmatlit Publishers [in Russian].
4. Smirnov A.A. (1966). *Molekuliarno-kineticheskaia teoriia metallov [Molecular-kinetic theory of metals]*. Moscow: Nauka [in Russian].
5. Anatychuk L.I., Manik O.N. (1994). A combined approach for thermoelectric material parameters calculation. 1 Methods of simulation in physics-chemical systems. *J. Thermoelectricity*, 1, 56-62.
6. Bugaiev V.A., Tatarenko V.A. (1989). *Vzaimodeistviie i raspredeleniie atomov v splavakh vnedreniia na osvove plotnoupakovannykh metallov [Interaction and distribution of atoms in the interstitial alloys based on closely packed metals]*. Kyiv: Naukova dumka [in Russian].
7. Gorsky V.S. (1928). *Zs. Phys*., 50, 64.
8. Bragg W.L., Williams E.S. (1935). *Proc. Roy. Soc. A*., 151, 540.
9. Golosov I.S., Pudan L.Ya., Golosova G.S., Popov L.E. (1972). Vlianiie sootnosheniia energii vzaimodeistviia v granetsentrirovannykh kubicheskikh nverdykh rastvorakh [The effect of the ratio of the interaction ratio in FCC solid solutions]. *Physics of the Solid State*, 14(5), 1494 - 1502.
10. Manik O.M. (1999). *Bahatofaktornyi pidhid v teoretychnomu materialoznavstvi [Multi-factor approach in theoretical materials research]*. Chernivtsi: Prut [in Ukrainian].
11. Almin K. E. The crystal structure of *CdSb* and *ZnSb* (1948). *Acta Chem. Scand*., 2, 400-407.
12. Manik O.N., Manik T.O., Bilinsky-Slotylo V.R. (2016). Peculiarities of electronic structure of hybrid orbitals and interatomic interaction in cadmium antimonide crystals. *J. Thermoelectricity*, 5, 57-64.
13. Belotskii D.P., Manik O.N. (1996). On the relationship between thermoelectric materials melts properties and structures and the state diagrams. 1. Regularities of cleavage manifestation in the state diagrams. *J. Thermoelectricity*, 1, 21-47.
14. Belotskii D.P., Manik O.N. (1996). On the relation of electronic properties and structure of melts to the diagrams of state in thermoelectric materials. 2. Phase changes and electronic properties of melts. *J.Thermoelectricity*, 2, 23-57.
15. Kirii V.G., Kirii A.V., Nikishchina I.V., Marenkin S.F. (1997). Sintez metastabilnogo soiedineniia Cd_4Sb_3 [Synthesis of metastable compound Cd_4Sb_3] *Neorganicheskiie materialy – Inorganic Materials*, 33(7), 781-783 [in Russian].
16. Psarev V.I. (1997). Termicheskaia peregruppirovka atomov v rasplavakh *Cd-Sb* [Technical rearrangement of atoms in *Cd-Sb* melts]. *Zhurnal fizicheskoi khimii- Journal of Physical Chemistry*, 21(6), 1022-1059 [in Russian].

Submitted 17.08.2018

V.A.Romaka[1], *doc technic sciences, professor*
L.P. Romaka[2], *cand. chemical of science*
Yu.V. Stadnyk[2], *cand. chemical of science*
V.V.Romaka[1,3], *doc technic sciences, cand. chemical of science, assistant professor*
A.M. Horyn[2], *cand. chemical of science,* **I.M. Romaniv**[2]

[1]National University "Lvivska Politechnika", 12, S. Bandera Str., Lviv, 79013, Ukraine;
e-mail: vromaka@polynet.lviv.ua
[2]Ivan Franko National University of Lviv, 6, Kyryla and Mefodiya Str., Lviv, 79005, Ukraine;
e-mail: lyubov.romaka@lnu.edu.ua,
[3]Institute for Solid State Research, IFW-Dresden, Helmholtzstr. 20, 01069 Dresden, Germany.

RESEARCH ON THE $Zr_{1-x}V_xNiSn$ THERMOELECTRIC MATERIAL

The crystalline and electronic structures, kinetic and energy characteristics of $Zr_{1-x}V_xNiSn$ thermoelectric material were investigated in the ranges: T=80–400 K, x=0.01–0.10. The mechanism of simultaneous generation of structural defects of the acceptor and donor nature, which determine the electric conductivity of material, was established. It was shown that energetically expedient is simultaneous occupation of the 4c position of Ni ($3d^8 4s^2$) atoms by V ($3d^3 4s^2$) atoms, which generates structural defects of the acceptor nature and the impurity acceptor band ε^1_A as well as the 4a position of Zr ($4d^2 5s^2$) atoms, which generates structural defects of the donor nature and the impurity donor band. ε^2_D. Bibl. 12, Fig. 8.

Keywords: electronic structure, electrical resistivity, Seebeck coefficient.

Introduction

It is known that semiconductor solid solutions based on half-Heusler phases *ZrNiSn*, *TiNiSn*, *HfNiSn* possess high efficiency of thermal into electrical energy conversion, stable characteristics in a wide temperature range, and the values of thermoelectric figure of merit (*ZT*) corresponding to the best figures of tellurides, clathrates and skutterudites [1,2]. At the same time, parameter optimization of thermoelectric materials based on the above compounds in order to obtain maximum values of thermoelectric figure of merit depends on a number of factors, such as current carrier concentration, scattering mechanisms, thermal conductivity, choice of crystallographic orientation, etc. [3]. One of the ways to increase the *ZT* values of said semiconductor materials is the appropriate doping with donor and/or acceptor impurities [1,3], and materials themselves become heavily doped and strongly compensated semiconductors [4]. Therefore, understanding the mechanisms of electrical conductivity of semiconductor solid solutions based on half-Heusler phases is a guarantee of successful choice of the type and concentration of doping impurity when optimizing the characteristics of material.

Experimental investigations of *ZrNiSn* phase and solid solutions on its basis have shown that it possesses semiconductor properties, and electrons are the majority carriers. Now there are two views about the nature of donors ("a priori doping") and electrical conductivity mechanisms in *ZrNiSn*. Understanding

the nature and origin of donors in *ZrNiSn* is extremely important, since such knowledge will enable one to develop a strategy for optimizing the characteristics by selecting the type and concentration of impurities. In fact, in [6] it was shown that in thermoelectric materials based on half-Heusler phases the prerequisite for achieving maximum efficiency of thermal into electrical energy conversion is doping of material with the type of impurity which coincides with the type of majority carriers of base semiconductor array.

In due time, the authors of [6] associated the nature of electron conductivity type ("a priori doping") of *ZrNiSn* with the disorder of crystalline structure of compound (structural type *MgAgAs*, space group $F\bar{4}3m$ [7]), the essence of which lies in partial, up to ~1%, occupation by *Ni* ($3d^8 4s^2$) atoms of the 4*a* position of *Zr* ($4d^2 5s^2$) atoms, which generates structural defects of the donor nature (*Ni* has six *d*-electrons more than *Zr*).

Noteworthy is a different view on the origin of donors in *ZrNiSn*. The analysis of the crystalline structure of the *ZrNiSn* compound showed that the absence of a centre of symmetry is caused by covalent bonds between atoms. This generates semiconducting properties, and also forms a volume in the unit cell which makes ~24% of the total, unoccupied by atoms (tetrahedral voids) (Fig. 1*a*). In [8], the effect of accumulation of *Ni* atoms in these voids, including the excess Ni_{1+x} atoms, to concentrations $x \leq 0.30$, which give rise to structural defects of the donor nature, was discovered. The accumulation of the smallest-size atoms (*Ni*) in the tetrahedral voids of the structure of *ZrNiSn* compound also consistently explains the nature of its "a priori doping" with donors. By the way, if all the four tetrahedral voids are occupied by *Ni* atoms, then a related compound $ZrNi_2Sn$ (*Heusler phase*, space group $Fm\bar{3}m$) [7]) is formed. That is, the tetrahedral void in the structure of *ZrNiSn* compound can be regarded as a vacancy (Vac) at the 4*d* position of Ni atoms in the structure of $ZrNi_2Sn$ compound.

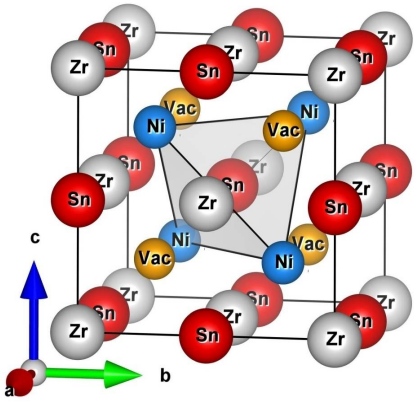

a)

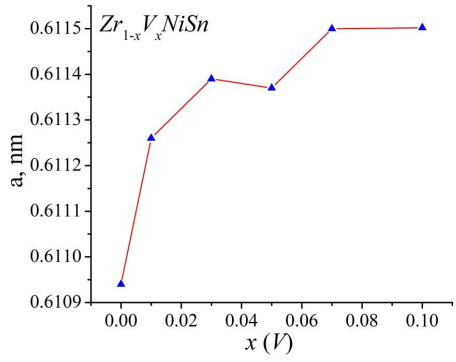

b)

Fig. 1. Crystalline structure of ZrNiSn compound(a) and change in the values of unit cell period a(x) *of* $Zr_{1-x}V_xNiSn$ *(b)*

The proposed work studies a new thermoelectric material $Zr_{1-x}V_xNiSn$ obtained by substitution in the *ZrNiSn* compound at the 4*a* position of *Zr* atoms by *V* ($3d^3 4s^2$) atoms, which must generate structural defects of the donor nature (*V* has more *d*-electrons than *Zr*). Such doping will correspond to conditions [5] related to achievement in semiconductor material of maximum efficiency of thermal into electrical energy conversion. The research pursued will also show that when analyzing the characteristics of thermoelectric materials based on half-Heusler phases one should simultaneously take into account different mechanisms of donor generation ("a priori doping"). In other words, in such compounds there simultaneously exist at least two methods of generation of structural defects of the donor nature, and their opposition or neglect in the analysis contradicts the numerous results of the experimental investigations [1, 8].

Investigation procedures

The crystalline structure, the distribution of the electronic density of states (DOS), the kinetic and energy characteristics of $Zr_{1-x}V_xNiSn$ were studied. The samples of $Zr_{1-x}V_xNiSn$ solid solution were synthesized by melting the charge of initial components in electric arc furnace in the inert argon atmosphere with subsequent homogenizing annealing for 720 hours at a temperature of 1073 K. The method of X-ray structural analysis (powder method) was used to obtain data arrays (diffractometer Guinier-Huber image plate system, $CuK\alpha_1$ radiation), and the structural characteristics were calculated by means of Fullprof program [9]. The chemical and phase compositions of samples were controlled by microprobe analyzer (EPMA, energy-dispersive *X*-ray analyzer). The simulation of the electronic structure of $Zr_{1-x}V_xNiSn$ was performed by the method of Green functions (the Korringa-Kohn-Rostoker method (KKR)) in coherent potential approximation (CPA) and local density approximation (LDA) [10]. For calculations by KKR method the licensed software AkaiKKR and SPR-KKR were used in LDA approximation for exchange-correlation potential with Moruzzi-Janak-Williams (MJW) parametrization [11]. The Brillouin zone was divided into 1000 *k*-points that were used for simulation of energy characteristics by calculation of DOS. The width of the energy window was 22 eV and selected so as to cover all semi-core states of *p*-elements.

In the calculations by method of linear MT orbital (Linear Muffin-Tin Orbital, LMTO) use was made of full potential (FP) in the representation of plane waves. The LDA approximation with MJW parametrization was also used as an exchange-correlation potential. The accuracy of calculation of the Fermi level position is ε_F ±6 meV. The temperature and concentration dependences of resistivity (ρ) and the Seebeck coefficient (α) with respect to copper of $Zr_{1-x}V_xNiSn$ are in the ranges: T=80–400 K, $N_D^V \approx 1.9\cdot10^{20}$ cm^{-3}–$1.9\cdot10^{21}\cdot$cm^{-3} (x=0.01–0.10).

Research on the crystalline and electronic structures of $Zr_{1-x}V_xNiSn$

The microprobe analysis of atomic concentration on the surface of $Zr_{1-x}V_xNiSn$ samples found that they correspond to the initial composition of the charge, and X-ray phase and structural analyzes showed that the diffractograms of the samples did not contain foreign phases. It was expected that the substitution of *Zr* atoms (r_{Zr}=0.160 nm) by smaller-size *V* atoms (r_V=0.134 nm) would reduce the values of unit cell period a(x) of $Zr_{1-x}V_xNiSn$. In this case, at the 4*a* crystallographic position of *Zr* atoms, structural defects of the donor nature will be generated, and an impurity donor zone ε_D^2 will be formed in the bandgap close to the conduction band ε_C.

However, the results of structural studies did not confirm the expectation of changing a(x) values of $Zr_{1-x}V_xNiSn$. As can be seen from Fig. 1*b*, in the concentration range x=0–0.07 the growth of the

dependence a(x) is observed. It is clear that the experimentally established behavior of the unit cell period a(x) of $Zr_{1-x}V_xNiSn$ reflects more complex processes in the structure of the solid solution than just substituting at the 4*a* position of *Zr* atoms by *V* atoms. Using the method of X-ray analysis, we failed to unambiguously establish the nature of such structural changes in $Zr_{1-x}V_xNiSn$, since the concentration of the impurity lies beyond the accuracy of the X-ray method.

At this stage of research we can only assume possible variants of unpredictable structural changes in $Zr_{1-x}V_xNiSn$. If we take into account that the atomic radius of *Sn* (r_{Sn}=0.162 nm) is greater than that of *V*, then we omit the option of a possible substitution at the *4b* position of *Sn* atoms by *V*. At the same time, the atomic radius of *Ni* (r_{Ni}=0.124 nm) is the smallest, and possible partial occupation by *V* atoms of the *4c* crystallographic position of *Ni* atoms can lead to an increase in the values of the unit cell period a(x) of $Zr_{1-x}V_xNiSn$, which is consistent with the results of structural investigations (Fig. 1*b*). In this case, in $Zr_{1-x}V_xNiSn$ thermoelectric material simultaneously with the structural defects of the donor nature (*V* atoms at the 4*a* position of *Zr* atoms) there will be generated structural defects of the acceptor nature (*V* has less *3d* electrons than *Ni* ($3d^8 4s^2$) and in the bandgap near the valence band ε_V an impurity acceptor zone ε_A^1 will be formed.

Thus, the structural investigations of $Zr_{1-x}V_xNiSn$ have not allowed us to consistently explain the changes in the spatial arrangement of atoms, which will lead to unpredictable changes in the electronic structure and kinetic properties of the thermoelectric material.

Research on the electronic structure of $Zr_{1-x}V_xNiSn$

To predict the behavior of the Fermi level ε_F, the bandgap width ε_g and the kinetic characteristics of $Zr_{1-x}V_xNiSn$, the distribution of the electronic density of states (DOS) (Fig. 2) was calculated for the ordered variant of a structure in which *Zr* atoms are substituted by *V* at the *4a* position.

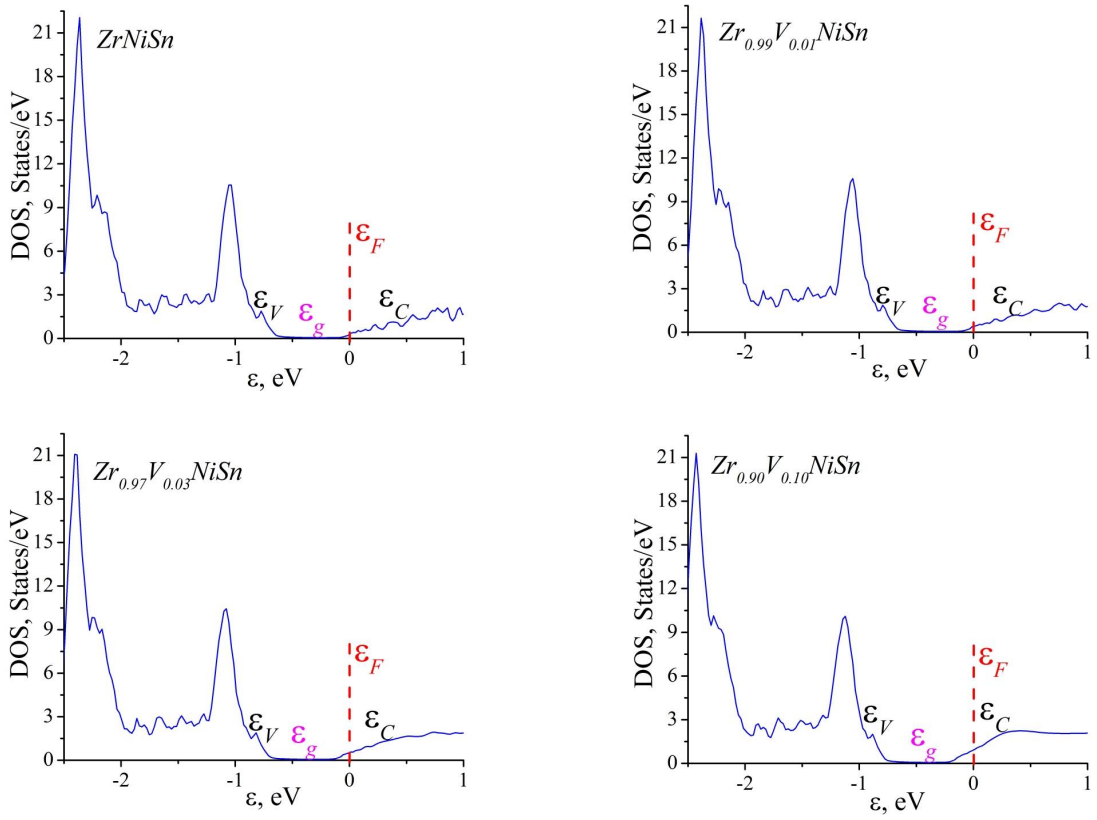

Fig. 2. Distribution of the electronic density of states DOS of $Zr_{1-x}V_xNiSn$ for the ordered structure

As is seen from Fig. 2, in the half-Heusler phase of *ZrNiSn* the Fermi level ε_F is located in the donor zone ε_D^1 close to percolation level of the conduction band ε_C, formed as a result of "a priori doping". We will not identify the nature of such doping so far. As long as the substitution of *Zr* atoms by *V* generates structural defects of the donor nature, already at the lowest concentrations of *V* in $Zr_{1-x}V_xNiSn$ and impurity donor band ε_D^2 will be formed. This will result in the growth of donor concentration, and the Fermi level ε_F will approach the percolation level of the conduction band ε_C, which will increase the density of states at the Fermi level $g(\varepsilon_F)$. The intersection of the Fermi level ε_F of the conduction band changes the conductivity from the activation to the metallic [4]: on the dependences ln (ρ (*1 / T*)) the activation regions disappear, and the values of resistance ρ will rise with temperature. At the same time, the change in the values of $g(\varepsilon_F)$ occurs much slower.

The calculation of the distribution of the electronic density of states DOS for the ordered structure $Zr_{1-x}V_xNiSn$ allows simulating the behavior of electrical resistivity, the Seebeck coefficient $\alpha(x,T)$, the thermoelectric power *Z**, etc. Fig. 2*a* shows a dependence inverse to the density of states at the Fermi level $g(\varepsilon_F)$, the values of which are proportional to the electrical resistivity of $Zr_{1-x}V_xNiSn$ thermoelectric material. We can see that with increasing concentration of donor impurity *V,* the conductivity of $Zr_{1-x}V_xNiSn$ grows. If we take into account that simulation of the Seebeck coefficient $\alpha(x,T)$ $Zr_{1-x}V_xNiSn$ (Fig. 4*a*) shows a drastic reduction of values with increasing concentration of donor impurity. The results of kinetic and energy studies of $Zr_{1-x}V_xNiSn$ will show the correspondence of these calculations to real processes in thermoelectric material.

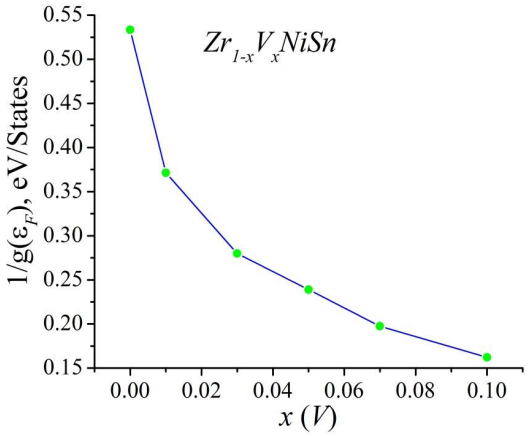

a)

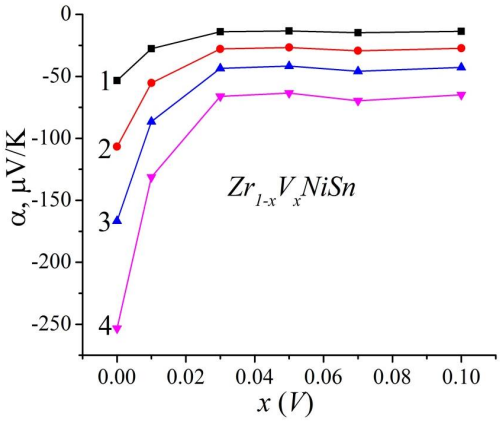

b)

Fig. 3. Simulation of a change in the values of $1/g(\varepsilon_F)$ (a) and the Seebeck coefficient $\alpha(x,T)$ at temperatures: 1 – 80 K; 2 – 160 K; 3 – 250 K; 4 – 380 K (b) for the ordered variant of $Zr_{1-x}V_xNiSn$ structure.

Research on the electrokinetic and energy characteristics of $Zr_{1-x}V_xNiSn$

The temperature and concentration dependences of the electrical resistivity ρ and the Seebeck coefficient α of $Zr_{1-x}V_xNiSn$ are given in Fig. 4, 5. Dependences ln(ρ(1/*T*)) (Fig. 4) and α (1/*T*) of $Zr_{1-x}V_xNiSn$ (Fig. 5*a*) are typical for heavily doped and strongly compensated semiconductors, and the available activation areas point to several charge carrier mechanisms.

Dependences ln(ρ(1/*T*)) of $Zr_{1-x}V_xNiSn$ are described by known relationship [4]:

$$\rho^{-1}(T) = \rho_1^{-1} \exp\left(-\frac{\varepsilon_1^{\rho}}{k_B T}\right) + \rho_3^{-1}\left(-\frac{\varepsilon_3^{\rho}}{k_B T}\right), \quad (1)$$

where the first term at high temperatures describes activation of current carriers ε_1^{ρ} from the Fermi level ε_F to percolation levels of continuous energy zones, and the second, low-temperature, – hopping conductivity ε_3^{ρ}. In turn, the temperature dependences of the Seebeck coefficient α(1/*T*) of $Zr_{1-x}V_xNiSn$ are described by the dependence [12]:

$$\alpha = \frac{k_B}{e}\left(\frac{\varepsilon_i^{\alpha}}{k_B T} - \gamma + 1\right), \quad (2)$$

where γ is a parameter that depends on scattering mechanisms. From the high-temperature areas of dependences α(1/*T*) the activation energies ε_1^{α} were calculated that are proportional to the amplitude of high-scale fluctuation of continuous energy zones, and from the low-temperature areas – the values of activation energies ε_3^{α} that are proportional to the modulation amplitude of small-scale fluctuation of heavily doped strongly compensated semiconductors [1,4]. For *ZrNiSn* at high temperatures the electron activation energy from the Fermi level ε_F was calculated to percolation level of the conduction band ε_1^{ρ}=97.6 meV, and at low temperatures – the activation energy of hopping conductivity ε_3^{ρ}=11.9 meV. From the high-temperature and low-temperature areas of dependence α(1/*T*) calculated were the values of activation energy ε_1^{α}=83.8 meV and ε_3^{α}=11.5 meV, respectively.

The doping of half-Heusler phase *ZrNiSn* with *V* atoms leads to a change in the behavior of the temperature and concentration dependences of resistivity ρ(*x*,*T*) and the Seebeck coefficient α(*x*,*T*) (Fig. 4,5). From the results of the DOS calculations we predicted that the substitution of *Zr* atoms by *V* will generate in $Zr_{1-x}V_xNiSn$ structural defects of the donor nature, which will be matched by the negative values of the Seebeck coefficient α(*x*,*T*). Indeed, as can be seen from Fig. 5, the values of the Seebeck coefficient α(*x*) of $Zr_{1-x}V_xNiSn$ for all concentrations and temperatures remain negative. Moreover, the generation of donors will increase the concentration of free electrons, which will cause a decrease in the values of resistivity ρ(*x,T*). It is precisely this behavior of ρ(*x,T*) that can be observed in Fig. 5, 6*a*.

Absolutely unexpected was preservation of high-temperature activation areas on the dependences ln(ρ(1/*T*)) for all investigated samples of $Zr_{1-x}V_xNiSn$ (Fig. 4). The presence of high-temperature activation on the dependences ln(ρ(1/*T*)) indicates the location of the Fermi level ε_F in the bandgap of semiconductor material. In turn, the negative values of the Seebeck coefficient α(*x,T*) of $Zr_{1-x}V_xNiSn$ testify that the Fermi level ε_F lies in the bandgap close to the conduction band ε_C. The experimental result obtained does not coincide with the results of simulation of the energy characteristics of $Zr_{1-x}V_xNiSn$ for the ordered structure variant in which there is a substitution at the 4*a* position of *Zr* atoms by *V*, which generates structural defects of the donor nature. In fact, according to the calculations (Fig. 2) already at the concentrations of $Zr_{1-x}V_xNiSn$, $x \geq 0.01$, the Fermi level ε_F had to cross the percolation level of the conduction band and enter the zone of continuous energies which would lead to the metallization of conductivity.

Thus, the presence of high-temperature activation due to the location of the Fermi level ε_F in the bandgap of $Zr_{1-x}V_xNiSn$ at all concentrations of *V* indicates that in the semiconductor, in addition to the donors, there appear structural defects of the acceptor nature by an unknown mechanism. The acceptors

capture free electrons, reducing their concentration, and inhibit movement of the Fermi level ε_F to the conduction band. Since the samples of $Zr_{1-x}V_xNiSn$ undergo thermal injection of electrons from the Fermi level ε_F to the percolation level of the conduction band with activation energy $\varepsilon_1^{\rho}(x)$, then, having calculated from the high-temperature activation areas of dependences $\ln(\rho(1/T))$ (Fig. 4) the values of energy $\varepsilon_1^{\rho}(x)$, we can identify the nature of motion of the Fermi level ε_F in the bandgap

Fig. 6 shows a change in the values of activation energy $\varepsilon_1^{\rho}(x)$ of the $Zr_{1-x}V_xNiSn$ thermoelectric material. The introduction into half-Heusler phase *ZrNiSn* of the lowest in the experiment concentration of donor impurity *V* predictably changes the position of the Fermi level ε_F, bringing it closer to the percolation level of the conduction band by the distance $\varepsilon_1^{\rho}(x=0.01)=19.8$ meV. Recall that in the half-Heusler phase *ZrNiSn* the Fermi level ε_F is at the distance of 97.6 meV from the percolation level of the conduction band. In so doing, at the concentration area $x=0–0.01$ the velocity of the Fermi level ε_F motion to the conduction band is $\Delta\varepsilon_F/\Delta x \approx 77.8$ meV/% *V*.

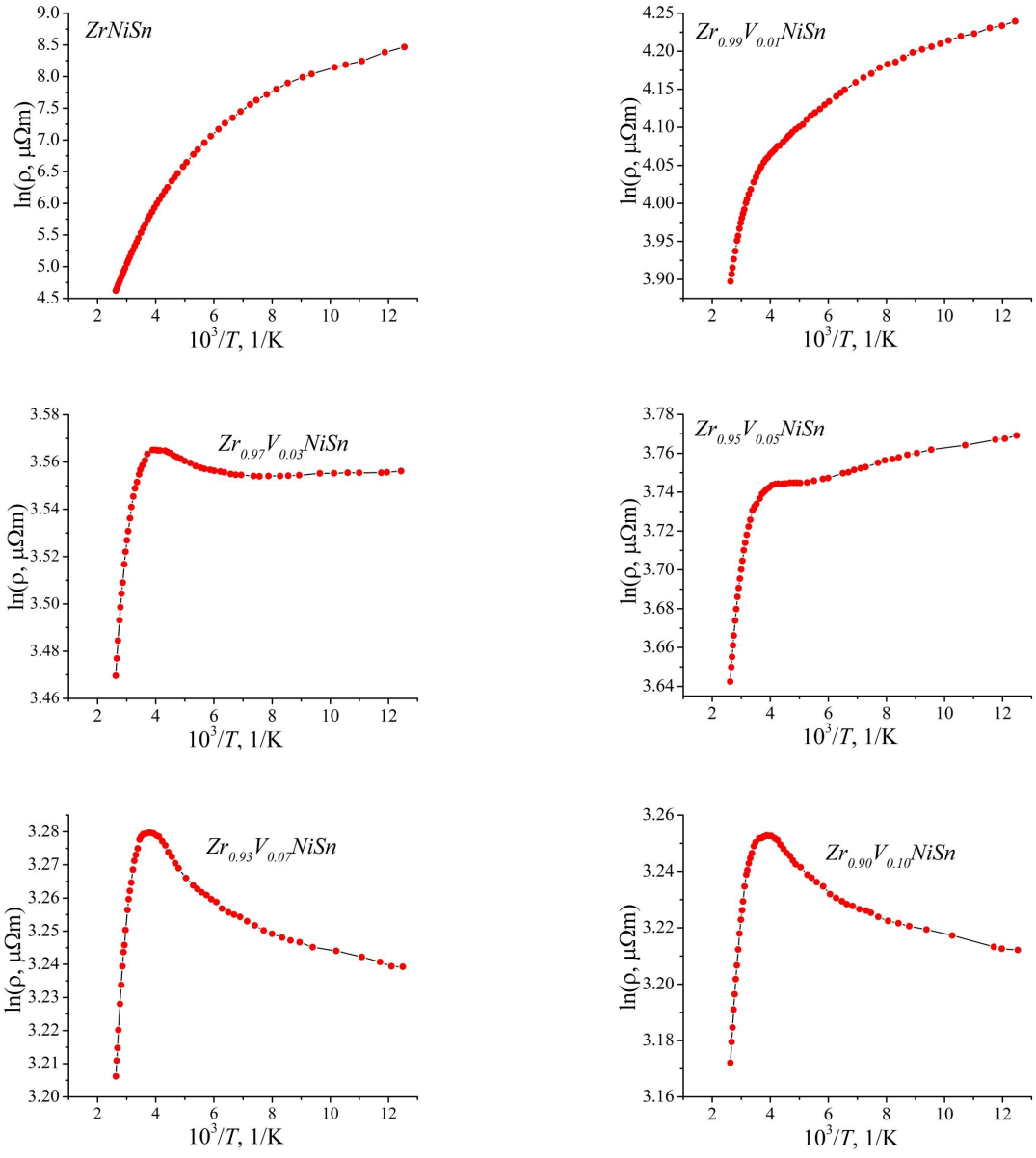

Fig. 4. Temperature dependences of resistivity ln(ρ(1/T)) in $Zr_{1-x}V_xNiSn$

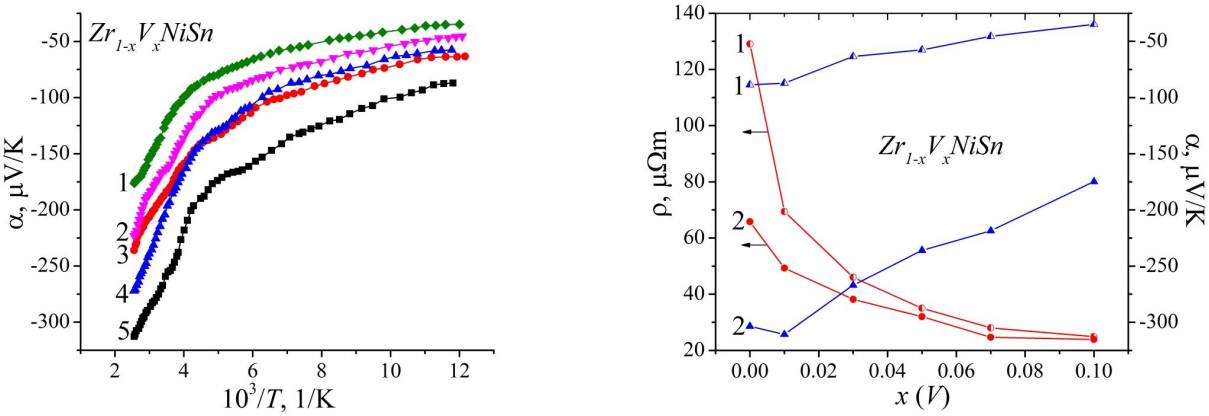

a) *b)*

Fig. 5. Temperature dependences of the Seebeck coefficient α(1/T): 1 – x=0.10, 2 – x=0.07, 3 – x=0.03, 4 – x=0.05, 5 – x=0.01 (a) and change in the values of resistivity ρ(x,T) and the Seebeck coefficient α(x,T) at different temperatures: 1 – 80 K, 2 –380 K (b) in $Zr_{1-x}V_xNiSn$

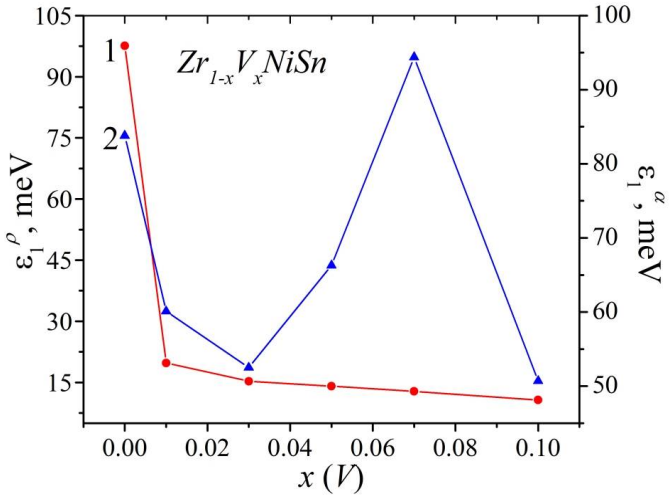

Fig. 6. Change in the values of activation energies $\varepsilon_1^{\rho}(x)$ (1) and ε_1^{α} (2) in $Zr_{1-x}V_xNiSn$

If the Fermi level ε_F even at higher concentrations of impurity *V* moved to the percolation level of the conduction band at the same velocity, then already at $x\approx0.015$ it would cross this level. However, at higher concentrations of the impurity *V* the velocity of the Fermi level ε_F rapidly decreased. Thus, at the concentration of impurity $Zr_{1-x}V_xNiSn$, x=0.03, the Fermi level ε_F approached the percolation level of the conduction band to the distance of $\varepsilon_1^{\rho}(x=0.03)$=15.3 meV. That is, at the concentration area x=0.01–0.03 the velocity of the Fermi level ε_F is $\Delta\varepsilon_F/\Delta x\approx2.2$ meV/% *V*, which is factor of ~35 less than at the concentration area x=0–0.01. At even higher concentrations of the donor impurity *V* the Fermi level ε_F will lie close to the percolation level of the conduction band at a distance of $\varepsilon_1^{\rho}(x=0.05)$=14.1 meV and $\varepsilon_1^{\rho}(x=0.10)$=10.7 meV. In this case, the velocity of the Fermi level ε_F at the area of x=0.03–0.10 becomes even lower and makes $\Delta\varepsilon_F/\Delta x\approx0.7$ meV/% *V*, which is two orders of magnitude smaller than at the area of x=0–0.01.

The number of *V* atoms introduced into the structure of half-Heusler phase ZrNiSn varied linearly. According to formal matter, if in $Zr_{1-x}V_xNiSn$ only the substitution at the 4*a* position of *Zr* atoms by *V*

atoms occurred, then only structural defects of the donor nature, whose concentration also grew by the linear law, would be generated. This would cause a linear change in the velocity of motion of the Fermi level ε_F to the valence band of $Zr_{1-x}V_xNiSn$. However, even at a considerable concentration of the donor impurity, $N_D^V \approx 1.9 \cdot 10^{21}$ cm^{-3} for $Zr_{1-x}V_xNiSn$, x=0.10, the Fermi level ε_F is still in the semiconductor bandgap.

The "inhibition" of the motion of the Fermi level ε_F in $Zr_{1-x}V_xNiSn$ can have the only reason – the generation, simultaneously with the donors, of the acceptors that capture free electrons, which changes the degree of compensation of semiconductor. To confirm this conclusion, from the activation areas of dependences $\alpha(1/T)$ (Fig. 5*a*) the values of activation energies ε_A^1 (Fig. 6) were calculated which represent the degree of compensation of $Zr_{1-x}V_xNiSn$ (the ratio between ionized donors and acceptors). From Fig. 6 we can see that for insignificant concentrations of impurity V the activation energy ε_1^α decreases from $\varepsilon_A^1(x=0)$=83.8 meV to $\varepsilon_A^1(x=0.01)$=60.1 meV and $\varepsilon_A^1(x=0.03)$=52.5 meV. Such a decrease in the activation energy ε_A^1 in a semiconductor of electron conductivity type indicates that donors are predominantly generated. Generation of acceptors is also possible, but the number of ionized donors is much in excess of the number of acceptors.

Even at higher concentrations of impurity V, x>0.03, there is an increase in the values of $\varepsilon_A^1(x)$ which achieve maximum for x=0.07. This behavior of $\varepsilon_A^1(x)$ definitely testifies that in semiconductor $Zr_{1-x}V_xNiSn$ acceptors are generated at a faster rate than donors. The experimental result obtained does not correspond to the conclusions drawn from the calculations of the distribution of the electronic density of states $Zr_{1-x}V_xNiSn$, provided that at the 4*a* position *Zr* atoms are substituted by *V*, which generates structural defects of the donor nature (Fig. 2). Obviously, in the $Zr_{1-x}V_xNiSn$ thermoelectric material there are unpredictable structural changes that affect the electronic structure and kinetic properties.The task is to identify these changes which will allow predicting the characteristics of $Zr_{1-x}V_xNiSn$.

Refinement of crystalline and electronic structures of $Zr_{1-x}V_xNiSn$

Thus, structural investigations of $Zr_{1-x}V_xNiSn$ using X-ray analysis did not reveal any deviations in the spatial arrangement of atoms, which made it possible to construct a model of an ordered structure of a semiconductor. However, the unpredicted behavior of the unit cell period a(x) of $Zr_{1-x}V_xNiSn$ (Fig. 1*b*) was just a signal that more complex structural changes occur in the structure of a semiconductor solid solution than simply substitution of *Zr* atoms at the 4*a* position with *V* atoms. A model of electronic structure $Zr_{1-x}V_xNiSn$, built on the results of structural studies for the ordered version of the crystalline structure, does not correspond to the results of kinetic characteristics, which is also a signal of more complex, than expected, structural changes in the semiconductor.

Any compound or, for example, semiconductor solid solutions based on half-Heusler phases, will only acquire the status of a *thermoelectric material* when their structural, energy, kinetic, etc. characteristics are clear and predictable. That is, when investigating a $Zr_{1-x}V_xNiSn$ semiconductor solid solution, we must identify the reasons for the unpredicted behavior of its characteristics.

It is known that to calculate the electron energy in the first Brillouin zone, it is necessary to know the spatial arrangement of atoms (or their absence - vacancies) in the nodes of the unit cell. On the other hand, the smallest structural changes affect the local symmetry and the distribution of the electronic density of states. Therefore, the adequacy of the calculation results of the distribution of the electronic density of states of semiconductor material and the results of experimental studies of the energy characteristics implies that the model of its crystalline structure is adequate to the spatial arrangement of atoms in a real

material. That is why the results of calculating the electronic structure in comparison with the results of, for example, kinetic and/or energy characteristics, make it possible to obtain information about the real crystalline structure, which is not available to X-ray methods of investigation [1].

Possessing the experimental results of the Fermi level ε_F drift velocity as the activation energy $\varepsilon_1^{\rho}(x)$ of $Zr_{1-x}V_xNiSn$, we searched for the degree of compensation (the ratio of structural defects of the acceptor and donor nature), which will set the velocity of the Fermi level ε_F as close as possible to $\varepsilon_1^{\rho}(x)$. The electronic structure of $Zr_{1-x}V_xNiSn$ was calculated for various variants of both the arrangement of atoms in the nodes of the unit cell and the degree of occupation of the crystallographic positions of all atoms by their own or foreign atoms. Based on the new results of the spatial arrangement of atoms in the $Zr_{1-x}V_xNiSn$ crystalline structure, the calculation of the distribution of the density of electronic states and, in particular, the density of states at the Fermi level $g(\varepsilon_F)$, was refined, as well as, for example, the Seebeck coefficient at different temperatures that are consistent with the results of experimental studies.

Fig. 7*a* shows the distribution of the electronic density of states for a disordered variant of the structure of a semiconductor solid solution $Zr_{1-x}V_xNiSn$. From Fig. 7a we can see that when *Zr* atoms are substituted by V, structural defects of the donor nature are generated, and a prolonged donor zone ε_D^2, which occupies a significant part of the band gap εg, is generated in the bandgap and is enlarged with increasing concentration of *V* atoms.

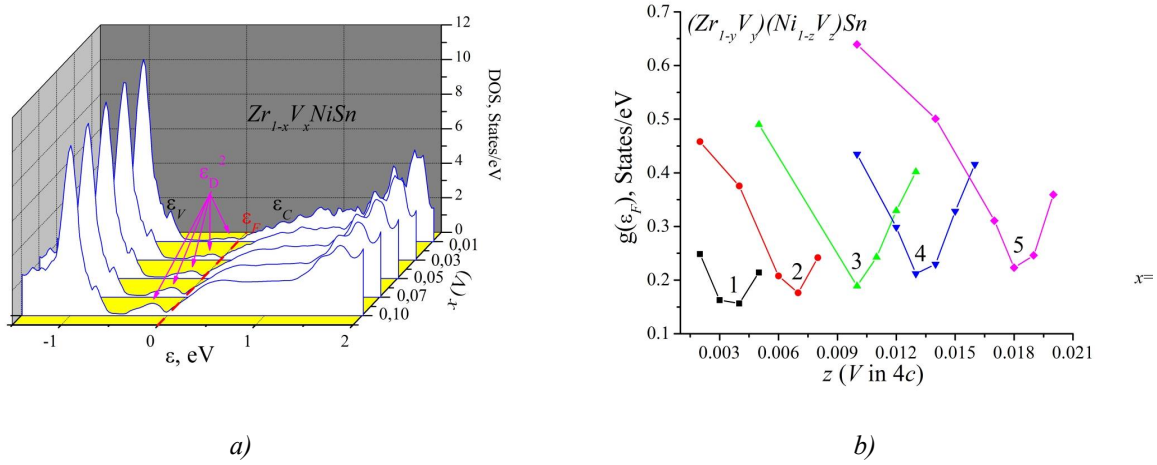

a) *b)*

Fig. 7. Calculation of DOS for the disordered structure (a) and change in the density of states values at the Fermi level $g(\varepsilon_F)$: 1 – x=0.01; 2 – x=0.03; 3 – x=0.05; 4 – x=0.07; 5 – x=0.10 (b) in $Zr_{1-x}V_xNiSn$

Let us take a closer look at the assumption made in the analysis of the structural characteristics of $Zr_{1-x}V_xNiSn$ concerning possible partial occupation by *V* atoms of the *4c* position of *Ni* atoms. After all, such a substitution, on the one hand, may increase the values of the unit cell period *a(x)* of $Zr_{1-x}V_xNiSn$, which is consistent with the results of structural investigations (Fig. 1*b*). On the other hand, at least partial occupation by *V (3d34s2)* atoms of the 4*c* position of *Ni* ($3d^8 4s^2$) atoms generates in the crystal structural defects of the acceptor nature, and in the bandgap an impurity acceptor band ε_A^1 is generated. This result is also consistent with the results of kinetic studies on $Zr_{1-x}V_xNiSn$.

Therefore, the distribution of the electronic density of states (Fig. 7b) was calculated for a case when the total concentration of *V(x)* atoms is distributed between two positions: 4*a* of *Zr(y)* atoms and 4*c* of *Ni (z)* atoms. In summation, *V(x)* atoms at the 4*a* position of *Zr (y)* atoms and the *4c* position of *Ni (z)* atoms are equal to the total concentration of vanadium impurity ($x=y+z$) in the samples $Zr_{1-x}V_xNiSn$: x=0.01, x=0.03, x=0.05, x=0.07 та x=0.10. In this case, the formula of the semiconductor solid solution is

transformed into $(Zr_{1-y}V_y)(Ni_{1-z}V_z)Sn$. In other words, by increasing the content of *V* atoms at the 4c position of *Ni* atoms, simultaneously, by the same amount, we reduce the concentration of *V* at the *4a* position of *Zr* atoms and vice versa. At the same time, by increasing the concentration of acceptors in $Zr_{1-x}V_xNiSn$, simultaneously we reduce the concentration of generated donors by the same amount. That is, the ratio of structural defects of the acceptor and donor nature (degree of compensation) provides the location of the Fermi level ε_F in the bandgap.

Fig. 7*b* shows a change in the density of states at the Fermi level $g(\varepsilon_F)$ $(Zr_{1-y}V_y)(Ni_{1-z}V_z)Sn$ depending on the concentration of *V* atoms at the 4*c* position of *Ni* atoms (*z*). For instance, for the sample $Zr_{1-x}V_xNiSn$, x=0.01, the density of states at the Fermi level $g(\varepsilon_F)$ passes through the minimum at a concentration of V at the 4*c* position of *Ni* atoms $Z\approx0.004$ (Fig. 7*b*, curve 1), and for the sample $Zr_{1-x}V_xNiSn$, x=0.10, the Fermi dependence $g(\varepsilon_F)$ passes through the minimum at the concentration of *V* at the 4*c* position $Z\approx0.018$ (Fig. 7*b*, curve 5).

Simultaneous generation of donors and acceptors in different ratios will change the degree of compensation of $Zr_{1-x}V_xNiSn$, which will change the position of the Fermi level ε_F, as well as the value of the density of states at the Fermi level $g(\varepsilon_F)$. The values of $g(\varepsilon_F)$ will be the smallest if the generated acceptors (*V* at the 4*c* position) change the degree of compensation in such a way that the Fermi level ε_F is located in the bandgap between the percolation level of conduction band and the energy states of the donor zone ε_D^2 (Fig. 7b). It is clear that the higher the total concentration of *V* atoms in $Zr_{1-x}V_xNiSn$, the lower the dependence on the density of states at the Fermi level $g(\varepsilon_F)$will occur at higher concentrations of acceptors (*V* at the 4*c* position). Fig. 8 shows the results of simulation of the distribution of the electronic density of states of the disordered structure $(Zr_{1-y}V_y)(Ni_{1-z}V_z)Sn$ for concentrations of *V* atoms at the 4*c* position of *Ni* atoms, where the minimum density of states appears at the Fermi level $g(\varepsilon_F)$, shown in Fig. 7*b*

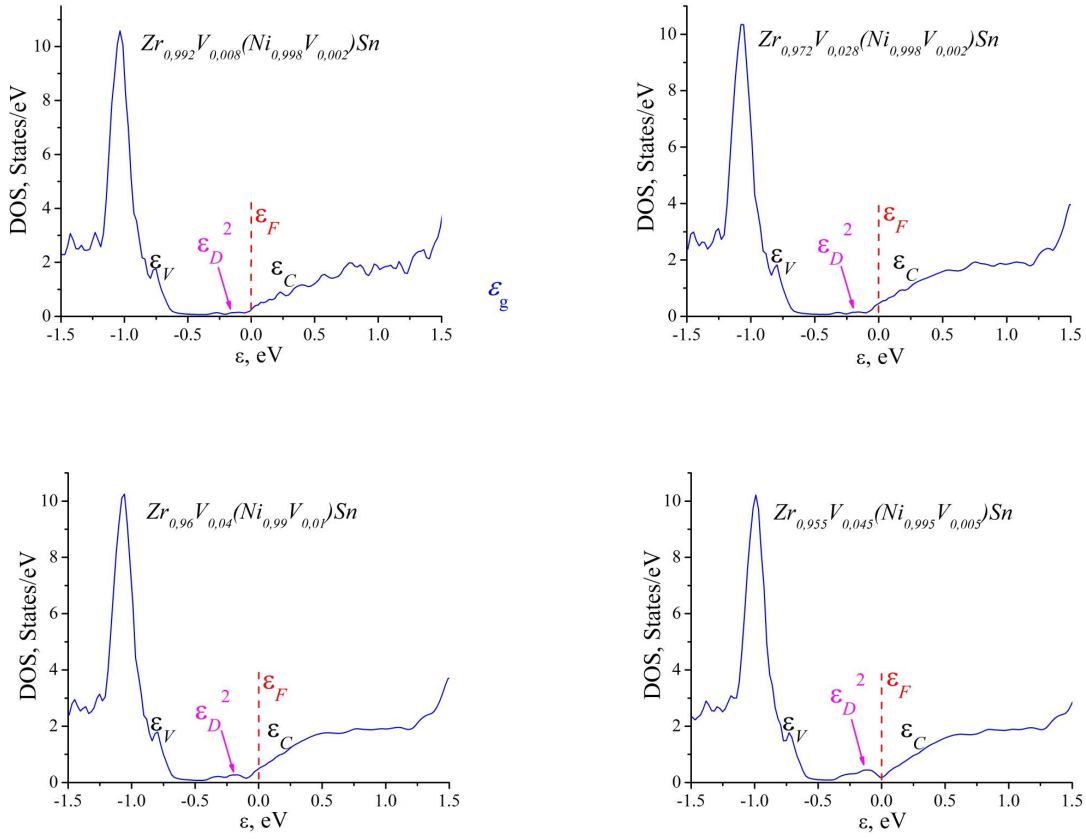

Fig. 8. Calculation of DOS for the disordered structure $(Zr_{1-y}V_y)(Ni_{1-z}V_z)Sn$ for the concentration of atoms V in position 4c of Ni atoms, where there appears density of states minimum at the Fermi level $g(\varepsilon_F)$

Conclusions

Thus, as a result of the complex study of crystalline and electronic structures, kinetic and energy characteristics of $Zr_{1-x}V_xNiSn$ thermoelectric material, the mechanism of simultaneous generation of structural defects of the acceptor and donor nature is established. It is shown that energetically expedient is simultaneous occupation of the 4*c* position of *Ni* $(3d^8 4s^2)$ atoms by *V* $(3d^3 4s^2)$ atoms, which generates the structural defects of the acceptor nature (in *V* there are less 3*d*-electrons than in *Ni*), and also the 4*a* position of *Zr* $(4d^2 5s^2)$ atoms, generating structural defects of the donor nature (in V there are more *d*-electrons than Zr). In the bandgap of the semiconductor solid solution $Zr_{1-x}V_xNiSn$ simultaneously in different ratios there appear energy states of the donor ε_D^2 and acceptor ε_A^1 zones (donor-acceptor pairs), which determine its mechanisms of electrical conductivity.

The work was performed in the framework of Ministry of Education and Science of Ukraine grant № 0118U003609.

References

1. Romaka V.A., Romaka V.V., Stadnyk Yu.V. (2011). *Intermetallic semiconductors: properties and applications.* Lviv: Lvivska Polytechnika.
2. Romaka V.V., Rogl P.-F., Carlini R., Fanciulli C. (2017). Prediction of the thermoelectric properties of Half-Heusler phases from the density functional theory. In *Alloys and Intermetallic Compounds. (*Artini C., Ed.) London-NY: Taylor & Francis Group.
3. Anatychuk L.I. (1979). *Termoelementy i termoelektricheskiie ustroistva. Spravochnik*
1. *[Thermoelements and thermoelectric devices. Handbook]*. Kyiv: Naukova Dumka [in Russian].
4. Shklovsky B.I., Efros A.L. (1979). *Electronic properties of doped semiconductors.* Moscow: Nauka [in Russian].
5. Romaka V.A., Frushart D., Stadnyk Yu.V., Tobola J., Gorelenko Yu.K., Shelyapina M.G., Romaka L.P., Chekurin V.F. (2006). A condition of maximum power characteristic to intermetallic semiconductors of the *MgAgAs* structure type. *Semiconductors*, 40 (11), 1289–1395.
6. Romaka V.A., Hlil E.K., Ya.V. Skolozdra, Rogl P., Stadnyk Yu.V., Romaka L.P., Goryn A.M.(2009). Features of the mechanisms of generation and "healing" of structural defects in the heavily doped intermetallic semiconductor *n-ZrNiSn. Semiconductors*, 43(9), 1115–1123.
7. Romaka V.V., Romaka L.P., Krayovskyy V.Ya., Stadnyk Yu.V. (2015). *Stanidy ridkisnozemelnykh ta perekhidnykh metaliv [Stannides of rare earth and transition metals]*. Lviv: Lvivska Polytechnika [in Ukrainian].
8. Romaka V.A., Rogl P., Romaka V.V., Stadnyk Yu.V., Hlil E.K., Kraiovskii V.Ya., Goryn' A.M. Effect of the accumulation of excess Ni atoms in the crystal structure of the intermetallic semiconductor *n-ZrNiSn* (2010). *Semiconductors*, 47(7), 892–898.
9. Roisnel T., Rodriguez-Carvajal J. (2001). WinPLOTR: a Windows tool for powder diffraction patterns analysis, *Mater. Sci. Forum, Proc. EPDIC7* 378–381, 118–123.
10. Schruter M., Ebert H., Akai H., Entel P., Hoffmann E., Reddy G.G. First-principles investigations of atomic disorder effects on magnetic and structural instabilities in transition-metal alloys (1995). *Phys. Rev*. B 52, 188–209.
11. Moruzzi V.L., Janak J.F., Williams A.R. *Calculated electronic properties of metals* (1978). NY: Pergamon Press.
12. Mott N.F., Davis E.A. (1979). *Electron processes in non-crystalline materials.* Oxford: Clarendon Press.

Submitted 10.09.2018

Ромака В.А.[1], *док. тех. наук*, *професcор*
Ромака Л.П.[2], *канд. хім. наук*
Стадник Ю.В[2], *канд. хім. наук*
Ромака В.В.[1,3], *док. тех. наук, канд. хім. наук, доц.*
Горинь А.М.[2], *канд. хім. наук*
Романів І.М.

[1]Національний університет "Львівська політехніка", вул. С. Бандери, 12, Львів, 79013, Україна; *e-mail: vromaka@polynet.lviv.ua*
[2]Львівський національний університет ім. І. Франка, вул. Кирила і Мефодія, 6, Львів, 79005, Україна; *e-mail: lyubov.romaka@lnu.edu.ua*,
[3]Інститут досліджень твердого тіла, IFW-Drezden, Гельмгольц штрасе, 20, 01069 Дрезден, Німеччина

ДОСЛІДЖЕННЯ ТЕРМОЕЛЕКТРИЧНОГО МАТЕРІАЛУ $Zr_{1-x}V_xNiSn$

Досліджено кристалічну та електронну структури, кінетичні та енергетичні характеристики термоелектричного матеріалу $Zr_{1-x}V_xNiSn$ у діапазонах: T=80–400 K, x=0.01–0.10. Встановлено механізми одночасного генерування структурних дефектів акцепторної та донорної природи, які визначають електропровідність матеріалу. Показано, що енергетично доцільним є одночасне часткове зайняття атомами V ($3d^34s^2$) позиції 4c атомів Ni ($3d^84s^2$), що генерує структурні дефекти акцепторної природи та домішкову акцепторну зону ε^1_A, а також позиції 4a атомів Zr ($4d^25s^2$), генеруючи структурні дефекти донорної природи та домішкову донорну зону ε^2_D. Бібл. 12, Рис.8.
Ключові слова: електронна структура, електроопір, коефіцієнт термоЕРС.

Ромака В.А.[1], *док. тех. наук*, *професcор*
Ромака Л.П.[2], *канд. хим. наук*
Стадник Ю.В[2], *канд. хим. наук*
Ромака В.В.[1,3], *док. тех. наук, канд. хим. наук, доц.*
Горынь А.М.[2], *канд. хим. наук*
Романов И.М.

[1]Национальный университет "Львовская политехника", ул. С. Бандеры, 12, Львов, 79013, Украина, *e-mail: vromaka@polynet.lviv.ua*,
[2]Львовский национальный университет им. И. Франко, ул. Кирилла и Мефодия, 6, Львов, 79005, Украина, *e-mail: lyubov.romaka@lnu.edu.ua*,
[3]Институт исследований твердого тела, IFW-Drezden, Гельмгольц штрассе, 2001069 Дрезден, Германия

ИССЛЕДОВАНИЕ ТЕРМОЭЛЕКТРИЧЕСКИХ МАТЕРИАЛОВ $Zr_{1-x}V_xNiSn$

Исследованы кристаллическая и электронная структуры, кинетические и энергетические характеристики термоэлектрического материала $Zr_{1-x}V_xNiSn$ в диапазонах: T = 80-400 K, x = 0.01-0.10. Установлены механизмы одновременного генерирования структурных дефектов акцепторной и донорной природы, которые определяют электропроводность материала. Показано, что энергетически целесообразно одновременное частичное занятие атомами V ($3d^34s^2$) позиции 4c атомов Ni ($3d8^4s^2$), генерирующий структурные дефекты акцепторной природы и примесную акцепторную зону, ε^1_A а также позиции 4a атомов Zr ($4d^25s^2$), генерируя структурные дефекты донорной природы и примесную донорных зону ε^2_D. Библ. 12, Рис.8.
Ключевые слова: электронная структура, электросопротивление, коэффициент термоЭДС.

References

1. Romaka V.A., Romaka V.V., Stadnyk Yu.V. (2011). *Intermetallic semiconductors: properties and applications.* Lviv: Lvivska Polytechnika.
2. Romaka V.V., Rogl P.-F., Carlini R., Fanciulli C. (2017). Prediction of the thermoelectric properties of Half-Heusler phases from the density functional theory. In *Alloys and Intermetallic Compounds. (*Artini C., Ed.) London-NY: Taylor & Francis Group.
3. Anatychuk L.I. (1979). *Termoelementy i termoelektricheskiie ustroistva. Spravochnik [Thermoelements and thermoelectric devices. Handbook]*. Kyiv: Naukova Dumka [in Russian].
4. Shklovsky B.I., Efros A.L. (1979). *Electronic properties of doped semiconductors.* Moscow: Nauka [in Russian].
5. Romaka V.A., Frushart D., Stadnyk Yu.V., Tobola J., Gorelenko Yu.K., Shelyapina M.G., Romaka L.P., Chekurin V.F. (2006). A condition of maximum power characteristic to intermetallic semiconductors of the *MgAgAs* structure type. *Semiconductors*, 40 (11), 1289–1395.
6. Romaka V.A., Hlil E.K., Ya.V. Skolozdra, Rogl P., Stadnyk Yu.V., Romaka L.P., Goryn A.M.(2009). Features of the mechanisms of generation and “healing” of structural defects in the heavily doped intermetallic semiconductor *n-ZrNiSn. Semiconductors*, 43(9), 1115–1123.
7. Romaka V.V., Romaka L.P., Krayovskyy V.Ya., Stadnyk Yu.V. (2015). *Stanidy ridkisnozemelnykh ta perekhidnykh metaliv [Stannides of rare earth and transition metals]*. Lviv: Lvivska Polytechnika [in Ukrainian].
8. Romaka V.A., Rogl P., Romaka V.V., Stadnyk Yu.V., Hlil E.K., Kraiovskii V.Ya., Goryn’ A.M. Effect of the accumulation of excess Ni atoms in the crystal structure of the intermetallic semiconductor *n-ZrNiSn* (2010). *Semiconductors*, 47(7), 892–898.
9. Roisnel T., Rodriguez-Carvajal J. (2001). WinPLOTR: a Windows tool for powder diffraction patterns analysis, *Mater. Sci. Forum, Proc. EPDIC7* 378–381, 118–123.
10. Schruter M., Ebert H., Akai H., Entel P., Hoffmann E., Reddy G.G. First-principles investigations of atomic disorder effects on magnetic and structural instabilities in transition-metal alloys (1995). *Phys. Rev*. B 52, 188–209.
11. Moruzzi V.L., Janak J.F., Williams A.R. *Calculated electronic properties of metals* (1978). NY: Pergamon Press.
12. Mott N.F., Davis E.A. (1979). *Electron processes in non-crystalline materials.* Oxford: Clarendon Press.

Submitted 10.09.2018

L.I. Anatychuk[1,2] *acad. National Academy of Sciences of Ukraine*
L.M. Vikhor [1]*doctor Phys.- math. Sciences*
A.V. Prybyla [1,2] *cand. Phys. - math. Sciences*

[1]Institute of Thermoelectricity of the NAS and MES of Ukraine,
1, Nauky str., Chernivtsi, 58029, Ukraine;
[2]Yu.Fedkovych Chernivtsi National University,
2, Kotsiubynskyi str., Chernivtsi, 58000, Ukraine
e-mail: anatych@gmail.com

THE INFLUENCE OF CONTACTS ON THE EFFICIENCY OF THERMOELECTRIC MODULES IN HEATING MODES UNDER MINIATURIZATION CONDITIONS

The paper presents the results of calculations of the influence of contacts on the heating coefficient of a thermoelectric module under miniaturization conditions. The possibilities of decreasing the weight and size parameters of a thermoelectric module in heating mode for various contact resistances with minimum heating coefficient losses are analyzed. Bibl. 9, Fig. 1, Tabl. 1.
Key words: thermoelectric heat pump, efficiency, miniaturization, simulation.

Introduction

General characterization of the problem. The use of thermoelectric converters in various-purpose cooling and heating systems is related to their unique advantages In the calculations, the physical model of a thermoelectric module in heating mode, described in detail in [7], was used.

An example of the successful use of thermoelectric modules in heating mode are systems for the regeneration of water from liquid waste products on board manned spacecraft (urine, atmospheric moisture condensate, sanitary water) [4 - 6].

The paper [7] presents the results of calculations of the influence of miniaturization of thermoelectric modules in heating mode. Through computer simulation, the influence of the height of thermoelectric material legs on the heating coefficient of the thermoelectric modules is determined and the optimum height of material leg is found, which provides the minimum losses of the energy conversion efficiency. Further reduction of the height of thermoelectric material legs leads to a sharp deterioration of the heating coefficient and is undesirable. In [7], calculations were made for the standard value of contact resistance $r_0 = 5 \cdot 10^{-6}\ \Omega \cdot cm^2$. However, it is obvious that under miniaturization conditions, the effect of contact resistance on the energy conversion efficiency increases. Therefore, studies are important to improve the quality of contacts, which, in general, will increase the heating coefficient of thermoelectric modules and reduce their overall dimensions.

The purpose of this work is to determine the influence of contacts on the efficiency of thermoelectric modules in heating mode under miniaturization conditions.

Mathematical and computer descriptions of the model

In the calculations, the physical model of the thermoelectric module in heating mode, described in detail in [7], was used.

The mathematical and computer descriptions of the model used in the calculations are given below.

To describe the heat and electricity fluxes, we will use the laws of conservation of energy

$$div\vec{E} = 0 \tag{1}$$

and electrical charge

$$div\vec{j} = 0, \tag{2}$$

where

$$\vec{E} = \vec{q} + U\vec{j}, \tag{3}$$

$$\vec{q} = \kappa\nabla T + \alpha T\vec{j}, \tag{4}$$

$$\vec{j} = -\sigma\nabla U - \sigma\alpha\nabla T. \tag{5}$$

Here, $\vec{E}$ is energy flux density, $\vec{q}$ is heat flux density, $\vec{j}$ is electrical current density, U is electrical potential, T is temperature, α, σ, κ are the Seebeck coefficient, electrical conductivity and thermal conductivity.

With regard to (3) – (5), one can obtain

$$\vec{E} = -(\kappa + \alpha^2\sigma T + \alpha U\sigma)\nabla T - (\alpha\sigma T + U\sigma)\nabla U. \tag{6}$$

Then the laws of conservation (1), (2) will take on the form:

$$-\nabla\left[(\kappa + \alpha^2\sigma T + \alpha U\sigma)\nabla T\right] - \nabla\left[(\alpha\sigma T + U\sigma)\nabla U\right] = 0, \tag{7}$$

$$-\nabla(\sigma\alpha\nabla T) - \nabla(\sigma\nabla U) = 0. \tag{8}$$

From the solution of equation (7) - (8) we obtain the distribution of physical fields, as well as the integral values of the efficiency and heat flux in the thermoelement.

To solve the above differential equations with the respective boundary conditions, the Comsol Multiphysics applied software package was used [8].

Computer simulation results

Thus, the dependences of the heating coefficient K of thermoelectric module on the value of contact electrical resistance for different heights of thermoelectric material legs and different temperature differences have been calculated.

The operating temperatures were chosen from the real thermal conditions of thermoelectric heat pump for water purification device of space application [5 - 7].

Fig.1 shows the dependence of the heating coefficient of thermoelectric module on the value of contact electrical resistance for two values of the height of thermoelement legs - 0.5 and 1 mm and for temperature differences ΔT = *5 - 25 K*. The temperature of the heat-absorbing surface T_c = 25ºC (as shown in [7], the value of the heating coefficient for the thermoelectric module is weakly dependent on the temperature of the heat-absorbing surface T_c and is determined mainly by the temperature difference ΔT).

As is seen from Fig., with an increase in the value of contact resistance, the influence of the height of thermoelectric material leg on the heating coefficient of thermoelectric module grows.

To analyze this influence, we will use Table, where we calculate the relative change in the value of the heating coefficient of a thermoelectric module with a change in the contact resistance for different

temperature differences and heights of the thermoelectric material leg.

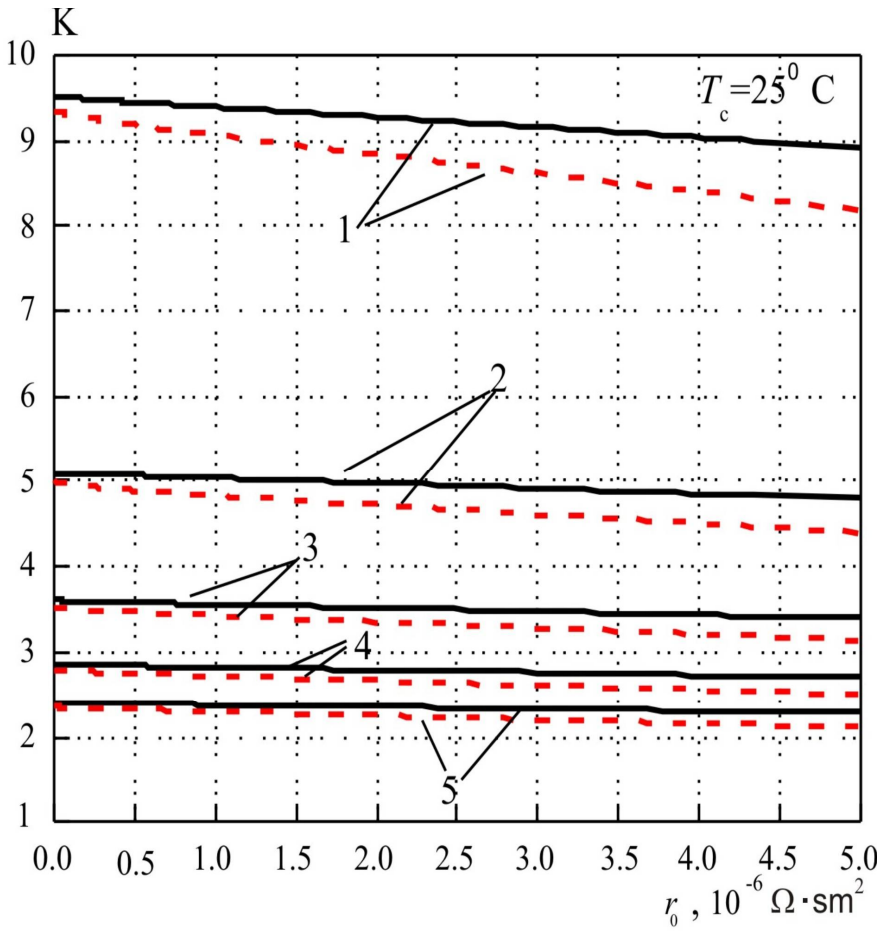

Fig. 1 Dependences of heating coefficient K of thermoelectric module on the value of contact resistance r_0 *for temperature differences 1 – ΔT=5 K, 2 - ΔT=10 K, 3 – ΔT=15 K, 4 – ΔT=20 K, 5 – ΔT=25 K. Solid lines – the length of leg h=0.5 mm, dashed lines - h=1 mm. Temperature of the heat-absorbing surface* T_c=25°C.

Table

Relative decrease of heating coefficient K of thermoelectric module on the value of contact resistance r_0 *for different temperature differences ΔT and leg heights h of thermoelectric material*

r_0, Ohm·cm^2	*h*, mm	K, Δ*T*=5°C	K, Δ*T*=10°C	K, Δ*T*=15°C	K, Δ*T*=20°C	K, Δ*T*=25°C
0	0.5	9.31	4.96	3.51	2.78	2.35
$5\cdot10^{-7}$		< by 1.4%	< by 1.3%	< by 1.1%	< by 1.0%	< by 1.3%
10^{-6}		<by 2.7%	<by 2.6%	<by 2%	<by 2%	<by 1.75%
$5\cdot10^{-6}$		<by 12%	<by 11.3%	<by 10.5%	<by 10.0%	<by 10.0%
0	1	9.51	5.1	3.61	2.86	2.41
$5\cdot10^{-7}$		< by 0.6%	< by 0.6%	< by 0.8%	< by 0.7%	< by 0.8%
10^{-6}		<by 0.63%	<by 1.0%	<by 1.0%	<by 1.1%	<by 1.0%
$5\cdot10^{-6}$		<by 6%	<by 6%	<by 5.8%	<by 5.6%	<by 10.4%

So, from Table it can be seen that the relative change in the heating coefficient depends weakly on the temperature difference and has a sharp dependence on the magnitude of contact resistance and the height of thermoelement leg. Moreover, for the leg height of h = 0.5 mm, a change in the value of contact resistance from 0 to 10^{-6} Ω· cm^2 leads to a slight decrease in the heating coefficient by ~ 1.75 - 2.7%, and from 10^{-6} to 5 · 10^{-6} Ω· cm^2 leads to its significant drop by ~ 10 - 12%. For the leg height h = 1 mm, a change in the magnitude of contact resistance from 0 to 10^{-6} Ω cm^2 leads to a decrease in the heating coefficient by ~ 0.6– 0.8%, and from 10^{-6} to 5 · 10^{-6} Ω cm^2 leads to its significant drop by ~ 6 - 10.4%.

From the above it is possible to draw a conclusion on the undoubted importance of improving the quality of contacts when miniaturizing thermoelectric modules. Thus, a decrease in contact resistance from 5 · 10^{-6} to 10^{-6} Ω·cm^2 is equivalent to reducing the height of the thermoelectric leg from 1 mm to 0.5 mm, which opens up possibilities for further reduction of mass-size indicators and is important for its practical use.

Conclusions

1. It has been established that with increasing the value of contact resistance, the influence of the height of thermoelectric material leg on the heating coefficient of thermoelectric module grows.
2. It has been calculated that for the leg height h=0.5 mm the change in the value of contact resistance from 0 to 10^{-6} Ω·cm^2 leads to a decrease in the heating coefficient by ~ 1.75 - 2.7 %, and from 10^{-6} to $5\cdot10^{-6}$ Ω·cm^2 leads to its significant drop by ~ 10 - 12 %; for the leg height h=1 mm the change in the value of contact resistance from 0 to 10^{-6} Ω·cm^2 leads to a decrease in the heating coefficient by ~ 0.6 - 0.8 %, and from 10^{-6} to $5\cdot10^{-6}$ Ω·cm^2 leads to its drop by ~ 6 - 10.4 %.
3. It has been determined that the reduction in the value of contact resistance from $5\cdot10^{-6}$ to 10^{-6} Ω·cm^2 is equivalent to decreasing the height of thermoelement leg from 1 mm to 0.5 mm, which opens up possibilities for further reduction of mass-dimensional parameters and is important for its practical use.

References

1. Anatychuk L.I., Vikhor L.M. (2013). The limits of thermoelectric cooling for photodetectors. *J. Thermoelectricity*, 5, 54-58.
2. Rozver Yu.Yu. (2003). Thermoelectric air-conditioner for vehicles. *J.Thermoelectricity*, 2, 52-56.
3. Anatychuk L.I., Vikhor L.N., Rozver Yu.Yu. (2004). Investigation on performance of thermoelectric cooler of liquid or gas flows. *J.Thermoelectricity*, 1, 73 – 80.
4. Anatychuk L.I., Barabash P.A., Rifert V.G., Rozver Yu.Yu., Usenko V.I., Cherkez R.G. (2013). Thermoelectric heat pump as a means of improving efficiency of water purification systems on space missions. *J. Thermoelectricity*, 6, 78 – 83.
5. Anatychuk L.I., Prybyla A.V. (2015). Optimization of power supply system of thermoelectric liquid-liquid heat pump. *J. Thermoelectricity*, 6, 53 – 58.
6. Anatychuk L.I., Prybyla A.V. (2017). Limiting possibilities of thermoelectric liquid-liquid heat pump. *J. Thermoelectricity,* 4, 33 – 39.
7. Anatychuk L.I., Vikhor L.M., Prybyla A.V. (2018). Effect of miniaturization on the efficiency of thermoelectric modules in heating mode. *J.Thermoelectricity*, 4, 38 – 45.
8. *COMSOL Multiphysics User's Guide* (2010). COMSOLAB.
9. Holm R. (1981). Elektricheskiie kontakty [Electrical contacts]. Moscow: Inostrannaia literatura [Russian transl].

Submitted 17.09.2018.

Анатичук Л.І.[1,2] *акад. НАН України*
Вихор Л.М.[1 1] *доктор фіз. - мат. наук*
Прибила А.В.[1,2] *канд. фіз. - мат. наук*

[1]Інститут термоелектрики НАН і МОН України,
вул. Науки, 1, Чернівці, 58029, Україна;
[2]Чернівецький національний університет
ім. Юрія Федьковича, вул. Коцюбинського 2,
Чернівці, 58000, Україна
e-mail: anatych@gmail.com

ВПЛИВ КОНТАКТІВ НА ЕФЕКТИВНІСТЬ ТЕРМОЕЛЕКТРИЧНИХ МОДУЛІВ У РЕЖИМІ НАГРІВУ В УМОВАХ МІНІТЮАРИЗАЦІЇ

У роботі наводяться результати розрахунків впливу контактів на опалювальний коефіцієнт термоелектричного модуля в умовах мініатюризації. Проаналізовані можливості зменшення масогабаритних показників термоелектричного модуля в режимі нагріву для різних контактних опорів за умови мінімальних втрат опалювального коефіцієнту. Бібл. 9, Рис. 1, Табл. 1.
Ключові слова: термоелектричний тепловий насос, ефективність, мініатюризація, моделювання.

Анатычук Л.И.[1,2] *акад. НАН Украины*
Вихор Л.Н.[1] *доктор физ. - мат. наук*
Прибыла А.В.[1,2] *канд. физ. - мат. наук*

[1]Институт термоэлектричества НАН и МОН Украины
ул. Науки, 1, Черновцы, 58029, Украина;
[2]Черновицкий национальный университет
им. Юрия Федьковича, ул. Коцюбинского 2
Черновцы, 58000, Украина
e-mail: anatych@gmail.com

ВЛИЯНИЕ КОНТАКТОВ НА ЭФФЕКТИВНОСТЬ ТЕРМОЭЛЕКТРИЧЕСКИХ МОДУЛЕЙ В РЕЖИМЕ НАГРЕВА В УСЛОВИЯХ МИНИТЮАРИЗАЦИИ

В работе приводятся результаты расчетов влияния контактов на отопительный коэффициент термоэлектрического модуля в условиях миниатюризации. Проанализированы возможности уменьшения массогабаритних показателей термоэлектрического модуля в режиме нагрева для различных контактных сопротивлений при условии минимальных потерь отопительного коэффициента. Библ. 9, Рис. 1, Табл. 1.
Ключевые слова: термоэлектрический тепловой насос, эффективность, миниатюризация, моделирование.

References

1. Anatychuk L.I., Vikhor L.M. (2013). The limits of thermoelectric cooling for photodetectors. *J. Thermoelectricity*, 5, 54-58.

2. Rozver Yu.Yu. (2003). Thermoelectric air-conditioner for vehicles. *J.Thermoelectricity*, 2, 52-56.
3. Anatychuk L.I., Vikhor L.N., Rozver Yu.Yu. (2004). Investigation on performance of thermoelectric cooler of liquid or gas flows. *J.Thermoelectricity*, 1, 73 – 80.
4. Anatychuk L.I., Barabash P.A., Rifert V.G., Rozver Yu.Yu., Usenko V.I., Cherkez R.G. (2013). Thermoelectric heat pump as a means of improving efficiency of water purification systems on space missions. *J. Thermoelectricity*, 6, 78 – 83.
5. Anatychuk L.I., Prybyla A.V. (2015). Optimization of power supply system of thermoelectric liquid-liquid heat pump. *J. Thermoelectricity*, 6, 53 – 58.
6. Anatychuk L.I., Prybyla A.V. (2017). Limiting possibilities of thermoelectric liquid-liquid heat pump. *J. Thermoelectricity,* 4, 33 – 39.
7. Anatychuk L.I., Vikhor L.M., Prybyla A.V. (2018). Effect of miniaturization on the efficiency of thermoelectric modules in heating mode. *J.Thermoelectricity*, 4, 38 – 45.
8. *COMSOL Multiphysics User's Guide* (2010). COMSOLAB.
9. Holm R. (1981). Elektricheskiie kontakty [Electrical contacts]. Moscow: Inostrannaia literatura [Russian transl].

Submitted 17.09.2018.

Dmytrychenko M.F., *Dr. of Technical Sciences*
Gutarevych Yu.F., *Dr. of Technical Sciences*
Trifonov D.M., *Cand. of Technical Sciences*
Syrota O.V., *Cand. of Technical Sciences*
Shuba E.V., *Cand. of Technical Sciences*

National Transport University
1, M.Omelianovycha-Pavlenka Str., Kyiv, 01010, Ukraine,
e-mail: kafedradvzntu@gmail.com

ON THE PROSPECTS OF USING THERMOELECTRIC GENERATORS WITH THE COLD START SYSTEM OF AN INTERNAL COMBUSTION ENGINE WITH A THERMAL BATTERY

According to the results of the analysis of the power capabilities of the internal combustion engine start system under low ambient temperatures, it has been found that this process is considerably affected by the temperature of the battery electrolyte. It is proposed to use a thermoelectric system that allows a thermoelectric generator to recover the exhaust gas thermal energy which is stored in a thermal battery to provide power to the infrared heating element in order to maintain the thermal state of the battery while the vehicle is kept at low temperatures. The description of the proposed system, its operating principle and the results of research are given. Fig. 4, Bibl. 15.
Key words: thermoelectric generator, recovery of exhaust gas thermal energy, phase change thermal battery, cold engine start, starter battery.

Introduction

Ensuring efficient operation of the car, in accordance with modern requirements to its fuel economy and environmental safety, is impossible without taking into account the operating conditions. Significant influence on fuel economy and ecological safety of a car is made by natural and climatic factors whereby the operation of a vehicle takes place. Under low ambient temperature, the main problem is to provide a reliable and trouble-free start of a cold internal combustion engine (IC engine).

Saving of fuel and energy resources can be realized through the recovery of part of the secondary energy resources, which arise in significant amounts during the operation of the internal combustion engine. The energy saving potential as a result of the use of secondary energy resources is quite large and can be up to 40% of the consumption of primary fuel and energy resources.

Many researchers recognize that the recovery of part of the thermal energy from the exhaust gases (EG) is one of the most effective measures, which allows reducing the total specific fuel consumption, while providing an increase in the total power of the power plant and a reduction in the negative environmental impact of the vehicle [1- 7]. EG recovery using thermoelectric generators (TEG) provides the generation of electrical energy.

Recent technological advances have made the recovery of secondary energy resources cost effective, and increased environmental and fuel-economic requirements to vehicles have made it absolutely necessary.

Therefore, increasing energy efficiency of a car power plant, primarily due to the reduction of

losses of secondary energy resources, is an urgent task and one of the priority directions of scientific research in this field.

The purpose of this study is to determine the feasibility and effectiveness of the use of a thermoelectric system, which will allow the optimal thermal state of the starter battery to be maintained while the vehicle is kept at low ambient temperatures, thus improving the cold start of the IC engine. The heat source in the proposed system is a phase change thermal battery which generates electrical energy by a thermoelectric generator upon the completion of the operation of an IC engine.

Analysis of previous research

When the ambient temperature decreases, the electric starter capacity of the IC engine starting system is dramatically lost due to the deterioration of the starter battery. When the temperature decreases, the power of the discharge current and the internal resistance of storage battery increase quite strongly. On the average, when the temperature of the electrolyte decreases by 1 ° C, the capacity of storage battery decreases by 1.0 ... 1.5%. At electrolyte temperatures below 30 ° C, the battery almost does not accept the charge and operates in fact discharged to 50 ... 60% of the nominal capacity [8-10].

According to the Battery Research Institute: at a temperature of 0 ° C, the current efficiency of the battery is 90%, and at minus 40 ° C - only 20%. That is, the battery becomes practically inoperable at a temperature of minus 30 ... 35 ° C [11].

The electrolyte temperature and density have a great influence on the internal resistance of storage battery. The minimal resistance of the electrolyte is at a temperature of plus 15 ° C and a density of 1.225 g / cm^3. With a decrease in the temperature of the electrolyte from plus 30 ° C to minus 40 ° C, its resistivity increases by a factor of 6 ... 8 [12-14].

Thus, lowering the temperature of the electrolyte leads to a decrease in voltage at the battery terminals, which leads to a decrease in the power of the starter in the process of cold engine start. So, to ensure the effective functioning of the starter battery, its optimum temperature should be maintained. To do this, heating the electrolyte of a storage battery by electric heaters embedded in a monoblock or placed in heat insulating containers for a storage battery powered by an external electrical network or a car generator during engine operation is widely used. However, the disadvantage of this method is the need for additional use of energy resources, the impossibility of using an external electrical network when holding cars in outdoor areas and the fact that maintenance of the optimum temperature of storage battery is possible only during the operation of the IC engine.

It is possible to overcome these drawbacks if the heat energy from the exhaust gases accumulated in a phase change thermal battery is used as a source of heat, which makes it possible to generate TEG electrical energy both during operation of the internal combustion engine and at the end of its operation.

The results of experimental studies

According to the chosen scheme of thermal energy recovery, the thermal model of the thermoelectric system has the form shown in Fig. 1. During the operation of the internal combustion engine, part of the thermal energy from the EG is transferred to a phase change thermal battery, in which thermal energy is accumulated. When the vehicle is kept at low ambient temperatures, after the operation of the IC engine is completed, a portion of the heat accumulated in a phase change thermal battery is transferred to the "hot" TEG junctions and further from the "cold" junctions of the TEG into the ambient air.

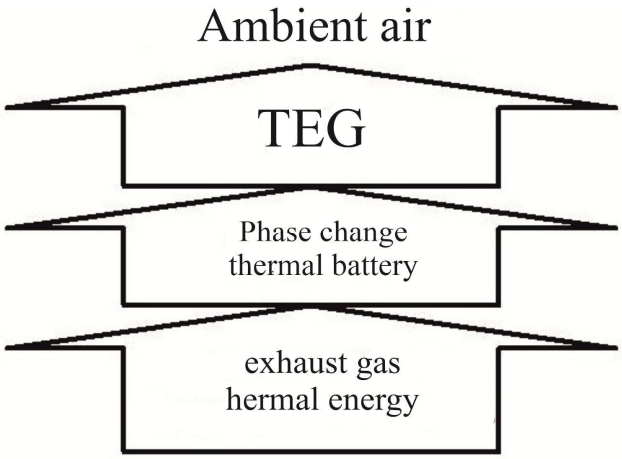

Fig. 1 – Schematic of thermal energy flows in the proposed thermoelectric system for the recovery of EG thermal energy with phase change thermal battery

The proposed thermoelectric system is composed (Fig. 2) of a phase change thermal battery 1, a layer of thermal-resistant compound 2, a thermoelectric generator that comprises series-connected elementary thermocouples 3, a heat controller 4 and an infrared heating element 5.

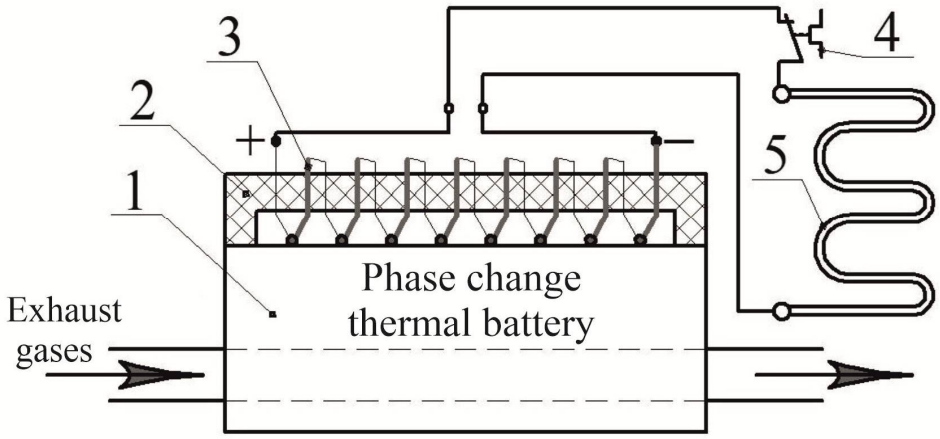

Fig. 2 – Thermoelectric system for the recovery of EG thermal energy with phase change thermal battery: 1 – phase change thermal battery, 2 – layer of thermal-resistant compound, 3 – thermoelectric generator, 4 – heat controller, 5 – infrared heating element

The operating principle of the proposed system is as follows (Fig. 2): during the operation of the internal combustion engine, the flow of exhaust gases passes along tube bundles through a phase change thermal battery 1, giving part of the thermal energy to the heat-accumulating material (HAM). During the storage of a car under low ambient temperatures, the thermoelectric generator 3, which functions according to the Seebeck effect, converts part of the thermal energy accumulated in a phase change thermal battery into electrical energy. The resulting electrical energy feeds the infrared heating film element 5. Heat controller 4 maintains the optimum temperature of the battery, creating the conditions necessary to improve the cold start of the IC engine.

The phase change thermal battery (Fig. 3), made at the Department of Engines and Heat Engineering of the National Transport University, with the participation of the employees of the Institute of Gas of the National Academy of Sciences of Ukraine, is a heat-exchange apparatus of a shell-tubular type with a box case consisting of a housing with a layer of thermal insulation, two gas tube bundles (heat exchangers) on pipe boards, between which there is the phase change HAM. The

heat-accumulating material is octahydrate of Barium hydroxide $Ba(OH)_2 \cdot 8H_2O$, the melting point of which is 351.2 K [15].

Thermoelectric generator (Fig. 3 a) is composed of thermoelectric converters of the type chromel-kopel thermocouple (chromel is an alloy of 90% nickel and 10% of chromium, kopel – an alloy of 56% copper and 44% nickel), connected in series.

Infrared heating element is made of aluminum-magnesium alloy protected by polymetals. This alloy combines a rather high strength and excellent corrosion resistance, a heating element with a surface temperature of + 60 ... 65 ° C, has high reliability and efficiency.

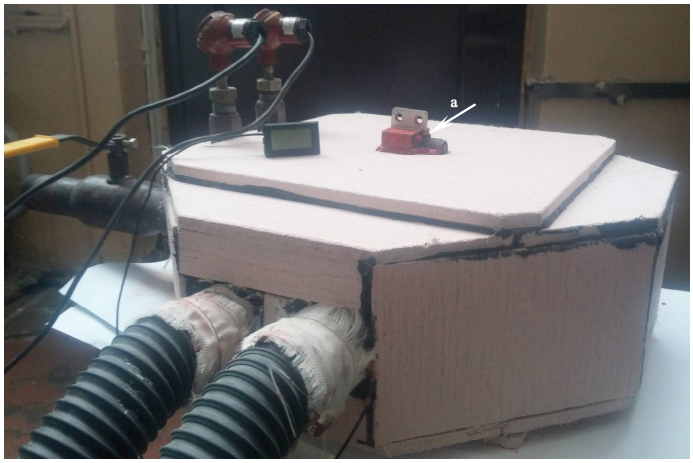

Fig. 3. Phase change thermal battery with thermoelectric generator (a)

When conducting experimental studies, the average ambient temperature was about 1.5° C, the surface temperature of a phase change thermal battery under a layer of thermal insulation at the point of contact with the "hot" junctions of the TEG was + 116 ° C.

With natural cooling, the discharge time of a phase change thermal battery in the temperature range from 116 ° C to 65 ° C was 320 minutes. During this time, the average rate of reduction in the temperature of a phase change thermal battery was about 0.16 ° C per minute. The amount of heat loss to the ambient air during storage of heat energy when the vehicle is kept without a garage depends on the quality of thermal insulation of a phase change thermal battery (Fig. 4).

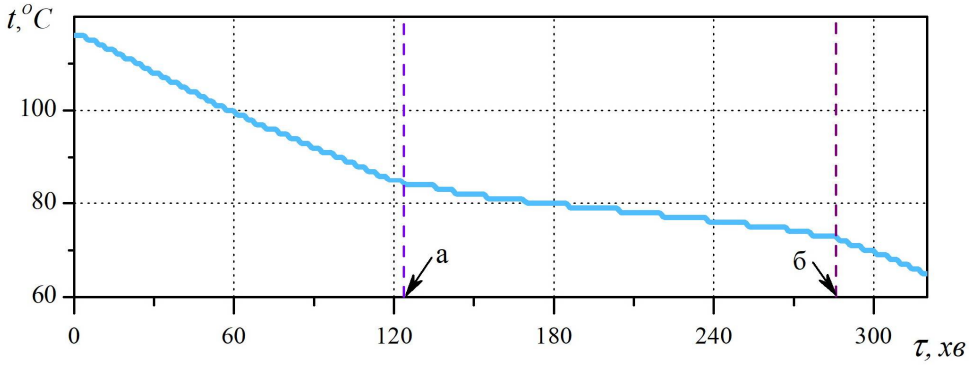

Fig. 4 – Change in the surface temperature of a phase change thermal battery under the layer of heat insulation at a point of contact with the "hot" junctions of TEG under natural cooling (a – beginning, b – end of crystallization of HAM)

Deceleration of the temperature decrease of a phase change thermal battery surface under a

layer of thermal insulation at a point of contact with the "hot" junctions of TEG is observed from 124 to 286 minutes (Fig. 4). This deceleration can be explained by the crystallization period of HAM. The duration of the HAM crystallization period is about 160 minutes. The temperature of a phase change thermal battery surface at a point of contact with the "hot" junctions of the TEG was relatively stable in the temperature range + 84 ... 73 ° C, the average temperature was + 78.5 ° C, while the rate of decrease in temperature was about 0.07 ° C per minute.

Thus, the study of a phase change thermal battery showed that a thermal battery located in the underhood space is able to ensure almost constant temperature difference between the "hot" and "cold" junctions of the TEG within 70 ... 80 ° C for about 320 minutes.

According to the results of experimental studies, it was found that, when fifteen thermocouples connected in series with temperature differences between hot and cold junctions of around 75 ° C were applied in the TEG, the thermal electromotive force (thermopower) reached 45 mV.

In the future, it is planned to carry out computational and experimental studies to determine the number of pairs of thermoelectric elements in the TEG to provide the necessary supply voltage to infrared heating element, the energy characteristics of the TEG, determine the dependence of the thermo-electromotive force of the TEG on the temperature difference between the "hot" and "cold" junctions of the TEG, studies of the physical model of the proposed thermoelectric system with a phase change thermal battery in the process of its operation

Conclusions

1. Testing of the proposed thermoelectric system has showed that it allows a recovery by a thermoelectric generator of IC engine exhaust gas thermal energy accumulated in a phase change thermal battery to power the infrared heating element in order to maintain the thermal state of the starter battery while the vehicle is kept under low ambient temperatures. At a temperature difference between the "hot" and "cold" junctions of the TEG about 75 ° C, the thermoEMF reached about 45 mV.
2. Testing of a phase change thermal battery, developed and manufactured at the Department of Engines and Heating Engineering of the National Transport University with the participation of the employees of the Institute of Gas of the National Academy of Sciences of Ukraine, at an ambient temperature of about 1.5ºC, has showed that the storage time for thermal energy is 320 minutes. During this time, the surface temperature of a phase change thermal battery under the thermal insulation layer at a point of contact with the "hot" junctions of TEG decreased from 116ºC to 65ºC.
3. The results of this study confirmed the possibility and efficiency of the use of thermoelectric generators in the system of starting a cold internal combustion engine with a thermal battery for generation of electric energy on board a car for a long time after the completion of the operation of the IC engine.

References

1. Vazaquez J., Zanz-Bobi M.A., Palacios R., Arenas A. (2002). State of the art of thermoelectric generators based on heat recovered from the exhaust gases of automobiles. *Proceedings of 7th European Workshop on Thermoelectrics.*
2. Gritsuk, I., Gutarevych, Y., Mateichyk, V., and Volkov, V. (2016). Improving the processes of preheating and heating after the vehicular engine start by using heating system with phase-

transitional thermal accumulator. *SAE Technical Paper 2016-01-0204*, 2016, https://doi.org/10.4271/2016-01-0204.

3. Trifonov D.M. (2018). Analiz napriamiv rekuperatsii teplovoi enerhii vidpratsiovanykh haziv dvyhuna vnutrishnioho zhorannia [Analysis of the directions of recovery of thermal energy of exhaust gases of internal combustion engine]. Suchasni energetychni ustavovky na transporti i tekhnologii ta obladnannia dlia ikh obsluhovuvannia [Modern energy installations on transport and technology and equipment for their maintenance]. *9-th International Scientific and Practical Conference.* Kherson: Kherson State Maritime Academy.
4. Sprouse C. Iii and Depcik C. (2013). Review of organic Rankine cycles for internal combustion engine exhaust waste heat recovery. *Applied Thermal Engineering*, 51, 711-722.
5. Jadhao J.S., Thombare D.G. (2013). Review on exhaust gas heat recovery for I.C. Engine. *International Journal of Engineering and Innovative Technology (IJEIT)*, 2 (12).
6. Aladayleh Wail, Alahmer Ali. (1915). Recovery of exhaust waste heat for ICE using the beta type stirling engine. *Journal of Energy*, Article ID 495418, 8 pages, http://dx.doi.org/10.1155/2015/495418.
7. Duraisamy Sivaprahasam, Subramaniam Harish, Raghavan Gopalan and Govindhan Sundararajan (2018). *Automotive waste heat recovery by thermoelectric generator technology, bringing thermoelectricity into reality,* Patricia Aranguren, IntechOpen, DOI: 10.5772/intechopen.75443.
8. Kuznetsov E.S., Boldin A.P., Vlasov V.M., et al. (2001). Tekhnicheskaia ekspluatatsia avtomobilei: uchebnik dlia vuzov [Technical maintenance of cars: textbook for higher schools]. 4-th ed., revised and supplemented. Moscow: Nauka [in Russian].
9. Lykov A.V. (1967). *Teoriia teploprovodnisti [Theory of thermal conductivity]*. Moscow: Vysshaia shkola [in Russian].
10. Krokhta G.M., Usatykh N.A., Guskov Yu.A., Voronin D.M. (2016). Operating peculiarities of starter storage batteries during self-heating of the engine in winter. *Dostizheniia nauki i tekhniki APK – Achievements of Science and Technology of Agro-Industrial Complex,* 30 (12), 94-97.
11. Pankratov N.I. (1985). Ekspluatatsiia akkumuliatornykh batarei pri nizkikh temperaturakh [Operation of storage batteries at low temperatures]. *Avtomobilnyi Transport*, 2, 16–19 [in Russian].
12. Timinskii V.I. (1985). *Spravochnik po elektrooborudovaniiu avtomobilei, traktorov, kombainov [Handbook of the electrical equipment of cars, tractors, combines]*. Moscow: Urozhai [in Russian].
13. Tyshkevich L.N., Zhuravskii B.V. (2017). *Issledovaniie teplovykh protsessov akkumuliatornoi batarei pri ekspluatatsii avtomobilia v usloviiakh nizkikh otritsatelnykh temperatur [Study of thermal processes of storage battery when operating a car under low negative temperatures]*. Omsk: Bulletin of Siberian Automobile and Highway Academy, 6 (58) [in Russian].
14. Markin A.G., Zhuravskii B.V., Zhigadlo A.P. (2015). *Energoobespecheniie puska dvigatelia vnutrennego sgoraniia avtomobilia [Power supply of the start of a car internal combustion engine]*. Omsk: Bulletin of Siberian Automobile and Highway Academy, 5 (45) [in Russian].
15. Trifonov D.M. (2018). Polipshennia palyvnoi ekonomichnosti i ekolohichnykh pokaznykov avtomobilia vykorystanniam teplovykh akumuliatoriv fazovoho perekhodu dlia prohrivu dvyhuna [Improvement of fuel economy and environmental performance of the car using phase change thermal batteries for engine warm-up]. *Candidate's thesis* (Operation and repair of means of transport). Kyiv (in Ukrainian).

Submitted 06.08.2018.

Дмитриченко М.Ф. *доктор техн. наук*
Гутаревич Ю.Ф. *доктор техн. наук*
Тріфонов Д.М. *канд. техн. наук*
Сирота О.В. *канд. техн. наук*
Шуба Є.В. *канд. техн. наук*

Національний транспортний університет
вул. М. Омеляновича-Павленка, 1, м. Київ, 01010, Україна,
e-mail: kafedradvzntu@gmail.com

ПРО ПЕРСПЕКТИВИ ВИКОРИСТАННЯ ТЕРМОЕЛЕКТРИЧНИХ ГЕНЕРАТОРІВ В СИСТЕМІ ПУСКУ ХОЛОДНОГО ДВИГУНА ВНУТРІШНЬОГО ЗГОРАННЯ З ТЕПЛОВИМ АКУМУЛЯТОРОМ

За результатами аналізу енергетичних можливостей системи пуску двигуна внутрішнього згорання в умовах низьких температур оточуючого повітря встановлено, що значний вплив на цей процес зумовлює температуру електроліту акумуляторної батареї. Запропоновано використання термоелектричної системи, що дозволяє утилізувати теплову енергію відпрацьованих газів термоелектричним генератором що акумульована в тепловому акумуляторі для забезпечення живлення інфрачервоного нагрівального елементу для підтримання теплового стану акумуляторної батареї під час утримування автомобіля в умовах низьких температур. Наведено опис запропонованої системи, принцип її функціонування та результати досліджень. Бібл. 15, рис. 4.
Ключові слова: термоелектричний генератор, тепловий акумулятор фазового переходу.

Дмитриченко М.Ф. *доктор техн. наук*
Гутаревич Ю.Ф. *доктор техн. наук*
Трифонов Д.М. *канд. техн. Наук*[1,2]
Сирота О.В. *канд. техн. Наук*[1,2]
Шуба Е.В. *канд. техн. Наук*[1,2]

Национальный транспортный университет
ул. Г. Емельяновича-Павленко, 1, г. Киев, 01010, Украина,
e-mail: kafedradvzntu@gmail.com

О ПЕРСПЕКТИВАХ ИСПОЛЬЗОВАНИЯ ТЕРМОЭЛЕКТРИЧЕСКИХ ГЕНЕРАТОРОВ В СИСТЕМЕ ПУСКА ХОЛОДНОГО ДВИГАТЕЛЯ ВНУТРЕННЕГО СГОРАНИЯ С ТЕПЛОВЫМ АККУМУЛЯТОРОМ

По результатам анализа энергетических возможностей системы пуска двигателя внутреннего сгорания в условиях низких температур окружающего воздуха установлено, что значительное влияние на этот процесс оказывает температура электролита аккумуляторной батареи. Предложено использование термоэлектрической системы, которая позволяет утилизировать тепловую энергию отработанных газов, аккумулируемую в тепловом аккумуляторе, при помощи термоэлектрического генератора и для обеспечения питания инфракрасного нагревательного элемента для поддержания теплового состояния аккумуляторной батареи во время содержания автомобиля в условиях низких температур. Приведены описание предложенной системы, принцип ее функционирования и результаты исследований. Библ. 15,Рис. 4.
Ключевые слова*:* термоэлектрический генератор, тепловой аккумулятор фазового перехода.

References

1. Vazaquez J., Zanz-Bobi M.A., Palacios R., Arenas A. (2002). State of the art of thermoelectric generators based on heat recovered from the exhaust gases of automobiles. *Proceedings of 7th European Workshop on Thermoelectrics*.
2. Gritsuk, I., Gutarevych, Y., Mateichyk, V., and Volkov, V. (2016). Improving the processes of preheating and heating after the vehicular engine start by using heating system with phase-transitional thermal accumulator. *SAE Technical Paper 2016-01-0204*, 2016, https://doi.org/10.4271/2016-01-0204.
3. Trifonov D.M. (2018). Analiz napriamiv rekuperatsii teplovoi enerhii vidpratsiovanykh haziv dvyhuna vnutrishnioho zhorannia [Analysis of the directions of recovery of thermal energy of exhaust gases of internal combustion engine]. Suchasni energetychni ustavovky na transporti i tekhnologii ta obladnannia dlia ikh obsluhovuvannia [Modern energy installations on transport and technology and equipment for their maintenance]. *9-th International Scientific and Practical Conference.* Kherson: Kherson State Maritime Academy.
4. Sprouse C. Iii and Depcik C. (2013). Review of organic Rankine cycles for internal combustion engine exhaust waste heat recovery. *Applied Thermal Engineering*, 51, 711-722.
5. Jadhao J.S., Thombare D.G. (2013). Review on exhaust gas heat recovery for I.C. Engine. *International Journal of Engineering and Innovative Technology (IJEIT)*, 2 (12).
6. Aladayleh Wail, Alahmer Ali. (1915). Recovery of exhaust waste heat for ICE using the beta type stirling engine. *Journal of Energy*, Article ID 495418, 8 pages, http://dx.doi.org/10.1155/2015/495418.
7. Duraisamy Sivaprahasam, Subramaniam Harish, Raghavan Gopalan and Govindhan Sundararajan (2018). *Automotive waste heat recovery by thermoelectric generator technology, bringing thermoelectricity into reality,* Patricia Aranguren, IntechOpen, DOI: 10.5772/intechopen.75443.
8. Kuznetsov E.S., Boldin A.P., Vlasov V.M., et al. (2001). Tekhnicheskaia ekspluatatsia avtomobilei: uchebnik dlia vuzov [Technical maintenance of cars: textbook for higher schools]. 4-th ed., revised and supplemented. Moscow: Nauka [in Russian].
9. Lykov A.V. (1967). *Teoriia teploprovodnisti [Theory of thermal conductivity]*. Moscow: Vysshaia shkola [in Russian].
10. Krokhta G.M., Usatykh N.A., Guskov Yu.A., Voronin D.M. (2016). Operating peculiarities of starter storage batteries during self-heating of the engine in winter. *Dostizheniia nauki i tekhniki APK – Achievements of Science and Technology of Agro-Industrial Complex,* 30 (12), 94-97.
11. Pankratov N.I. (1985). Ekspluatatsiia akkumuliatornykh batarei pri nizkikh temperaturakh

[Operation of storage batteries at low temperatures]. *Avtomobilnyi Transport*, 2, 16–19 [in Russian].

12. Timinskii V.I. (1985). *Spravochnik po elektrooborudovaniiu avtomobilei, traktorov, kombainov [Handbook of the electrical equipment of cars, tractors, combines]*. Moscow: Urozhai [in Russian].
13. Tyshkevich L.N., Zhuravskii B.V. (2017). *Issledovaniie teplovykh protsessov akkumuliatornoi batarei pri ekspluatatsii avtomobilia v usloviiakh nizkikh otritsatelnykh temperatur [Study of thermal processes of storage battery when operating a car under low negative temperatures]*. Omsk: Bulletin of Siberian Automobile and Highway Academy, 6 (58) [in Russian].
14. Markin A.G., Zhuravskii B.V., Zhigadlo A.P. (2015). *Energoobespecheniie puska dvigatelia vnutrennego sgoraniia avtomobilia [Power supply of the start of a car internal combustion engine]*. Omsk: Bulletin of Siberian Automobile and Highway Academy, 5 (45) [in Russian].
15. Trifonov D.M. (2018). Polipshennia palyvnoi ekonomichnosti i ekolohichnykh pokaznykov avtomobilia vykorystanniam teplovykh akumuliatoriv fazovoho perekhodu dlia prohrivu dvyhuna [Improvement of fuel economy and environmental performance of the car using phase change thermal batteries for engine warm-up]. *Candidate's thesis* (Operation and repair of means of transport). Kyiv (in Ukrainian).

Submitted 06.08.2018.


V.S. Zakordonets

V.S. Zakordonets, *Cand.Sc. (Physics and Mathematics)*
N.V. Kutuzova

Ivan Puyul Ternopil National Technical University,
56, Rus'ka str., Ternopil, 46001
e-mail:wladim21@gmail.com


N.V. Kutuzova

CALCULATION OF HEAT PIPE-BASED LED COOLING SYSTEM

The mathematical thermal model of heat pipe-based LED cooling system is constructed. The system of differential equations is solved, which includes stationary equation of thermal conductivity and the Joule thermal generation equation, both supplemented by thermal boundary conditions. The distribution of temperature in structural elements of the cooling system is calculated depending on the power of LED, the parameters of heat pipe and the ambient temperature. Bibl. 10, Fig. 3, table. 1.
Key words: LED, luminous flux, thermal mode, thermal resistance, thermal stabilization, heat pipe.

Formulation of the problem

In modern high-power LED lighting systems, active cooling systems are widely used, which are based on the forced circulation of air or liquid in the circuit [1]. However, active cooling is associated with noise. Fan motors and airflow itself create sound waves that are often undesirable. In particular, when lighting residential premises, concert halls, classrooms, etc. In addition, they require additional capital investments and maintenance. All this leads to the search for alternative cooling systems.

Heat pipes (HPs) are one of the most efficient passive methods for the selection and transfer of thermal energy. Due to the use of latent heat of vaporization for heat transfer, its effective thermal conductivity is thousands of times greater than the thermal conductivity of Cu, Ag or Al, and reaches ~ 10^7 W/m K.

Analysis of recent research and publications

Thermal stabilization of electronic equipment using heat pipes indicates high efficiency of this cooling method [2, 3]. Obviously, it can be efficient for stabilizing the thermal mode of LEDs. In particular, in [4 – 6], a LED cooling system, which operates according to the heat pipe principle, was experimentally investigated. It is proved that the considered cooling systems provide the necessary thermal mode of LEDs in a wide range of temperatures. In [7], a LED cooling system was studied for various HP operating modes. Its high efficiency compared with a radiator, which has an identical profile and surface area, was experimentally proved.

However, these works considered only practical designs. Moreover, the thermal mathematical model of the cooling system was not considered and the theoretical analysis was not carried out.

The purpose of the work is to create the mathematical thermal model of heat pipe-based LED cooling system and to calculate on its basis the temperature of the active zone of LED.

Formulation of the task

Through theoretical analysis, to establish analytical relationships between the power of LED, the heat pipe parameters, the temperature of the medium and the active zone of LED. This will allow you to rationally choose the cooling circuit to ensure adequate thermal mode of LED.

Presentation of the main material

To calculate the thermal mode of LED, consider the thermal mathematical model of a LED attached to the end surface of the heat pipe as the base. We will assume that the thermal power of LED is completely absorbed by its hot end

$$P_t = P_h, \tag{1}$$

and from the lateral and end surfaces, due to convective heat transfer, excess power is diverted. The schematic of heat pipe-based cooling system is shown in Fig.1.

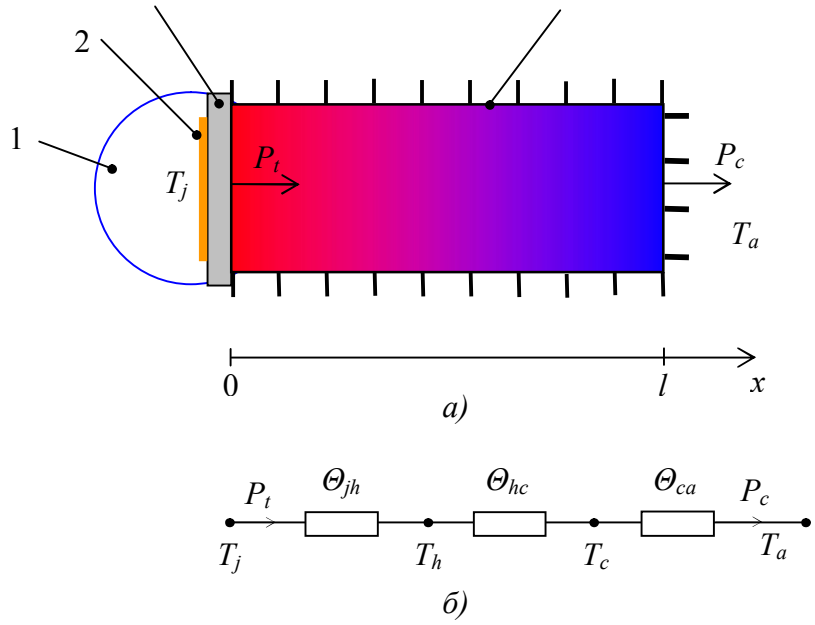

Fig. 1. Schematic of heat pipe-based LED cooling system (a) and its thermal circuit (b). Here, 1is LED, 2 is active zone, 3 is contact pad, 4 is heat pipe. T_j is temperature of the active zone of LED, T_h and T_c are the temperatures of the hot and cold ends of heat pipe, respectively, T_a is ambient temperature.

Consider the distribution of heat in a heat pipe with a constant cross-section along its length. For intensification of heat exchange, its lateral and end surfaces have a radiator profile. We believe that the pipe is in a medium with a constant temperature. The propagation of heat in the pipe is described by the stationary heat equation [8]

$$\nabla^2 t - \gamma^2 t = 0. \tag{2}$$

and the Joule thermal generation equation

$$P_t = \left(1 - \eta_e\right) I_f U_f, \tag{3}$$

where $\nabla = \vec{i}\frac{\partial}{\partial x} + \vec{j}\frac{\partial}{\partial y} + \vec{k}\frac{\partial}{\partial z}$ is the Hamiltonian operator, $t = T - T_a$ is overheat temperature of the pipe surface, T_a is ambient temperature, P_t is thermal generation power, U_f is direct voltage, I_f is direct current, η_e is quantum efficiency of LED,

$$\gamma = \sqrt{\frac{\alpha_p p}{\kappa S}}, \tag{4}$$

p and S are the perimeter of the lateral surface and the cross-sectional area, α_p and α_l are coefficients of heat transfer between the lateral and end surfaces of the pipe and the medium, respectively.

We believe that the heat flux is evenly distributed in the pipe plane. Then, for the density of the heat flux, we obtain:

$$q_t = \frac{P_t}{S}. \tag{5}$$

The written equations should be supplemented with the boundary conditions. At the interfaces between the structures of the cooling system, we define the traditional matching conditions for heat fluxes.

$$-\kappa \frac{dt}{dx}|_{x=0} = q_t, -\kappa \frac{dt}{dx}|_{x=l} = \alpha_l t|_{x=l}. \tag{6}$$

The solution of the system of equations (2-6) will be sought in the form:

$$t(x) = C_1 e^{\gamma x} + C_2 e^{-\gamma x}, \tag{7}$$

where C_1 and C_2 are integration constants which are determined from the boundary conditions.

As a result of solving the system of equations, the following distribution of overheat temperature was obtained

$$t(x) = \frac{P_t}{\alpha_l S}\frac{\alpha_l}{\kappa\gamma}\left\{\frac{\mathrm{ch}\left[\gamma(l-x)\right] + \mathrm{sh}\left[\gamma(l-x)\right]}{\mathrm{sh}(\gamma l) + (\alpha_l/\kappa\gamma)\mathrm{ch}(\gamma l)}\right\}. \tag{8}$$

Let us find the temperature of the hottest and coldest ends of the heat pipe and the average linear temperature difference. At $x = 0$ and $x = l$ we obtain, respectively:

$$T_h = T_a + \frac{P_t}{\alpha_l S}\frac{\alpha_l}{\kappa\gamma}\left[\frac{1 + (\alpha_l/\kappa\gamma)\,\mathrm{th}(\gamma l)}{(\alpha_l/\kappa\gamma) + \mathrm{th}(\gamma l)}\right], \tag{9}$$

$$T_c = T_a + \frac{P_t}{\alpha_l S\left[(\alpha_l/\kappa\gamma) + \mathrm{th}(\gamma l)\right]}\frac{\alpha_l}{\kappa\gamma}. \tag{10}$$

For the average linear temperature difference we have:

$$\lambda(\gamma l) = \frac{T_h - T_c}{l} = \frac{P_t}{\alpha_l S}\left(\frac{\alpha_l}{\kappa\gamma}\right)^2 \frac{\mathrm{th}(\gamma l)}{(\alpha_l/\kappa\gamma) + \mathrm{th}(\gamma l)}. \tag{11}$$

From the analysis of (11) it follows that due to the large thermal conductivity of the heat pipe $\lim_{\gamma l \to 0}\lambda(\gamma l) = 0$ in a wide range of lengths. This indicates that the pipe surface is an isothermal surface. The result is a uniform and and efficient heat dissipation along the entire length.

The temperature of the active zone of LED will be determined by the method of electrothermal analogy from Ohm's law for the thermal leg [9]

$$T_j = T_h + \Theta_{jh} P_t, \tag{12}$$

Taking into account (9), we get

$$T_j = T_a + P_t \left[\frac{\varepsilon}{\alpha_l S} \left(\frac{1 + \varepsilon \ \mathrm{th}\ \beta}{\varepsilon + \mathrm{th}\ \beta} \right) + \Theta_{jh} \right]. \tag{13}$$

where $\beta = \gamma l$ is a relative length of the heat pipe, $\varepsilon = \alpha_l / \kappa\gamma$ is a relative heat-transfer coefficient.

The temperature of the active zone decreases with an increase in the relative length of the heat pipe, and at $\beta \to \infty$ it asymptotically approaches the boundary value

$$T_j = T_a + P_t \left[\frac{\alpha_l}{\alpha_p} \frac{1}{\kappa p} + \Theta_{jh} \right]. \tag{14}$$

For numerical analysis, we choose a white LED Gree XL1310CXA whose parameters are presented in Table 1. In this case, its quantum efficiency is $\eta_e = 0.25$, and the thermal resistance is $\theta_{jh} = 1.2$ K/W. For conditions of free convection of air the value of heat-transfer coefficient is $\alpha_p = (5 \div 25)$ (W/m^{2}K). Under forced convection, the heat-transfer coefficient varies within $\alpha_p = (10 \div 200)$ (W/m^{2}K). We use heat pipes with coeffcieints of thermal conductivity $\kappa = 4 \cdot 10^4$ W/m and $2 \cdot 10^4$ W/m·K. For comparison, we choose a copper thermal conductor of the same length which has and identical profile and surface area, and the coefficient of thermal conductivity is $\kappa = 400$ W/m·K.

The dependences of the active zone of LED on the relative length of HP are presented in Fig. 2. It is obvious that with the increase in length the temperature of the active zone decreases.

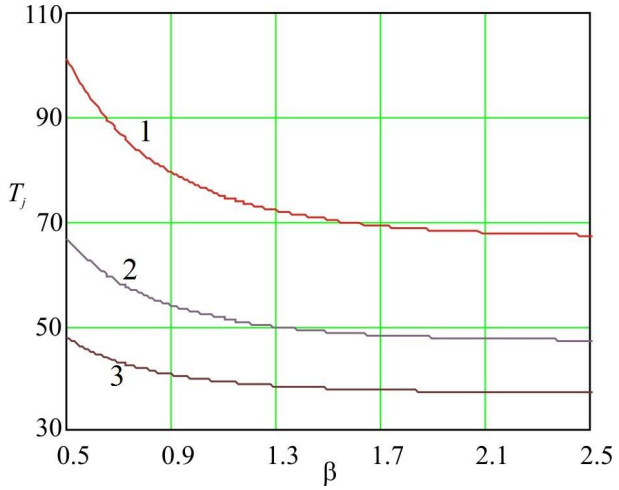

Fig. 2. Dependence of the temperature of the active zone of LED with thermal power P_t=20 W on the relative length of HP at different relative heat-transfer coefficients. The lines 1, 2, and 3 are at ε=0.1 (copper radiator), ε=0.05 (HP) and ε=0.025 (HP), respectively.

This is due to the increase in the surface area of heat exchange with the environment. The increase in the product γl which is responsible for the propagation of heat through the lateral surface contributes to the increase in the relative length of the heat pipe.

The temperature of the active zone is also significantly affected by the relative heat- transfer coefficient.

$$\varepsilon = \frac{\alpha_l}{\kappa\gamma} = \alpha_l \sqrt{\frac{S}{\alpha_p \kappa p}} . \qquad (15)$$

Its reduction also leads to a decrease in temperature T_a. The reduction of ε is aided by the increase in the product $\alpha_p \kappa p$ which is responsible for a wide propagation of heat along the heat pipe. The dependence of the temperature of the active zone of LED on the relative heat-transfer coefficient is shown in Fig. 3.

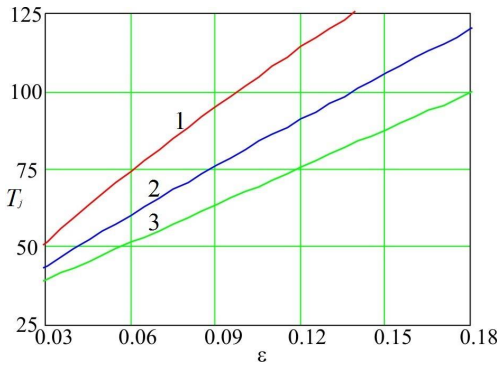

Fig. 3. Dependence of the temperature of the active zone of LED with thermal power P_t=20 W on the relative heat-transfer coefficient at different relative lengths of HP. The lines 1, 2, 3 are at β=0.50, β=0.85, β=2.5, respectively.

Thus, heat pipe-based LED cooling system has a higher efficiency compared to a copper radiator having an identical profile and surface area. This advantage is due to the uniform distribution of temperature over the surface of the heat pipe, and hence, more efficient removal of thermal energy.

Table 1

Series	Rated voltage *(V)*	Direct current (μ*A*)	Maximum power (W)	Luminous flux (*lm*)	Thermal resistance (K/W)	Maximum temperature of the active zone (C°)
XL1310CXA	18	700-1050	20	1400-2100	1.2	125
XL1310CXA	36	350-525	20	1400-2100	1.2	125
XL1520CXA	35	500-900	33	2000-4000	1.2	125
XL1850CXA	35	1400-2100	78	6000-9400	0.6	125
XL2590CXA	69	1200-1800	130	8000-15600	0.6	125

An alternative to efficient and quiet cooling of LEDs with the help of heat pipes is the use of thermoelectric cooling [10].

Conclusions

Heat pipe (HP) is one of the most efficient passive methods of LED cooling. Moreover, cooling efficiency is increased with increasing HP length, perimeter, heat transfer coeficient and the coeficient

of thermal conductivity. The use of HP will significantly reduce the size and mass of the passive cooling system.

The heat pipe-based LED cooling system is more efficient than a copper radiator, which has an identical profile and surface area. Such an advantage is due to the uniform temperature distribution along the HP surface and more efficient removal of thermal energy.

The use of HP-based cooling circuit will increase the luminous flux of LED (increase the power) without rising the temperature of the active zone. This will allow reducing the quantity of LEDs in a lamp and its cost without shortening the lifetime.

HPs have a relatively narrow range of effective use. If the calculated temperature is exceeded, the entire coolant can vaporize, and vice versa, if the temperature is insufficient, the the liquid evaporates badly. It will lead to a sharp decrease in the thermal conductivity of LED cooling system, with all the negative consequences.

References

1. Lotar Noel (2010). Okhlazhediie i regulirovanie temperaturnykh rezhimov svetodiodov [Cooling and control of temperature modes of LEDs]. Poluprovodnikovaia svetotekhnika – Semiconductor Illumination Engineering, 3, 13-15 [in Russian].
2. Khairnasov S.M. (2015). Primeneniie teplovykh trub v sistemakh obespecheniia teplovykh rezhimov REA: sovremennoie sostoianiie i perspektivy [The use of heat pipes in the systems providing thermal modes of electronic equipment]. Tekhnologiia i konstruirovaniie v elektronnoi apparature, 2-3, 19 – 33 [in Russian].
3. Alekseiev V.A., Arefiev V.A. (1979). Teplovyie truby dlia okhlazhdeniia i termostatirovaniia radioelektronnoi apparatury [Heat pipes for cooling and thermostating radioelectronic equipment]. Moscow: Energiia [in Russian].
4. Soule Christopher A. (2004). Heat pipe reliability in high-power applications. Power Electronics Technology, 40-44.
5. Patent of Ukraine №40882, Bul. №8. (2009). Stozhok V.M., Zaguliaiev O.I. LED lighting device [in Ukrainian].
6. Patent of RF №2568105, Bul.№ 31 (2015). Sysun V.V. Powerful LED lamp with heat pipe cooling [in Russian].
7. Rassamakin A.B., Bykov E.V., Khairnasov S.M. (2013). Teplovi rezhymy okholodzhennia svitlodiodnykh svitylnykiv na osnovi teplovykh trub [Thermal modes of system for cooling LED lamps on the basis of heat pipes]. Tekhnologiia i konstruirovaniie v elektronnoi apparature, 5, 28-30 [in Ukrainian].
8. Tikhonov A.N., Samarskii A.A. (1977). Uravneniia matematicheskoi fiziki [Mathematical physics equations]. Moscow: Nauka [in Russian].
9. Beliaiev N.M., Riadno A.A. (1982). Metody teorii teploprovodnosti. Chast1. [Methods of thermal conductivity theory. P.1] – Moscow: Vysschaia shkola [in Russian].
10. Shostakovski P. (2009). Sovremennyie resheniia termoelektricheskogo okhlazhdeniia . [Modern solutions of thermoelectric cooling]. Komponenty i tekhnologii – Components and Technologies,12, 40-46 in Russian].

Submitted 08.08.2018

Закордонець В.С., *канд. фіз.-мат наук*
Кутузова Н.В.

Тернопільський національний технічний університет,
імені Івана Пуюля, вул. Руська,56, Тернопіль, 46001, Україна
e-mail:wladim21@gmail.com

РОЗРАХУНОК СИСТЕМИ ОХОЛОДЖЕННЯ СВІТЛОДІОДА НА БАЗІ ТЕПЛОВОЇ ТРУБИ

Побудована математична теплова модель системи охолодження світлодіода на базі теплової труби. *Розв'язана система диференціальних рівнянь, яка включає стаціонарне рівняння теплопровідності та рівняння термогенерації Джоуля доповнена тепловими граничними умовами. Розрахований розподіл температури в структурних елементах* системи охолодження *в залежності від потужності* світлодіода, *параметрів теплової труби і температури середовища. Бібл. 10, рис. 3, табл. 1.*
Ключові слова: світлодіод, світловий потік, тепловий режим, тепловий опір, термостабілізація, теплова труба.

Закордонец В.С., *канд. физ.-мат. наук, доцент*
Кутузова Н.В.

Тернопольський национальный технический университет,
имени Ивана Пуюля, ул. Русская, 56, Тернополь, 46001, Украина,
e-mail:wladim21@gmail.com

РАСЧЕТ СИСТЕМЫ ОХЛАЖДЕНИЯ СВЕТОДИОДА НА БАЗЕ ТЕПЛОВОЙ ТРУБЫ

Разработаны физическая и математическая тепловые модели системы охлаждения светодиода (СД) на базе тепловой трубы (ТТ). Решена система дифференциальных уравнений, включающая стационарное уравнение теплопроводности и уравнение термогенерации Джоуля, дополненная тепловыми граничными условиями. Расчитано распределение температуры в структурных элементах системы охлаждения в зависимости от мощности СД, параметров ТТ и температуры среды. Библ. 10, рис.3, табл. 1.
Ключевые слова: светодиод, световой поток, тепловой режим, тепловое сопротивление, термостабилизация, тепловая труба.

References

1. Lotar Noel (2010). Okhlazhdeiie i regulirovanie temperaturnykh rezhimov svetodiodov [Cooling and control of temperature modes of LEDs]. Poluprovodnikovaia svetotekhnika – Semiconductor Illumination Engineering, 3, 13-15 [in Russian].

2. Khairnasov S.M. (2015). Primeneniie teplovykh trub v sistemakh obespecheniia teplovykh rezhimov REA: sovremennoie sostoianiie i perspektivy [The use of heat pipes in the systems providing thermal modes of electronic equipment]. Tekhnologiia i konstruirovaniie v elektronnoi apparature, 2-3, 19 – 33 [in Russian].
3. Alekseiev V.A., Arefiev V.A. (1979). Teplovyie truby dlia okhlazhdeniia i termostatirovaniia radioelektronnoi apparatury [Heat pipes for cooling and thermostating radioelectronic equipment]. Moscow: Energiia [in Russian].
4. Soule Christopher A. (2004). Heat pipe reliability in high-power applications. Power Electronics Technology, 40-44.
5. Patent of Ukraine №40882, Bul. №8. (2009). Stozhok V.M., Zaguliaiev O.I. LED lighting device [in Ukrainian].
6. Patent of RF №2568105, Bul.№ 31 (2015). Sysun V.V. Powerful LED lamp with heat pipe cooling [in Russian].
7. Rassamakin A.B., Bykov E.V., Khairnasov S.M. (2013). Teplovi rezhymy okholodzhennia svitlodiodnykh svitylnykiv na osnovi teplovykh trub [Thermal modes of system for cooling LED lamps on the basis of heat pipes]. Tekhnologiia i konstruirovaniie v elektronnoi apparature, 5, 28-30 [in Ukrainian].
8. Tikhonov A.N., Samarskii A.A. (1977). Uravneniia matematicheskoi fiziki [Mathematical physics equations]. Moscow: Nauka [in Russian].
9. Beliaiev N.M., Riadno A.A. (1982). Metody teorii teploprovodnosti. Chast1. [Methods of thermal conductivity theory. P.1] – Moscow: Vysschaia shkola [in Russian].
10. Shostakovski P. (2009). Sovremennyie resheniia termoelektricheskogo okhlazhdeniia . [Modern solutions of thermoelectric cooling]. Komponenty i tekhnologii – Components and Technologies,12, 40-46 in Russian].

Submitted 08.08.2018

O.J. Luste

Luste O.J.[1,2], *Doctor Phys.-math. Science*

Institute of Thermoelectricity of the NAS and MES of Ukraine,
1, Nauky str, Chernivtsi, 58029, Ukraine; *e-mail: anatych@gmail.com,*
[2]Yu.Fedkovych Chernivtsi National University,
2, Kotsiubynskyi str., Chernivtsi, 58000, Ukraine

ACCELERATED TESTING METHODS FOR RELIABILITY PREDICTION

Traditional testing methods are expensive and ineffective to predict the reliability of systems that are expected to function reliably over the years, such as components of space-purpose thermoelectric systems. An alternative to traditional testing are accelerated methods. These include, in particular, accelerated life testing (ALT, HALT)), accelerated degradation testing (ADT), highly accelerated stress screening (HASS).

The paper considers the classification of accelerated methods and options for their mutual harmonization. Bibl. 9, Fig. 3.

Key words: reliability testing methods, time to failure, prediction of reliability.

Introduction

The paper describes accelerated testing methods for predicting the reliability of complex thermoelectric systems under the condition of a minimum sample size. The purpose of the work is the classification of accelerated methods and options for their mutual harmonization.

Accelerated testing methods

Reliability theory is a mathematical discipline that has two aspects - purely theoretical, as a sublime departure from reality, and applied, like a passionate desire for life. In our previous work on the theory of reliability [1], we have already noted that of the two extremes - "mathematics without common sense" and "common sense without mathematics" – the latter should undoubtedly be given the advantage. Of course, it is best to have both working, when mathematical calculations are constantly checked by “common sense”. But this is not always the case. The mathematical apparatus has some kind of hypnotic property, and researchers are often inclined to unconditionally believe in their calculations and the more they believe, the more complex mathematical apparatus is used.

The real practical work aims to point out the importance of abandoning the traditional mistakes in the use of mathematical methods of the reliability theory. For this, two important problems of the reliability of thermoelectric devices and systems were examined in [1] —the determination of the minimum allowable sample size for testing and building reliable complex systems from unreliable elements.

Many systems have extremely high reliability requirements over a long period of operation or storage – space applications of thermoelectric products are a vivid example. Moreover, systems and components often have to be developed in terms that are much shorter than their reliable operating periods. These requirements are a challenge to traditional reliability technology, in which elements are checked for failure in the expected operating conditions to provide a reliable system life. When lifetime is measured in years or decades, this approach is impossible.

Reliability can be defined as the ability of an element to perform the required function, under specified environmental conditions and operation, and for a specified period of time [2]. Formally, if *F (t)* is the probability of failure at time *t* or before time *t*, the reliability function

$$R(t) = 1 - F(t)$$

gives the probability that the element will still function at time *t*. Derived values include the probability density of failure, $f(t) = dF(t) / dt$, and the risk degree $h(t) = f(t) / R(t)$. The hazard rate gives a failure rate at time *t*, with regard to survival before *t*. Knowing whether *h (t)* increases or decreases or is a constant value is useful when predicting the service life.

The standard reliability theory assumes that the mean time to failure for a complex system can be described as a “trough-shaped curve”, as shown in Fig. 1. At the beginning, in the so-called infantile period, the system may exhibit a high failure rate due to manufacturing defects or structural defects. It is expected that these problems will pass and the time will come when the failure rate will be constant and relatively low. At the end of its service life, the failure rate increases due to "aging", which may be associated with certain components of the system, or some physical or chemical degradation processes.

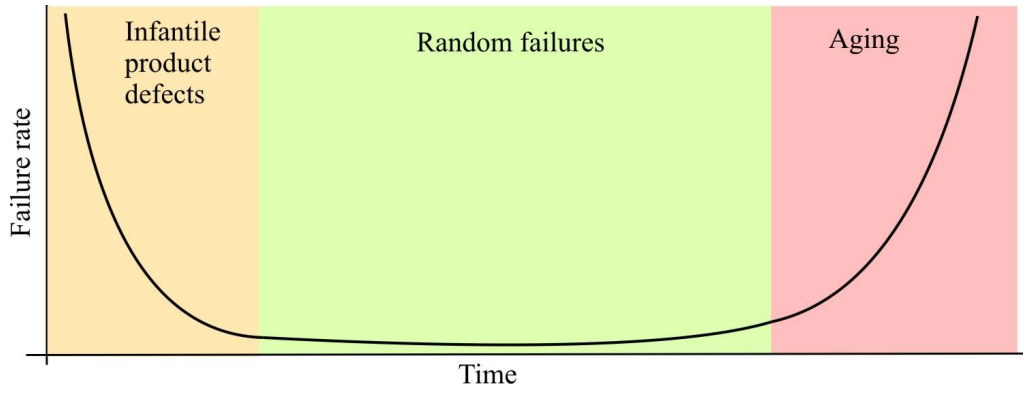

Fig. *1. “Trough-shaped” reliability model.*

If, in the infantile period, failures are determined and *corrected* [2], [3], then reliability grows. This process requires accelerated test methods that quickly reveal failures. Fig. 2 depicts test data where product samples are selected with a small groove, and then subjected to multiple bending up to cracking and elongation. The plots in the upper part of the figure are the calculated probability density of failures (flexibility cycles) to achieve the critical crack length. This density can be used to predict the product lifetime prior to its replacement [4].

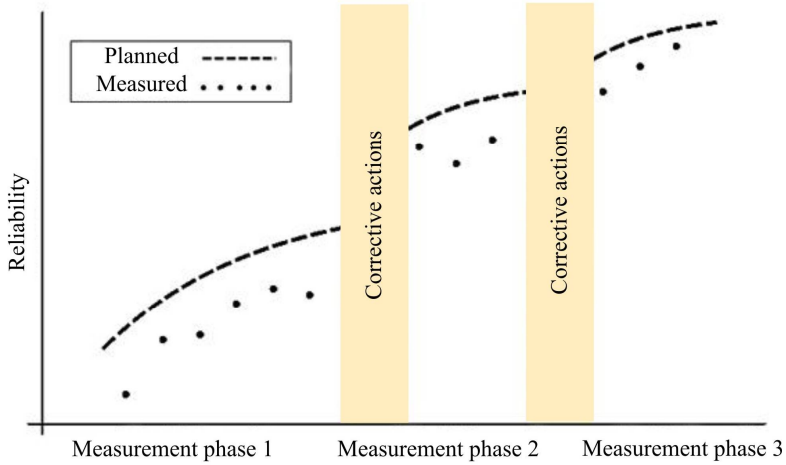

Fig. 2. Reliability growth.

For highly reliable components and systems, the described type of testing cannot be completed within the acceptable period of time, if it is carried out under normal operating conditions - the collection of a significant number of failures may take years. Approaches to overcoming this problem are accelerated life testing (ALT) and accelerated degradation testing (ATD), where elements are tested in conditions of high temperature, mechanical loading, vibration, etc. that are outside the normal operating range [5]. ALT can include increased stresses or multiple stresses at the same time. LANL, ALT / ADT have been applied to various materials [6] [7]. The purpose of ALT / ADT is to accelerate the failure or degradation that may occur in normal use. For accelerated tests, in order to have predictive value, the experimenter must be able to simulate a reduction in the life of the element due to overloading. In this case, the exponential distribution of failure rate is often used:

$$R(t) = \exp(-\lambda t),$$

where λ is the average failure rate. The Arrhenius model for the temperature dependence of the reaction rate is used to predict changes in reliability with increasing temperature, establishing dependence

$$\lambda = \lambda(\tau) = \alpha \exp(-\beta / \tau),$$

where α and β are experimentally determined.

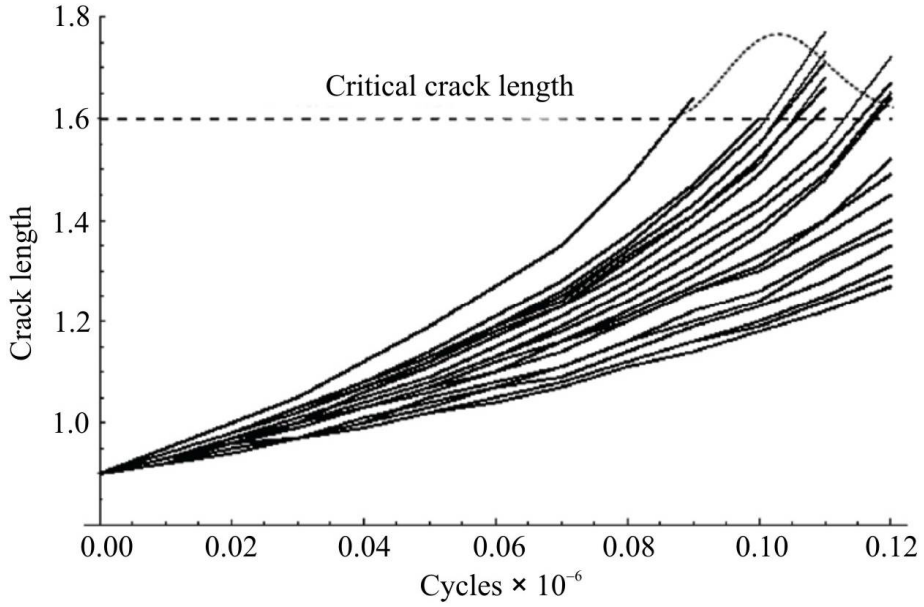

Fig 3. Crack length versus the number of cycles.

Highly accelerated life testing (HALT), which uses a combination of factors at significantly higher levels, although similar to ALT, aims only at finding and correcting design failures during development [8]. Highly accelerated stress screening (HASS) is a related method used to eliminate defective elements from the production process [9]. HALT is effective in accelerating the growth of reliability, but quite often the demonstration reliability requirements may include statistically-oriented methods such as ALT. This creates a certain conflict and may lead to a non-optimal distribution of limited testing options. Ways to overcome this conflict were found in [2 – 9].

Conclusion

A classification of accelerated methods for determining the reliability of complex thermoelectric systems has been developed and options for mutual harmonization of these methods have been determined.

References

1. Anatychuk L.I., Luste O.J. (2017). The effect of degradation on the service life properties of thermoelectric materials. *J.Thermoelectricity*, 5, СТОР?
2. ISO 8402 (1986). *Quality vocabulary.* International Organization for Standardization, Geneva, Switzerland.
3. MIL-HDBK-189C (2011). *Reliability growth management.* US Department of Defense, Washington, DC.
4. Duane, J.T. (1964). *IEEE Trans Aerosp* **2,** 563.
5. Lu, C.J. and W.Q. Meeker (1993). *Technometrics* **35,** 161.
6. Nelson, W.B. (1990). *Accelerated testing: statistical models, test plans, and data analysis*. Hoboken, NJ: John Wiley & Sons .
7. Labouriau, A. and Stephens T.S. (2008). Report on assessment of aging in polymers. *LANL Technical Report LA-UR-08-6800)*.
8. Martz, J.C. and Schwartz A.J. (2003). *J. Miner Met Mater Soc* **55,** 19.
9. Hobbs, G.K. (2000). *Accelerated reliability engineering: HALT and HASS.*Chichester, UK : John Wiley & Sons.

Submitted 20.07.2018

Лусте О.Я. *доктор фіз.-мат. наук, професор*[1,2]

[1]Інститут термоелектрики НАН і МОН України,
вул. Науки, 1, Чернівці, 58029, Україна;
[2]Чернівецький національний університет
ім. Юрія Федьковича, вул. Коцюбинського 2,
Чернівці, 58000, Україна, *e-mail: anatych@gmail.com*;

ПРИСКОРЕНІ МЕТОДИ ВИПРОБУВАНЬ ДЛЯ ПРОГНОЗУВАННЯ НАДІЙНОСТІ

Традиційні методи тестування є дорогими та неефективними для прогнозування надійності систем, які, як очікується, надійно функціонуватимуть протягом багатьох років, таких як компоненти термоелектричних систем космічного призначення. Альтернативою традиційним випробуванням є прискорені методи. Вони включають зокрема прискорене тестування ресурсу (ALT, HALT)), прискорене тестування деградації (ПТД), прискорення сильних механічних напружень (ПСМН). В роботі розглянуто класифікацію прискорених методів і варіанти їх взаємного узгодження. Бібл. 9, рис. 3.

Ключові слова: методи випробувань надійності, наробіток на відмову, прогноз надійності.

Лусте О. Я. *доктор физ.-мат. наук, професор*[1,2]

[1]Институт термоэлектричества НАН и МОН Украины, ул. Науки, 1,
Черновцы, 58029, Украина, *e-mail: anatych@gmail.com*;
[2]Черновицкий национальный университет им. Ю. Федьковича,
ул. Коцюбинского, 2, Черновцы, 58012, Украина,

УСКОРЕННЫЕ МЕТОДЫ ИСПЫТАНИЙ ДЛЯ ПРОГНОЗИРОВАНИЯ НАДЕЖНОСТИ

Традиционные методы тестирования являются дорогостоящими и неэффективными для прогнозирования надежности систем, которые, как ожидается, надежно будут функционировать в течение многих лет, таких как компоненты термоэлектрических систем космического назначения. Альтернативой традиционным испытаниям являются ускоренные методы. Они включают, в частности, ускоренное тестирование ресурса (ALT, HALT)), ускоренное тестирование деградации (ПДТ), ускорение больших механических напряжений (ПСМН). В работе рассмотрена классификация ускоренных методов и варианты их взаимного согласования. Библ. 9, рис. 3.

Ключевые слова: методы испытаний надежности, наработка на отказ, прогноз надежности.

References

1. Anatychuk L.I., Luste O.J. (2017). The effect of degradation on the service life properties of thermoelectric materials. *J.Thermoelectricity*, 5, СТОР?
2. ISO 8402 (1986). *Quality vocabulary.* International Organization for Standardization, Geneva, Switzerland.
3. MIL-HDBK-189C (2011). *Reliability growth management.* US Department of Defense, Washington, DC.
4. Duane, J.T. (1964). *IEEE Trans Aerosp* **2,** 563.
5. Lu, C.J. and W.Q. Meeker (1993). *Technometrics* **35,** 161.
6. Nelson, W.B. (1990). *Accelerated testing: statistical models, test plans, and data analysis*. Hoboken, NJ: John Wiley & Sons .
7. Labouriau, A. and Stephens T.S. (2008). Report on assessment of aging in polymers. *LANL Technical Report LA-UR-08-6800)*.
8. Martz, J.C. and Schwartz A.J. (2003). *J. Miner Met Mater Soc* **55,** 19.
9. Hobbs, G.K. (2000). *Accelerated reliability engineering: HALT and HASS*.Chichester, UK : John Wiley & Sons.

Submitted 20.07.2018

P.D.Mykytiuk

P.D.Mykytiuk. *Cand.Sc. (Physics and Mathematics)*[1,2]
O.Yu.Mykytiuk. *Cand.Sc. (Physics and Mathematics), Assistant Professor*[3]

[1]Institute of Thermoelectricity of the NAS and MES of Ukraine, 1, Nauky str, Chernivtsi, 58029, Ukraine;
e-mail: anatych@gmail.com;
[2]Yuriy Fedkovych Chernivtsi National University, 2, Kotsiubynsky str., Chernivtsi, 58012, Ukraine;
e-mail: anatych@gmail.com;
[3]Higher State Educational Institution of Ukraine "Bukovinian State Medical University", 2, Theatre Square, Chernivtsi, 58002, Ukraine

O.Yu. Mykytiuk.

PROTECTION OF THERMOELECTRIC CONVERTERS AGAINST ELECTRICAL OVERLOADS

Mars Science The analysis of the known methods for protection of thermoelectric converters (TC) against electrical overloads is made. The description and operating principle of the developed electronic protection device with a galvanic decoupling on the electric circuit of the heater is given. The created device allows protection of TC from at least 10 times the load. Tabl. 2, Fig. 2, Bibl. 6.

Key words: thermoelectric converter, overload capacity, heater, sensitivity.

Introduction

In electrical equipment, when measuring the operating values of the alternating voltage and current, wide application has been found by thermoelectric converters (TC) [1].

One of the important parameters of TC is its ability to withstand electrical overloads - the so-called overload capacity. As in most TC, the junction temperature of a thermocouple at a nominal voltage value is 100 ÷ 150 ° C, the 3-4-fold voltage increase at the TC heater leads to the destruction of the thermocouple and, accordingly, to TC failure. Therefore, the overload capacity of TC, as a rule, does not exceed 150 ÷ 200 % of the nominal voltage or current value.

The relevance of the work is due to the lack of a reliable way to protect TC against electrical overloads, which does not affect TC sensitivity.

The purpose of this paper is to analyze the known methods for protection of TC against electrical overloads and to develop an electronic protection device which introduces minimal additional error to the measuring electrical circuit and reliably protects TC against overloads.

Analysis of existing methods for TC protection

One of the easiest methods for protection of TC against accidental overloads is the inclusion of a low-melting fuse made of a microwire in series with a TC heater [2]. However, due to the highly technological difficulties in the creation of microwire fuses for currents less than 20 mA and low

reliability, this method for protection of TC against overloads has not found a wide practical application.

In the search for other ways to solve this problem, the attention of researchers was drawn to the possibility of using silicon diodes to protect TC. Such methods of TC protection were considered in [3, 4]. The authors of these studies investigated a series of silicon diodes and zener diodes. To protect TC, the property of silicon diodes was used to sharply increase the current with a small change in voltage in the region close to the bend of the current-voltage characteristics of the diode. The essence of the device was that parallel to the TC heater there was connected a combination of diodes, and the voltage to the TC heater was applied through the current-limiting resistance. As the voltage on the heater increased to a value exceeding its nominal value, the diodes opened and shunted the heater.

Such devices for protection of TC relatively reliably protect it against overloads, are distinguished by simplicity and low cost design, but introduce a large (up to 1 %) additional error in measurements. In addition, due to the shunting effect of the diodes and resistors included in the measuring circuit, the sensitivity of TC is significantly reduced.

Another way of protecting TC against overloads using transistors is discussed in [5], where TC protection device is described, in which the use of transistors for shunting TC heater allows expanding the dynamic range and increasing the sensitivity of the device. However, this method of protecting TC also did not find widespread use due to the disadvantages inherent in TC protection with diodes.

The best known method of TC protection against electrical overloads is considered in [6], in which an automatic electronic device for the protection of TC was investigated. Such a device contains an electronic circuit that controls either an electronic relay that disconnects TC heater from the current source, or a TC heater bypass transistor.

The use of electronic protection devices allows you to reliably protect TC against overloads, but since the electronic device is connected to the TC input, the additional errors introduced by the circuit are quite significant. Therefore, the use of such electronic TC protection devices is undesirable for use in precision metrological TC.

Electronic device for TC protection with a galvanic decoupling along the heater circuit

In all devices for TC protection against electrical loads mentioned in Section 1, the signal necessary to control the protecting element is taken from the electrical circuit of the heater. This necessarily distorts the measuring circuit and leads to relatively large measurement errors. To eliminate the influence of the protection scheme on the input circuit, a TC protection device was developed with a galvanic decoupling along the TC heater circuit

The operating principle of such a device is based on the change in the slew rate of the overload output pulse. Fig. 1 shows the schematic diagram of the protection device, which operates as follows.

When an input voltage is applied to a TC heater, its thermocouple generates a thermoEMF with a value proportional to this voltage. The thermocouple thermoEMF is fed to the CIP3 differential link, which forms a pulse whose amplitude is proportional to the rate of rise of thermocouple thermoEMF. The pulse is applied to the pulse amplifier input (transistor T1 and operational amplifier A_1). The amplified signal from the output of the pulse amplifier, whose value is regulated by the feedback value (P_{11}-P_{14}) of the operating amplifier, is fed to trigger 1.1. If the amplitude of the pulse is sufficient for switching the trigger (that is, the rate of increase of thermoEMF is greater than its nominal value), then the trigger switches by closing the transistor key T_3, the electronic circuit of whose collector includes a reed switch coil. The reed switch will be de-energized and with its contacts will open the circuit of the TC heater from the source of the input voltage, thus protecting TC from failure.

If there are two heaters in the TC design, the protection device operates in the same way. The only difference will be that the polarity of thermoEMF on the thermocouple will have the opposite sign. Therefore, after a pulse amplifier, there is a phase inverter on the transistor T_2, which turns the negative signal of the pulse into a positive one and the trigger 1.2 will be switched by a positive pulse.

Experimental studies of TC protection device

Studies of TC protection devices for additional comparing error

One of the main characteristics of the differential voltage TC is comparing error, which was investigated on a single differential TC of DTC type with a nominal voltage of 1V at a frequency of 1 kHz. Measurements were carried out with and without a protection device. 6 variants of TC protection devices were investigated. Measurement data are shown in Table 1.

Table 1

Results of experimental studies of TC protection devices for additional comparing error

№ of TC protection device	Error without TC protection device, %	Error with protection device, %	Additional error introduced by protection device, %
1	0.0002	0.0003	0.0001
2	0.0002	0.0003	0.0001
3	0.0002	0.0002	0
4	0.0002	0.0004	0.0002
5	0.0002	0.0002	0
6	0.0002	0.0006	0.0004

Studies have shown that electronic devices created by the Institute of Thermoelectricity for protecting TC against electrical overloads practically do not add any significant additional error to comparing TC of the type DTC.

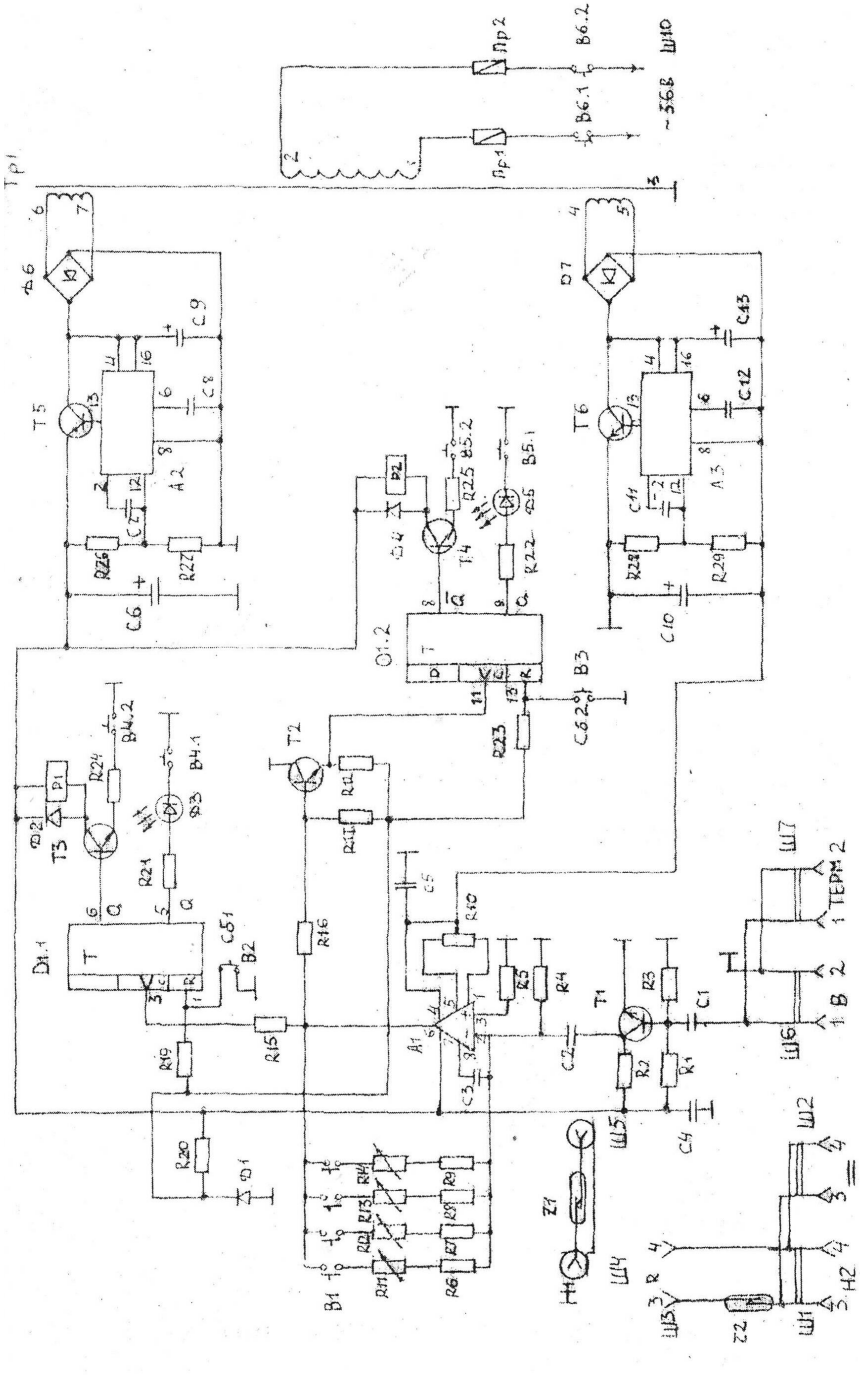

Fig.1. Schematic diagram of TC electrical device

Frequency error of voltage TC introduced by its protection device

Another important characteristic of TC is its frequency error. Frequency error was measured on the same differential DTC with a nominal voltage of 1V. Measurements were made with and without an electronic TC protection device, as well as with six variants of TC protection device. The results of the studies are presented in Table 2.

As can be seen from Table 2, electronic devices for TC protection do not introduce a significant contribution to the frequency error of DTC.

Table 2

Study of TC protection devices for frequency error

Types of TC studies	Frequency error of DTC at frequencies, kHz (%)					Additional error for DTC frequency error at frequencies, kHz (%)				
	0.02	0.4	1.0	10	100	0.02	0.4	1.0	10	100
Without electronic protection device	0.018	0.0073	0	0.0027	0.013					
With electronic protection device										
№ 1	0.02	0.0095	0	0.0031	0.018	0.002	0.0022	0	0.0004	0.005
№ 2	0.029	0.0094	0	0.0103	0.019	0.011	0.0021	0	0.0076	0.006
№ 3	0.031	0.0098	0	0.0110	0.025	0.013	0.0025	0	0.0083	0.012
№ 4	0.023	0.0085	0	0.0052	0.021	0.005	0.0012	0	0.0025	0.008
№ 5	0.021	0.0093	0	0.0065	0.018	0.004	0.0020	0	0.0038	0.005
№ 6	0.027	0.0086	0	0.0079	0.020	0.009	0.0013	0	0.0052	0.007

Speed of TC protection device

An important parameter of TC electronic protection device is the response time when a voltage accidentally hits the TC input, the value of which exceeds its nominal value.

The speed of TC protection device was determined as follows: TC was connected to protection device and to its input from the square-wave generator for 1 s an overload pulse was fed; parallel to TC heater an oscilloscope with a memory function was connected; the response time (speed) of TC protection device was measured as the duration of the overload pulse generated by it on TC heater.

Fig.2 shows the dependence of the protection device speed t_{cep} on the ratio between overload voltage u and the nominal voltage of TC $u_н$.

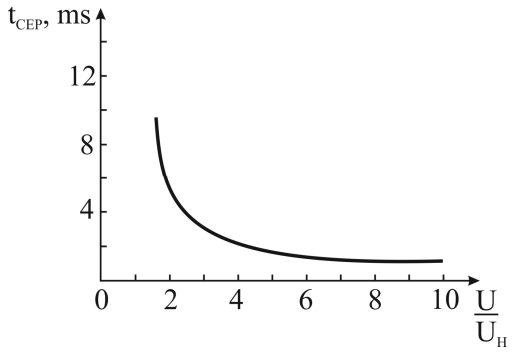

Fig.2. The dependence of TC protection device speed on the ratio between overload voltage and the nominal voltage of TC.

From Fig.2 it is seen that with increasing overload, the response time of the protection device decreases and at 10-fold overload it is less than 1 ms, which corresponds to the release of energy on the TC heater, the value of which is less than 1 mJ. This amount of heat is not enough to overheat the thermocouple junction and to put TC out of action.

Conclusions

The developed electronic device for protection of TC against electrical overloads with a galvanic decoupling on the heater electrical circuit practically does not affect the basic TC parameters and reliably protects it against accidental overloads that are 10 or more times higher than the nominal voltage or current in the TC.

References

1. Anatychuk L.I. (1979). *Termoelementy i termoelektricheskiie ustroistva: Spravochnik [Thermoelements and thermoelectric devices: Handbook]*. Kyiv: Naukova dumka [in Russian].
2. Badinter E.Ya. (1969). *O nominalnom toke slabotochnykh predokhranitelei. V sbornike: Mikroprovod i pribory soprotivleniia, vypusk 6 [On the nominal current of low current fuses. In: Microwire and resistance devices, issue 6]*. Kishinev: Cartea Moldoveneasca [in Russian].
3. Volodin V.A. (1965). Ispolzovaniie poluprovodnikovykh diodov dlia zashchity ot peregruzok po toku [The use of semiconductor diodes for protection against overcurrent]. *Voprosy radioelektroniki*, ser. III, issue 5 [in Russian].
4. Zeldich Yu.V. (1964). Zashchita elektroizmeritelnykh priborov ot peregruzok [Overload protection of electrical measuring devices]. *Izmeritelnaia tekhnika – Measurement Techniques*, 9 [in Russsian].
5. Certificate of Authorship № 144927 (1962). Panchishin V.I. *Bulletin of inventions,* № 4.
6. Kotelnikov N.I. (1981). Avtomat dlia zashchity termopreobrazovatelei [Automatic device for the protection of thermal converters].]. *Izmeritelnaia tekhnika – Measurement Techniques,* № ? [in Russian].

Submitted 14.09.2018.

Микитюк П.Д. *канд. фіз.-мат. наук*[1,2]
Микитюк О.Ю. *канд. фіз.-мат. наук, доцент*[3]

[1]Інститут термоелектрики НАН і МОН України, вул. Науки,
1, Чернівці, 58029, Україна, *e-mail: anatych@gmail.com*;
[2]Чернівецький національний університет імені Юрія
Федьковича, вул. Коцюбинського 2,
Чернівці, 58012, Україна, *e-mail: anatych@gmail.com*
[3]Вищий державний навчальний заклад України
«Буковинський державний медичний університет»,
Театральна площа, 2, Чернівці, 58002, Україна

ЗАХИСТ ТЕРМОПЕРЕТВОРЮВАЧІВ ВІД ЕЛЕКТРИЧНИХ ПЕРЕВАНТАЖЕНЬ

Зроблено аналіз відомих способів захисту термоперетворювачів (ТП) від електричних перевантажень. Наведено опис та принцип дії розробленого електронного пристрою захисту ТП з гальванічною розв'язкою по електричному колу нагрівника. Створений пристрій дозволяє захищати ТП не менше як від 10-ти кратного навантаження. Бібл. 6,табл. 2, рис. 2.
Ключові слова: термоперетворювач, перевантажувальна здатність, нагрівник, чутливість.

Микитюк П.Д. *канд. физ.-мат. наук*[1,2]
Микитюк О.Ю. *канд. физ.-мат. наук, доцент*[3]

[1]Институт термоэлектричества НАН и МОН Украины, ул. Науки, 1, Черновцы, 58029, Украина, *e-mail: anatych@gmail.com*;
[2]Черновицкий национальный университет имени Юрия Федьковича, ул. Коцюбинского 2, Черновцы, 58012, Украина
[3]Высшее государственное учебное заведение Украины «Буковинский государственный медицинский университет», Театральная площадь, 2, Черновцы, 58002, Украина

ЗАЩИТА ТЕРМОПРЕОБРАЗОВАТЕЛЕЙ ОТ ЭЛЕКТРИЧЕСКИХ ПЕРЕГРУЗОК

Сделан анализ известных способов защиты термопреобразователей (ТП) от электрических перегрузок. Приведено описание и принцип действия разработанного электронного устройства защиты ТП с гальванической развязкой по электрической цепи нагревателя. Созданное устройство позволяет защищать ТП не менее как от 10-ти кратной перегрузки. Библ. 6, Рис. 2, Табл. 2.
Ключевые слова: термопреобразователь, перегрузочная способность, нагреватель, чувствительность.

References

1. Anatychuk L.I. (1979). *Termoelementy i termoelektricheskiie ustroistva: Spravochnik [Thermoelements and thermoelectric devices: Handbook]*. Kyiv: Naukova dumka [in Russian].
2. Badinter E.Ya. (1969). *O nominalnom toke slabotochnykh predokhranitelei. V sbornike: Mikroprovod i pribory soprotivleniia, vypusk 6 [On the nominal current of low current fuses. In: Microwire and resistance devices, issue 6]*. Kishinev: Cartea Moldoveneasca [in Russian].
3. Volodin V.A. (1965). Ispolzovaniie poluprovodnikovykh diodov dlia zashchity ot peregruzok po toku [The use of semiconductor diodes for protection against overcurrent]. *Voprosy radioelektroniki*, ser. III, issue 5 [in Russian].
4. Zeldich Yu.V. (1964). Zashchita elektroizmeritelnykh priborov ot peregruzok [Overload protection of electrical measuring devices]. *Izmeritelnaia tekhnika – Measurement Techniques*, 9 [in Russsian].
5. Certificate of Authorship № 144927 (1962). Panchishin V.I. *Bulletin of inventions,* № 4.
6. Kotelnikov N.I. (1981). Avtomat dlia zashchity termopreobrazovatelei [Automatic device for the protection of thermal converters].]. *Izmeritelnaia tekhnika – Measurement Techniques,* № ? [in Russian].

Submitted 14.09.2018.

T. Somkina *Professor, Doctor of Economic Sciences*
O. Lytvynova *Associate professor without tenure, PhD in Economic sciences*
R. Dymenko *Associate professor without tenure, PhD in Economic sciences,* **O. Loban**

Department of Enterprise, Trade and Exchange Activities;
State University of Telecommunications, 7, Solomenska st.,
Kyiv, 03680, Ukraine, *e-mail lobanoo@ukr.net*

FEATURES OF THE UKRAINIAN SOFTWARE DEVELOPERS

It is determined that Ukraine has a mid-size IT market which is more USA- and Europe-oriented, less Russia and Belarus though. IT sector in Ukraine has grown by 15-20% over the last 2 years (from $2.5 billion to $3 billion). What makes extremely attractive for establishing business, it's a solid number of IT talents (over 230,000 IT specialists are employed in 4% companies from the total number of companies in Ukraine). As to the main software development hubs, Kyiv, Lviv, and Odesa are the leaders. As to the preferences, Ukrainian IT market is developing in the following main directions – software development, consulting and support as well as data processing. At least quarter of Ukrainian companies provides system software development services. Moreover it was possible to identify seven groups of IT enterprises, depending on the certain business model implementation. Only 2 enterprises – are most experienced from the Top-50, are selected into the product model group. The numerous group of companies consist of the second sized enterprises (10-49 employees) are operating by using the hybrid model, they also have experience above 5 years. Bibl. 6, Fig. 7.

Keywords: Ukrainian software development companies, IT market, vendors, software are made for business, CRM system.

Introduction

According to analys by using methods of systematization, primary data processing and interpretation of the obtained results from a database of 9866 IT firms, which are represented at clutch.co platform in Category Web&Software Development, were chosen Top-50 Web&Software Development Firm with a mention in the structure of activities such directions as SRM systems development or Customer Software Development. Only 43 enterprises were the permanent elements of the Top-50. They were the basis for the study, the results of which are presented in this paper. Also, during the analysis conducting process, 50 requests to the companies management for public information were formulated.

*The article is published in order to draw attention to the possibilities of using the potential of software in Ukraine for the research, development and business in the field of thermoelectricity.

A lot of international organizations, analytical agencies confirm the importance of Ukrainian software developers on the world stage. So World Economic Forum (WEF) ranks the countries which has the Information technology business performance by the fact of ranging them according to the Networked Readiness Index (NRI), which consist of several pillars: political and regulatory environment, business and innovation environment, skills, government usage, and social impact. Although Ukraine occupied 64th place in 2016, it has the rank improvement, according to the NRI, by 17 points from 2009 till 2016. Moreover WEF forecasts the 40th place for Ukrainian IT Industry in 2020. However, this index cannot

objectively show the situation within R&D in IT industry or directly take into consideration software sales and starting-up/maintenance works. Besides, the revenue of numbers middle-sized software development companies in Ukraine depend on one or few major clients. In Ukraine, there are more than 160 mid-size companies with 50+ employees. The number of developers in the given companies has a steady growth pattern (on average 6-7% per month).

According to PwC analysis, Ukraine is ranked 5th among Top 25 IT services exporters. The value of software outsourcing export in 2015 reached $2,7 bn and it is showing double-digit growth year after year. The contribution of IT to the Ukrainian GDP increased from 0.6% to 3.3% (i.e. from $ 1.1 billion to $ 2.7 billion) during the 2011-2015 period. Compared to its neighboring countries in Europe, Ukraine has the most moderate prices for IT services.

The purposes of scientific article are to determine the development states, features of Ukrainian IT companies business models, which in fact operate as manufacturers and vendors of software (CRM-products) on the world customized or standart software development market. This requires:

(1) to analyze the top-50 IT companies activities along the software development & sales direction, for distributing them by clusters according to selected parameters (from the point of geographical distribution, client orientation and work experience) (section 1, 2);

(2) to analyze the company's personnel management and the corresponding market share, taking into account the characteristics of periodical operating variety in the market (section 3);

(3) to distribute the selected companies by the relevant business models they are uses as an operational activity basis (section 4);

(4) and make the conclusions – new challenges and issues (section 5).

Geographical Framework

Many of the large software development companies operating in Ukraine are headquartered in other countries, including the USA, Israel, EU-members. Moreover, some of Ukrainian companies are expanding outside of Ukraine by opening offices in Poland, Bulgaria, Romania, Belarus, Russia and Spain.

Resources are spread among the country, only 40% in the biggest city (Kyiv). Although there are Top 5 tech hubs in Ukraine: Kyiv, Lviv, Kharkiv, Dnipropetrovsk, and Odessa (fig. 1).

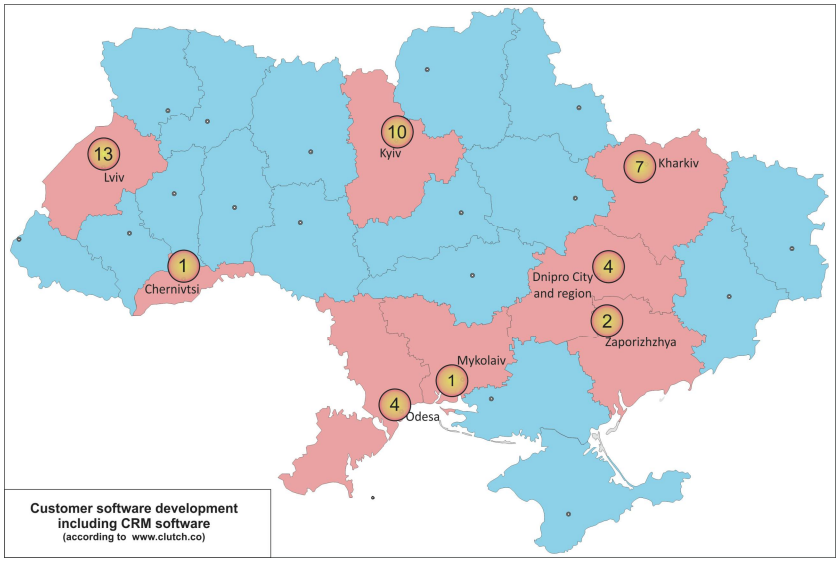

Fig. 1. Spreading of Customer software developers including CRM software developers within Ukrainian borders [compieled based on www.clutch.co and official Top-50 webcites].

The main parameters for choosing the main office location Top-50 enterprise are: proximity to the EU (Lviv), the availability of specialized enterprises that use services in the central region as an administrative country division (Kyiv), the development of industry, primarily heavy industry (Dnipro, Kharkiv, Zaporizhzhya, Odesa). This distribution indicates the diversity of consumers interests at services and requires a clear specialization of developers who, in accordance with this distribution, work both within the domestic and foreign markets.

The enterprises specialization due to the users specialization implies the futher approach of the developer to the consumer so it allows to better orient oneself in the users arising problems (the peculiarities of countries legislation, domestic consumption market where users work and the territorial availability of places for specialists training considerable for replenishing the working resources). As for the conditions of the developers external market, they are less connected to the territory, but there is a clear difference in the developers working for the Western and Eastern markets.

At the same time, it can be assumed that enterprises deployed in Lviv and Kiev can work with great opportunities in the EU and US markets, Australia (this includes language training of the staff located in the Eastern and Centeral regions of Ukraine), and those in the Eastern regions are oriented more towards the CIS countries, which may also be due to the preference for the language environment (fig. 2). Moreover, only a 2-3 hour flight separates Ukraine from Germany, the UK, and other Western European countries. Also, time zone in Ukraine is GMT+2, which is a great advantage for European clients, because of business hours is practically the same as the working hours of Ukrainian remote team.

Fig. 2. Geographic spread of Ukrainian software developers` key clients [compieled based on www.clutch.co and official Top-50 webcites.]

As for the directions of the direct developers specialization, there is a tendency of specialization of both internal and external markets. And if the developers of the Central, the Southern and Eastern parts are oriented more toward the IT sphere and services, then the country's East developers are oriented to large TNCs, primarily having a dislocation in these same industrial areas.

Client Focus

As a result of the analysis of the Top-50 expirience at the market under these study, the tendency of client-orientedness of their work was manifested, which showed that expirience from 1-3 years determines the operational focus on small and medium-sized enterprises (43% and 44 %, respectively), share of large enterprises is about 13 %; enterprises with an operational experience of 4-5 years have in the client base not only small and average (67.2 % and 30.2 %), but also large enterprises (2.6 %), which number is less than has inexperienced group as their clients.

As for enterprises that have been on the market above 5 years, their client base covers all consumer organizational forms with significant growth large enterprises numbers approximately at quarter share (24 %) (fig. 3). This suggests a more even distribution of the client base according to the diversity of their sizes.

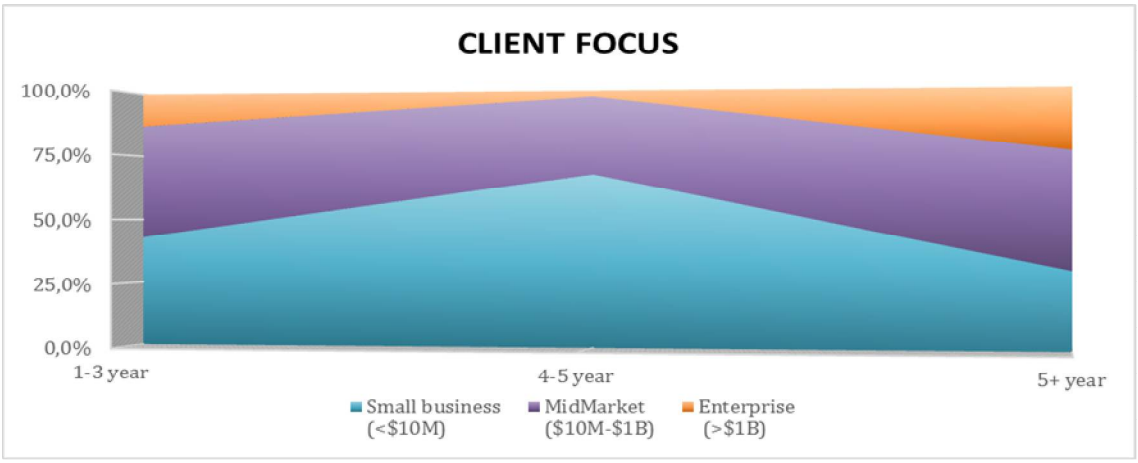

Fig. 3. Client focus of Ukrainian software developers according to their size [compieled based on www.clutch.co and official Top-50 webcites].

It is necessary for scientific investigation to show off the main specialization among Ukrainian software developers at internal and external markets. To deal with it the grouping of all enterprises` clients was done as an analysis of the sphere of clients' interests (fig.4).

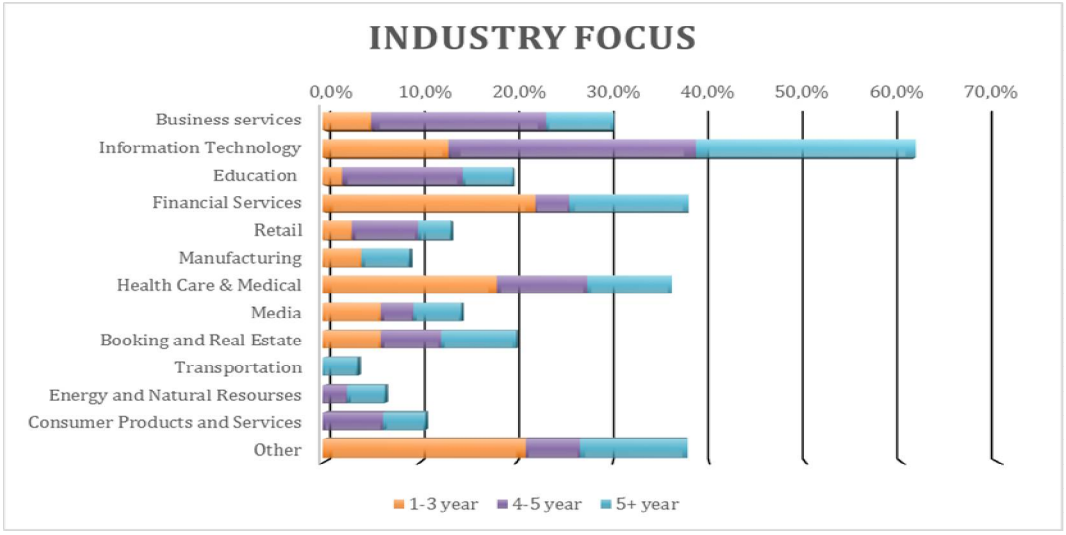

Fig. 4. Industry focus of Ukrainian software developers [compieled based on www.clutch.co and official Top-50 webcites].

So, client focus analisis is showed that the main development direction is making business services software, CRM systems for IT, finantial services companies, education sectors, health care & medical sphere, manufacturing etc. Other less popular business domains include media, retail, travel tech, and energy & natural resources sphere.

The Ukrainian software developer market was formed on the basis of client-orientation, depending on developers experience: inexperienced ones have significant share at finantial services (22 %), healthcare and medical services (18 %), IT sphere (13 %) and others (21 %); experienced companies (4+ years) have another structure of clients` business directions – the biggest one is information technology sphere (above 20 %), business services the second one for the companies with 4-5 year experience (18.1 %) but for the most experience developers with 5+ years market practice the share of business services count only 7%, the second place for them is finantial sphere (12.4 %). Also there is tendencies for the most experienced developers that they have the biggest client focus diversification than other two groups.

The following conclusions were made as a result of the research: almost 72 % of the Top-50 companies list one of these industries among their core competencies (fig. 4). This developers specialization determines the specifics of the services market formation and, accordingly, guides new enterprises to work with this client base. Insufficient attention to customers of such areas as transportation, consumer products and services etc. leads to incomplete coverage of all Ukrainian developers` clients, and, accordingly, the search for customers abroad also taking into account the specialization of the developers.

Classification Aspects

To continue the analysis of the software developers specialization within Ukrainian market, 50 largest and most important companies in that direction were clustering, taking into account their place at the market and the activity field.

The results of the analysis (fig. 5) showed, that the the most numerical group of enterprises (it counts 18 developers or 36% of Top-50), which have a share of CRM in their activities of 20-40 % and 5+ experience, are the most qualified and specialized enterprises using the specifics of the Ukrainian software development market.

The second largest group with the share of CRM in their activities of 20-40 % includes 6 enterprises or 12 % of all developers (Perfsys, FreshCode, US Informatics, CuboRubo, DVG, 482.solutions) and consist of experienced ones (the market experience 4-5 years).

The third group which has a 4 developers with 10% share of the CRM in their activities and expand their share in the current time, that is, enter both into Ukrainian and foreign markets with their specialization.

The least numerical group consists of companies (WD Expert, Syntech Software and Noltic) that work on the market for up to 1 year, but have a specialization of 20-40% of the CRM developments (2 of that companies) and above 51% of the CRM system developments one of them (Noltic), that is, they are young enterprises that occupy a niche and are able to increase their market share in the near future.

The analysis of Top-50 companies from the point of view of internal management and staff training showed that the largest share of the SRM developers is owned by enterprises with a staff of up to 50 people, which indicates the specialists training level and the companies personnel policy and aimed to improving the quality of employees, taking into account their interests and specialization (fig. 6).

The second group consists of large enterprises with a staff of up to 250 people, which are focused on individualizing not only the development process but also the customer base (fig. 6). This gives an opportunity to hold positions within the range of 20-40 % of the development volume. At the same time, 4 enterprises with different numbers of employees specialize directly only in the CRM-systems development.

These enterprises are focused on the internal consumer and fixed on the client base, taking into account the needs of each client, selecting personnel for each development project.

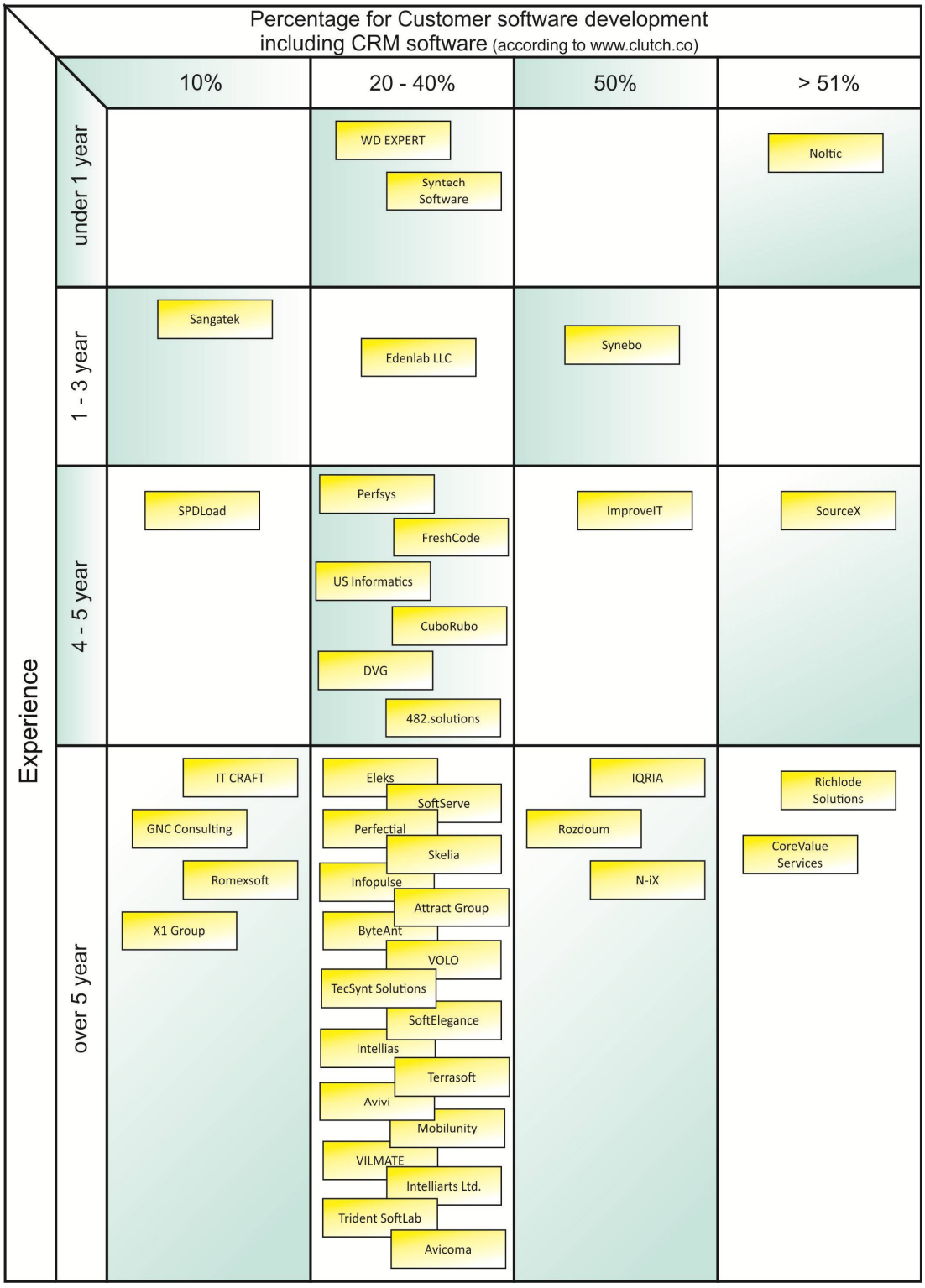

Figure 5. Clustering of Ukrainian software developers according to their experience and SRM software development share [compieled based on www.clutch.co and official Top-50 webcites].

It is impossible to estimate apart market share of customized CRM system development and the market of services related to CRM development in Ukraine: the most software development companies offer both customized and development services, such as SRM installation, consultations and SI.

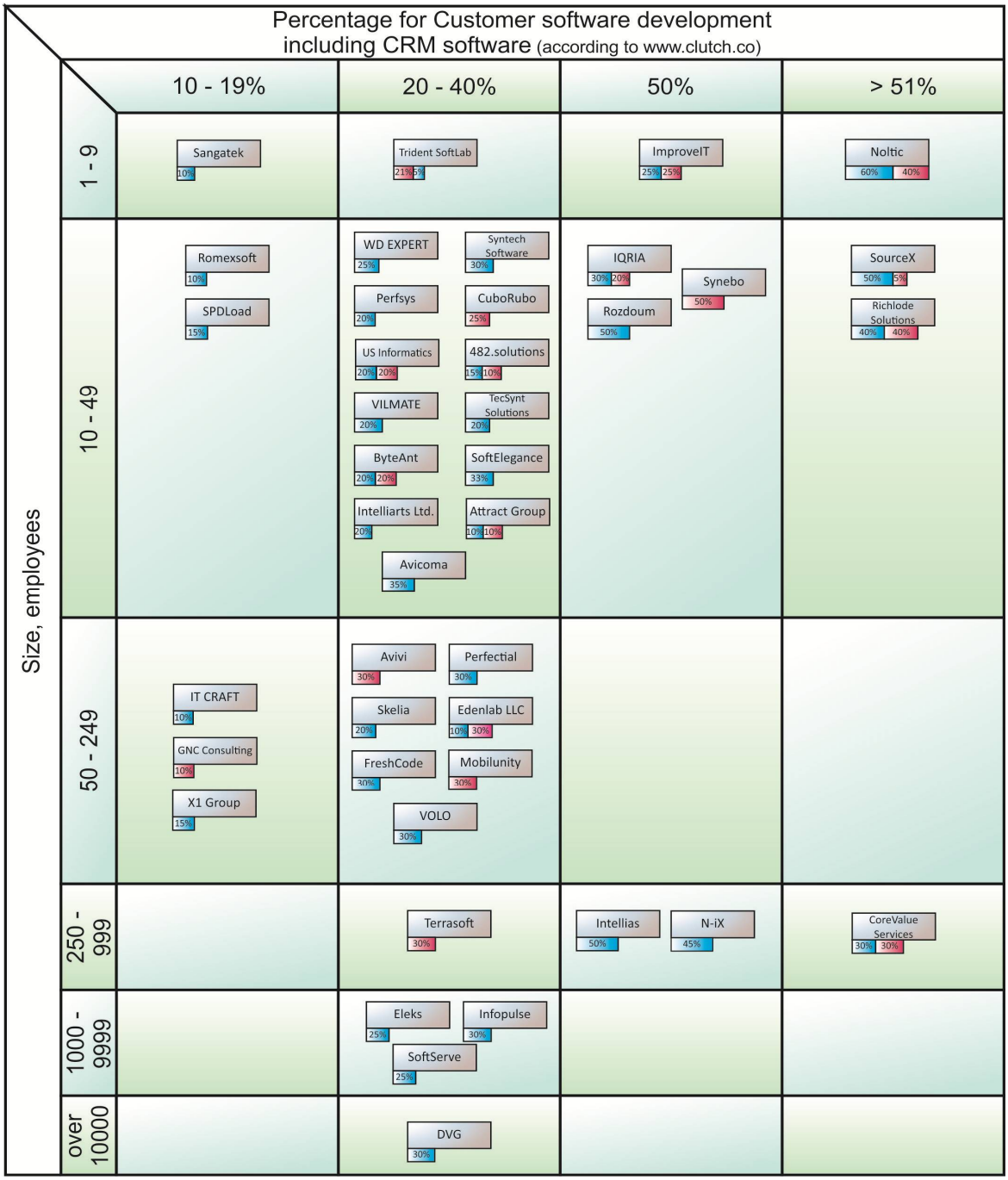

Fig. 6. Clustering of Ukrainian software developers according to their size and SRM software development share [compieled based on www.clutch.co and official Top-50 webcites].

Business environment

Ukraine is one of the leading IT outsourcing destinations in Eastern Europe for multiple reasons, such as highly-qualified developers, moderate prices, good English proficiency, innovative approach to development etc. Ukraine is on the list of top 10 emerging-market locations for offshore services according to Gartner. T. Kearney research indicates that Ukrainian currency depreciation has led to a major gain in its

compensation cost score, accompanied by the improvement in the competitiveness of its tax (Sethi, Gott, 2017).

At the end of the analysis, a business model classification was made for Top-50 software developers headqutered in Ukraine, taking into account not only internal management but also the competitive component of the market environment. The basis was the classification of business models implemented by Cusumano, Nabisan, based on the typification of business models, taking into account the final form of the development product (Cusumano, 2004; Nabisan, 2001). As a result of the analysis, the following conclusions can be drawn (fig. 7).

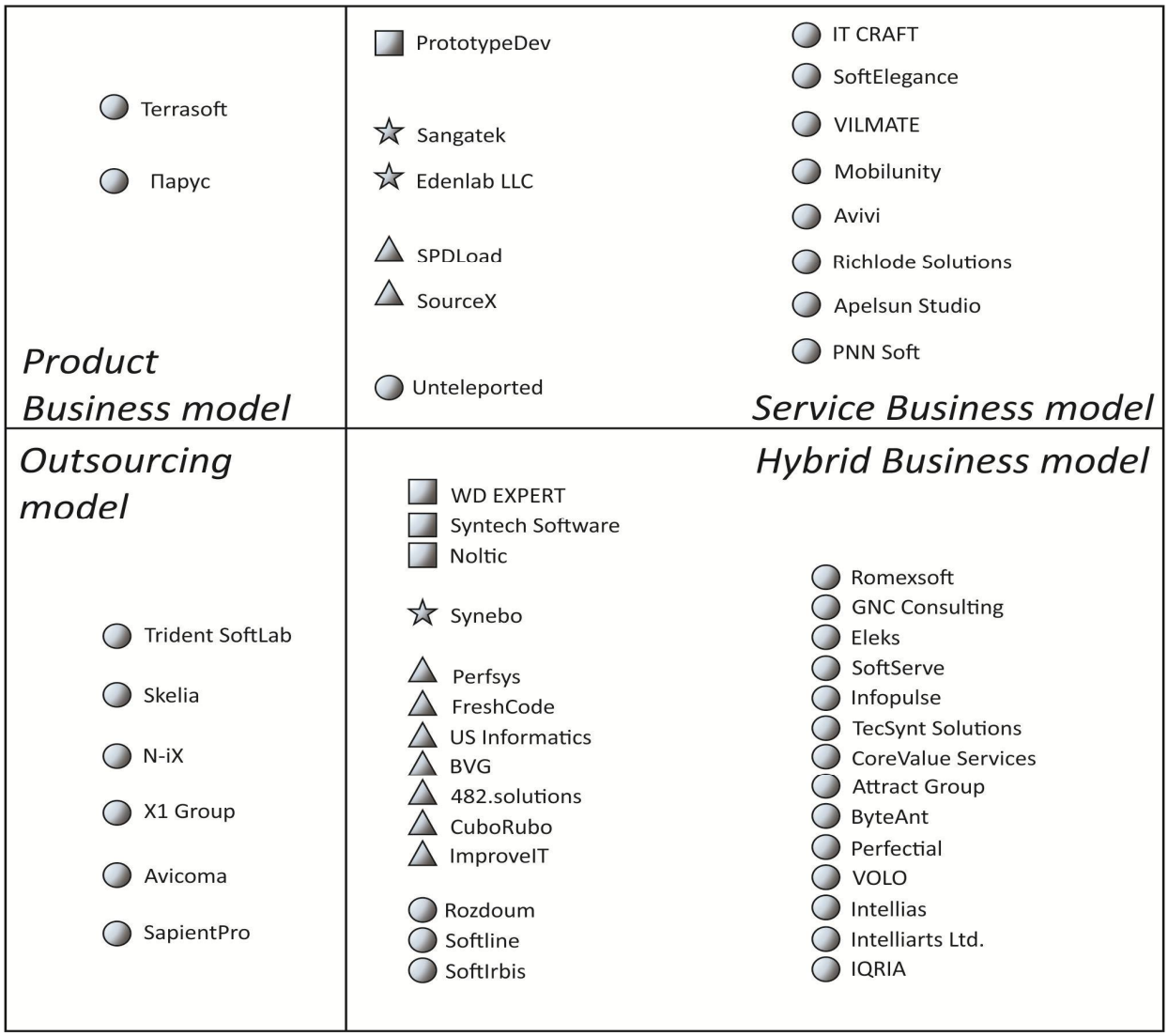

Figure 7. Clustering of Ukrainian software developers according to their business model [compieled based on www.clutch.co and official Top-50 webcites].

The largest number of Ukrainian software developers today from the group under this study presupposes a hybrid functioning business model that represents an intermediate stage of the enterprise's development from service to product, which shows the transitional state of the Ukrainian software market and the orientation of the enterprises majority into the software development segment (nowdays is the most modern world analogues of a business constructions) to reduce the risks level both on domestic and abroad market.

Conclusions: Challenges and issues

We and others must keep expanding and elaborating software economics theory, in particular about the differences between SaaS, outsourcing, customized software development etc., in the face of the fragmentation of knowledge and inability to address with systematic knowledge and analysis many current problems in that scientific issue. So developing the idea of seven business models to cover everything in the software business, remove the legal and theory collisions and replace them with appropriate economic knowledges, especialy taking into account the ukrainians players specifics of activities – is the number one goal for ukrainian researchers. The traditional business model, one has been used for many years by vendors such as SAP, Oracle, and Microsoft, is unappropriate for ukrainian developers, because of the internal specifications they need more flexible one.

A lot of outsourcing companies within Ukrainian software development market explained by uncomplicated buying by clients the software from the other worlwide software vendor, but higher maintenance fees for supporting which can be easly change to less amount of money than what you'll spend doing it yourself, or less ammount annualy from worldwide software leader.

References

1. A database platform www.clutch.co. Retrieved March 01, 2018, from https://clutch.co/web-developers.
2. Arjun Sethi, Johan Gott (2017). The Widening Impact of Automation. Global Services Location Index. Research Report. Retrieved March 01, 2018, from https://www.atkearney.com/digital-transformation/gsli/full-report.
3. Cusumano M. (2004). The Business of Software: What Every Manager, Programmer, and Entrepreneur Must Know to Thrive and Survive in Good Times and Bad. Retrieved March 28, 2018, fromhttp://library.globalchalet.net/Authors/Startup%20Collection/%5BCusumano,%202004%5D%20The%20Business%20of%20Software.pdf.
4. International Organization for Public-Private Cooperation Word economic forum. Retrieved March 4, 2018, from http://reports.weforum.org/global-information-technology-report-2016/networked-readiness-index.
5. Nambisan S. (2001).Why Service Business are not Product Businesses. MIT Sloan Management Review, 42 (4), 72-80.
6. PricewaterhouseCoopers. Retrieved April 10, 2018, from https:// https://www.pwc.com/gx/en.html.

Submitted 18.09.2018

Анатичук Л.І.[1,2] *акад. НАН України*
Вихор Л.М.[1 1] *доктор фіз. - мат. наук*
Прибила А.В.[1,2] *канд. фіз. - мат. наук*

[1]Інститут термоелектрики НАН і МОН України,
вул. Науки, 1, Чернівці, 58029, Україна;
[2]Чернівецький національний університет
ім. Юрія Федьковича, вул. Коцюбинського 2,
Чернівці, 58000, Україна
e-mail: anatych@gmail.com

ВПЛИВ КОНТАКТІВ НА ЕФЕКТИВНІСТЬ ТЕРМОЕЛЕКТРИЧНИХ МОДУЛІВ У РЕЖИМІ НАГРІВУ В УМОВАХ МІНІТЮАРИЗАЦІЇ

У роботі наводяться результати розрахунків впливу контактів на опалювальний коефіцієнт термоелектричного модуля в умовах мініатюризації. Проаналізовані можливості зменшення масогабаритних показників термоелектричного модуля в режимі нагріву для різних контактних опорів за умови мінімальних втрат опалювального коефіцієнту. Бібл. 9, Рис. 1, Табл. 1.
Ключові слова: термоелектричний тепловий насос, ефективність, мініатюризація, моделювання.

Сомкина Т.,, *док. эконом. наук, профессор*
Литвинова О., *канд. эконом. наук, доцент*
Дыменко Р., *канд. эконом. наук*
Лобан О.

Государственный университет телекоммуникаций
03680, ул. Соломенская 7, Киев, Украина
[2]Черновицкий национальный университет
им. Юрия Федьковича, ул. Коцюбинского, 2,
Черновцы, 58012, Украина

ХАРАКТЕРНЫЕ ОСОБЕННОСТИ УКРАИНСКИХ РАЗРАБОТОК ПРОГРАММНОГО ОБЕСПЕЧЕНИЯ

Установлено, что Украина имеет рынок информационных технологий (ИТ) среднего размера, который в большей степени ориентирован на США и Европу, и меньше на Россию и Беларусь. Сектор информационных технологий в Украине вырос на 15-20% за последние 2 года (с 2.5 млрд долларов до 3 млрд долларов). Что делает этот бизнес чрезвычайно привлекательным. Это большое количество ИТ-талантов (свыше 230,000 ИТ-специалистов заняты в 4% компаний от общего числа компаний в Украине). Что касается основных центров разработки программного обеспечения, то лидерами являются Киев, Львов и Одесса. Украинский рынок информационных технологий развивается по следующим основным направлениям: разработка программного обеспечения, консалтинг и поддержка, а также обработка данных. Как минимум четверть украинских компаний предоставляют услуги по разработке системного программного обеспечения. Кроме того, удалось выделить семь групп ИТ-предприятий в зависимости от реализации конкретной бизнес-модели. Тольто 2 предприятия – наиболее опытные из ТОП-50 - отобраны в группу моделей продукции. Многочисленная группа компаний состоит из предприятий второго размера (10-49 сотрудников), которые работают по гибридной модели. Они имеют опыт работы более 5 лет.
Ключевые слова: Украинские компании по разработке программного обеспечения, рынок информационных технологий, поставщики, программное обеспечение для бизнеса, система управления отношениями с клиентами (CRM system).

References

1. A database platform www.clutch.co. Retrieved March 01, 2018, from https://clutch.co/web-developers.

2. Arjun Sethi, Johan Gott (2017). The Widening Impact of Automation. Global Services Location Index. Research Report. Retrieved March 01, 2018, from https://www.atkearney.com/digital-transformation/gsli/full-report.
3. Cusumano M. (2004). The Business of Software: What Every Manager, Programmer, and Entrepreneur Must Know to Thrive and Survive in Good Times and Bad. Retrieved March 28, 2018, fromhttp://library.globalchalet.net/Authors/Startup%20Collection/%5BCusumano,%202004%5D%20The%20Business%20of%20Software.pdf.
4. International Organization for Public-Private Cooperation Word economic forum. Retrieved March 4, 2018, from http://reports.weforum.org/global-information-technology-report-2016/networked-readiness-index.
5. Nambisan S. (2001).Why Service Business are not Product Businesses. MIT Sloan Management Review, 42 (4), 72-80.
6. PricewaterhouseCoopers. Retrieved April 10, 2018, from https:// https://www.pwc.com/gx/en.html.

Submitted 18.09.2018

ARTICLE SUBMISSION GUIDELINES

For publication in a specialized journal, scientific works are accepted that have never been printed before. The article should be written on an actual topic, contain the results of an in-depth scientific study, the novelty and justification of scientific conclusions for the purpose of the article (the task in view).

The materials published in the journal are subject to internal and external review which is carried out by members of the editorial board and international editorial board of the journal or experts of the relevant field. Reviewing is done on the basis of confidentiality. In the event of a negative review or substantial remarks, the article may be rejected or returned to the author(s) for revision. In the case when the author(s) disagrees with the opinion of the reviewer, an additional independent review may be done by the editorial board. After the author makes changes in accordance with the comments of the reviewer, the article is signed to print.

The editorial board has the right to refuse to publish manuscripts containing previously published data, as well as materials that do not fit the profile of the journal or materials of research pursued in violation of ethical norms (for instance, conflicts between authors or between authors and organization, plagiarism, etc.). The editorial board of the journal reserves the right to edit and reduce the manuscripts without violating the author's content. Rejected manuscripts are not returned to the authors.

Submission of manuscript to the journal

The manuscript is submitted to the editorial office of the journal in paper form in duplicate and in electronic form on an electronic medium (disc, memory stick). The electronic version of the article shall fully correspond to the paper version. The manuscript must be signed by all co-authors or a responsible representative.

In some cases it is allowed to send an article by e-mail instead of an electronic medium (disc, memory stick).

English-speaking authors submit their manuscripts in English. Russian-speaking and Ukrainian-speaking authors submit their manuscripts in English and in Russian or Ukrainian, respectively. Page format is A4. The number of pages shall not exceed 15 (together with References and extended abstracts). By agreement with the editorial board, the number of pages can be increased.

To the manuscript is added:

1. Official recommendation letter, signed by the head of the institution where the work was carried out.

2. License agreement on the transfer of copyright (the form of the agreement can be obtained from the editorial office of the journal or downloaded from the journal website – Dohovir.pdf). The license agreement comes into force after the acceptance of the article for publication. Signing of the license agreement by the author(s) means that they are acquainted and agree with the terms of the agreement.

3. Information about each of the authors – full name, position, place of work, academic title, academic degree, contact information (phone number, e-mail address), ORCID code (if available). Information about the authors is submitted as follows:

authors from Ukraine - in three languages, namely Ukrainian, Russian and English;

authors from the CIS countries - in two languages, namely Russian and English;

authors from foreign countries – in English.

4. Medium with the text of the article, figures, tables, information about the authors in electronic

form.

5. Colored photo of the author(s). Black-and-white photos are not accepted by the editorial staff. With the number of authors more than two, their photos are not shown.

Requirements for article design

The article should be structured according to the following sections:

- *Introduction*. Contains the problem statement, relevance of the chosen topic, analysis of recent research and publications, purpose and objectives.
- *Presentation of the main research material* and the results obtained.
- *Conclusions* summing up the work and the prospects for further research in this direction.
- *References*.

The first page of the article contains information:

1) in the upper left corner – UDC identifier (for authors from Ukraine and the CIS countries);

2) surname(s) and initials, academic degree and scientific title of the author(s);

3) the name of the institution where the author(s) work, the postal address, telephone number, e-mail address of the author(s);

4) article title;

5) abstract to the article – not more than 1 800 characters. The abstract should reflect the consistent logic of describing the results and describe the main objectives of the study, summarize the most significant results;

6) key words – not more than 8 words.

The text of the article is printed in Times New Roman, font size 11 pt, line spacing 1.2 on A4 size paper, justified alignment. There should be no hyphenation in the article.

Page setup: "mirror margins" – top margin – 2.5 cm, bottom margin – 2.0 cm, inside – 2.0 cm, outside – 3.0 cm, from the edge to page header and page footer – 1.27 cm.

Graphic materials, pictures shall be submitted in color or, as an exception, black and white, in .opj or .cdr formats, .jpg or .tif formats being also permissible. According to author's choice, the tables and partially the text can be also in color.

Figures are printed on separate pages. The text in the figures must be in the font size 10 pt. On the charts, the units of measure are separated by commas. Figures are numbered in the order of their arrangement in the text, parts of the figures are numbered with letters – a, b, .. On the back of the figure, the title of the article, the author (authors) and the figure number are written in pencil. Scanned images and graphs are not allowed to be inserted.

Tables are provided on separate pages and must be executed using the MSWord table editor. Using pseudo-graph characters to design tables is inadmissible.

Formulae shall be typed in Equation or MatType formula editors. Articles with formulae written by hand are not accepted for printing. It is necessary to give definitions of quantities that are first used in the text, and then use the appropriate term.

Captions to figures and tables are printed in the manuscript after the references.

Reference list shall appear at the end of the article. References are numbered consecutively in the order in which they are quoted in the text of the article. References to unpublished and unfinished works are inadmissible.

Attention! In connection with the inclusion of the journal in the international bibliographic abstract database, the reference list should consist of two blocks: CITED LITERATURE and REFERENCES (this requirement also applies to English articles):

CITED LITERATURE – sources in the original language, executed in accordance with the Ukrainian standard of bibliographic description DSTU 8302:2015. With the aid of VAK.in.ua

(http://vak.in.ua) you can automatically, quickly and easily execute your "Cited literature" list in conformity with the requirements of State Certification Commission of Ukraine and prepare references to scientific sources in Ukraine in understandable and unified manner. This portal facilitates the processing of scientific sources when writing your publications, dissertations and other scientific papers.

REFERENCES – the same cited literature list transliterated in Roman alphabet (recommendations according to international bibliographic standard APA-2010, guidelines for drawing up a transliterated reference list "References" are on the site http//www.dse.org.ua, section for authors).

To speed up the publication of the article, please adhere to the following rules:

- in the upper left corner of the first page of the article – the UDC identifier;
- family name and initials of the author(s);
- academic degree, scientific title;

begin a new line, Times New Roman font, size 12 pt, line spacing 1.2, center alignment;

- name of organization, address (street, city, zip code, country), e-mail of the author(s);

begin a new line 1 cm below the name and initials of the author(s), Times New Roman font, size 11 pt, line spacing 1.2, center alignment;

- the title of the article is arranged 1 cm below the name of organization, in capital letters, semi-bold, font Times New Roman, size 12 pt, line spacing 1.2, center alignment. The title of the article shall be concrete and possibly concise;
- the abstract is arranged 1 cm below the title of the article, font Times New Roman, size 10 pt, in italics, line spacing 1.2, justified alignment in Ukrainian or Russian (for Ukrainian-speaking and Russian-speaking authors, respectively);
- key words are arranged below the abstract, font Times New Roman, size 10 pt, line spacing 1.2, justified alignment. The language of the key words corresponds to that of the abstract. Heading "Key words" - font Times New Roman, size 10 pt, semi-bold;
- the main text of the article is arranged 1 cm below the abstract, indent 1 cm, font Times New Roman, size 11 pt, line space spacing 1.2, justified alignment;
- formulae are typed in formula editor, fonts Symbol, Times New Roman. Font size is "normal" – 12 pt, "large index" – 7 pt, "small index" – 5 pt, "large symbol" – 18 pt, "small symbol" – 12 pt. The formula is arranged in the text, center aligned and shall not occupy more than 5/6 of the line width, formulae are numbered in parentheses on the right;
- dimensions of all quantities used in the article are represented in the International System of Units (SI) with the explication of the symbols employed;
- figures are arranged in the text. The figures and pictures shall be clear and contrast; the plot axes – parallel to sheet edges, thus eliminating possible displacement of angles in scaling; figures are submitted in color, black-and-white figures are not accepted by the editorial staff of the journal;
- tables are arranged in the text. The width of the table shall be 1 cm less than the line width. Above the table its ordinary number is indicated, right alignment. Continuous table numbering throughout the text. The title of the table is arranged below its number, center alignment;
- references should appear at the end of the article. References within the text should be

enclosed in square brackets behind the text. References should be numbered in order of first appearance in the text. Examples of various reference types are given below.

Examples of LITERATURE CITED

Journal articles

Anatychuk L.I., Mykhailovsky V.Ya., Maksymuk M.V., Andrusiak I.S. Experimental research on thermoelectric automobile starting pre-heater operated with diesel fuel. *J.Thermoelectricity*. 2016. №4. P.84–94.

Books

Anatychuk L.I. *Thermoelements and thermoelectric devices. Handbook.* Kyiv, Naukova dumka, 1979. 768 p.

Patents

Patent of Ukraine № 85293. Anatychuk L.I., Luste O.J., Nitsovych O.V. Thermoelement.

Conference proceedings

Lysko V.V. *State of the art and expected progress in metrology of thermoelectric materials.* Proceedings of the XVII International Forum on Thermoelectricity (May 14-18, 2017, Belfast). Chernivtsi, 2017. 64 p.

Authors' abstracts

Kobylianskyi R.R. *Thermoelectric devices for treatment of skin diseases*: extended abstract of candidate's thesis. Chernivtsi, 2011. 20 p.

Examples of REFERENCES

Journal articles

Gorskiy P.V. (2015). Ob usloviakh vysokoi dobrotnosti i metodikakh poiska perspektivnykh sverhreshetochnykh termoelektricheskikh materialov [On the conditions of high figure of merit and methods of search for promising superlattice thermoelectric materials]. *Termoelektrichestvo - J.Thermoelectricity,* 3, 5 – 14 [in Russian].

Books

Anatychuk L.I. (2003). *Thermoelectricity. Vol.2. Thermoelectric power converters*. Kyiv, Chernivtsi: Institute of Thermoelectricity.

Patents

Patent of Ukraine № 85293. Anatychuk L. I., Luste O.Ya., Nitsovych O.V. Thermoelements [In Ukrainian].

Conference proceedings

Rifert V.G. Intensification of heat exchange at condensation and evaporation of liquid in 5 flowing-down films. In: *Proc. of the 9th International Conference Heat Transfer.* May 20-25, 1990, Israel.

Authors'abstracts

Mashukov A.O. *Efficiency hospital state of rehabilitation of patients with color carcer.* PhD (Med.) Odesa, 2011 [In Ukrainian].